

Spring 1985

Fluvial Depositional Processes of a Tropical River, Colombia, South America

Michael L. Babuin
Old Dominion University

Follow this and additional works at: https://digitalcommons.odu.edu/oeas_etds



Part of the [Geology Commons](#)

Recommended Citation

Babuin, Michael L.. "Fluvial Depositional Processes of a Tropical River, Colombia, South America" (1985).
Master of Science (MS), Thesis, Ocean & Earth Sciences, Old Dominion University, DOI: 10.25777/
6t6q-2049
https://digitalcommons.odu.edu/oeas_etds/109

This Thesis is brought to you for free and open access by the Ocean & Earth Sciences at ODU Digital Commons. It has been accepted for inclusion in OES Theses and Dissertations by an authorized administrator of ODU Digital Commons. For more information, please contact digitalcommons@odu.edu.

FLUVIAL DEPOSITIONAL PROCESSES
OF A TROPICAL RIVER, COLOMBIA, SOUTH AMERICA

by

Michael L. Babuin

B.S. May 1980, Campbell University

A Thesis Submitted to the Faculty of
Old Dominion University in Partial Fulfillment of the
Requirements for the Degree of

MASTER OF SCIENCE
GEOLOGICAL SCIENCES
OLD DOMINION UNIVERSITY

February 1985

Approved by:

(Director)

© Copyright by Michael L. Babuin 1985
All Rights Reserved

ABSTRACT

FLUVIAL DEPOSITIONAL PROCESSES OF A TROPICAL RIVER, COLOMBIA, SOUTH AMERICA

Michael L. Babuin
Old Dominion University, 1985
Director: Dr. G. R. Whittecar

Fluvial depositional processes along the Rio Magui in southwestern Colombia are primarily controlled by localized uplift downstream of the mouth of the river, sediment sources that produce both coarse-and-fine-grained load, and numerous over-bank flows each caused by torrential rainfall. Sedimentologic and bathymetric data also indicate that the geomorphic processes and features may reflect recent geologic history of the river and human influence in the region. Fluvial processes and sedimentary environments along the Rio Magui are generally similar to those formed along other tropical and temperate rivers. Several unusual features exist along the Rio Magui including levee-dammed tributary lakes, anomalous textural trends of levee sediments, well-preserved leaf mat accumulations on point and side bars, and a relatively high river gradient for the sinuosity and discharge.

Dedication

Mom and Dad

In recognition of 26 years
of faithful service

Acknowledgments

I am greatly indebted to Dr. G. R. Whittecar, my thesis director and friend, who has offered countless hours of ideas and suggestions regarding this thesis. Without his constructive input and enthusiasm this final product would not exist. Special thanks are also in order to my committee members Dr. Dennis A. Darby and Dr. Harris B. Stewart, Jr. Dr. Darby provided the opportunity of a lifetime through his association with Cal-Colombian Mines, Ltd., that enabled me to undergo my thesis research in the remote tropical rain-forest region of Colombia, South America. Additionally, his continual willingness and patience in assisting me with numerous problems throughout my studies is warmly appreciated. Dr. Stewart, Director of the Center for Marine Studies, in Norfolk, Virginia, also offered many informative discussions concerning a wide variety of topics and for that I am grateful.

A word of thanks is in order for my two colleagues, Jim Garrett and Rick Barringer, who were instrumental in mapping the Rio Magui during the summer of 1983. The memories of the three long months we endured the hardships of living in the jungle will never be forgotten.

I would like to thank Dr. Ramesh Venkatakrishnan who offered many supportive comments regarding structural geologic interpretations, remote sensing techniques, and other helpful bits of advice. Additionally, the assistance of other colleagues and friends such as Rob McDaniel, Yu Wen, and JoAnn Goshorn undoubtedly enhanced the overall quality of this thesis. The tireless assistance of Dori Donn, Linda Ruff, Jeanne Ashmore, and Charlie Fox throughout my graduate studies

at Old Dominion University is also recognized.

Special thanks goes out to Mr. Bruce Harvey, Dr. Robert Perkins, Dr. R. C. Hope, Mr. Steve Westbrook and Dr. Andrew Button, my former professors at Campbell University, who provided me with the necessary training, motivation, and ambition to pursue graduate studies. I am equally indebted to Dr. Robert O. Bloomer, professor emeritus (retired) St. Lawrence University, my close friend, who initially inspired me to pursue a career in geology.

Last but not least, I am grateful to my parents, in-laws and wife, Teresa. Without their financial and moral support this thesis would not exist. I clearly remember many trying moments when I questioned the usefulness and practicality of obtaining an advanced degree. During moments such as these, I was ready to "throw-the-towel-in", but their constant reminders as to the importance of an education provided me with additional stamina to endure the entire "ordeal".

Inevitably, there are some people who I have unconsciously omitted from these acknowledgments, therefore, I express my gratitude to those individuals at this time.

Michael L. Babuin

April, 1985

TABLE OF CONTENTS

	PAGE
LIST OF TABLES	<i>ix</i>
LIST OF FIGURES	<i>x</i>
LIST OF PLATES	<i>xiv</i>
 Chapter	
1. INTRODUCTION	1
SCOPE OF THESIS	1
LOCATION AND SETTING OF STUDY AREA	1
PRIOR RESEARCH IN STUDY AREA	1
IMPORTANCE OF RESEARCH	3
2. RIVER HYDROLOGY	5
METHODOLOGY	5
RESULTS	6
DISCHARGE AND RAINFALL RECORDS	6
SUSPENDED SEDIMENT CONCENTRATION	6
DISCUSSION	10
3. STREAM BATHYMETRY AND CHANNEL MORPHOLOGY	14
METHODOLOGY	14
RESULTS	15
BATHYMETRY AND OTHER MAP FEATURES	15
CHANNEL MORPHOLOGY	16
DISCUSSION	18

	PAGE
4. CHANNEL BAR MORPHOLOGY	29
METHODOLOGY	29
RESULTS	29
MID-CHANNEL BARS	29
POINTS BARS	34
SIDE BARS	37
DISCUSSION	40
5. CHANNEL BAR SEDIMENTARY STRUCTURES	44
METHODOLOGY	44
RESULTS	46
SURFACE FEATURES	46
CROSS-BEDDING	53
VARIATIONS IN SEDIMENTARY STRUCTURES	57
INTRA-BAR COMPARISONS	61
INTER-BAR COMPARISONS	62
DISCUSSION	65
6. TEXTURAL CHARACTERISTICS OF CHANNEL BARS	70
METHODOLOGY	70
RESULTS	70
INTRA-BAR COMPARISONS	70
INTER-BAR COMPARISONS	74
DISCUSSION	76
7. DEPOSITION OF ORGANIC MATTER	80
METHODOLOGY	80
RESULTS	80

	PAGE
DESCRIPTION OF ORGANIC DEBRIS AND DEPOSITS	80
SIZE CHARACTERISTICS OF ORGANIC MATTER	81
IMBRICATION OF WOOD DEBRIS	83
DISCUSSION	87
8. LEVEE ENVIRONMENTS	94
METHODOLOGY	94
RESULTS	96
LATERAL VARIATIONS IN GRAIN SIZE PARAMETERS	96
CHANGES IN SAND/MUD RATIO	96
CHANGES IN MEAN GRAIN SIZE	96
CHANGES IN SORTING	105
DISCUSSION	105
9. BACKSWAMP ENVIRONMENTS	113
METHODOLOGY	113
PLANE TABLE AND ALIDADE	113
AUGERING	113
RESULTS	115
DISCUSSION	118
10. SUMMARY AND CONCLUSIONS	125
REFERENCES CITED	133

LIST OF TABLES

TABLE	PAGE
1. Characteristics of river channel bars within the Rio Magui	30
2. Location of levee samples with respect to geomorphic features	99

LIST OF FIGURES

FIGURE	PAGE
1. Map of Nariño, Colombia, showing the location of Payan, major rivers and roads in the area	2
2. Plot of rainfall compared to river height measured at Payan for one year beginning August 8, 1982	7
3. Rating curve for the Rio Magui at Payan gauging station	8
4. Plot of daily suspended sediment in the Rio Magui at Payan for the summer of 1983	9
5. Plot of suspended sediment concentration and discharge for a single flood event.	11
6. Plot of discharge (Q) and suspended sediment concentrations (SS) for one flood event.	12
7. Sketch of hydraulic and topographic sinuosity	17
8. Longitudinal profile of the Rio Magui levees between Payan and the Rio Patia.	19
9. Map of Rio Magui from Payan to the mouth of the Rio Patia showing the extent of river pools and shape of meanders.	20
10. Plot of river slope versus bankfull discharge for meandering and braided streams	22
11. Plot of radius of curvature (Rc) for individual meanders on the Rio Magui between Payan and the Rio Patia	23
12. Inferred lineament control map of topographic elements in the Rio Magui area	26
13. Sketch depicting modes of channel migration.	27
14. Sketch of surface topography of Rio Magui channel bars as seen in cross-section.	31

FIGURE	PAGE
15. Sketch depicting planar view of shape and configuration of river channel bars with respect to channel walls within the Rio Magui.	32
16. Plot of size characteristics for all mid-channel bars along the Rio Magui	33
17. Photograph of Mid-channel bar 1, downstream of the village of Payan in a transitional form	35
18. Plot of size characteristics of all point bars along the Rio Magui.	36
19. Photograph of Point bar 1 approximately one kilometer downstream of the village of Payan	38
20. Plot of size characteristics of all side bars along the Rio Magui.	39
21. Photograph of Side bar 9 approximately eight kilometers downstream of the village of Payan.	41
22. Sketch of flow patterns in pools and riffles	42
23. Map showing location of mid-channel side and point bars examined in the study area.	45
24. Photograph and block diagram of straight-crested ripples.	47
25. Photograph and block diagram of undulatory ripples.	48
26. Photograph and block diagram of lingoid ripples.	49
27. Photograph and block diagram of lunate megaripples.	52
28. Photograph of winnowed concentrations of heavy minerals along the edges of the downstream portion of Mid-channel bar 1	54
29. Photograph and block diagram of planar cross-bedding	55
30. Photograph and block diagram of trough cross-bedding	56
31. Photograph and sketch of small ripple cross-bedding.	58

FIGURE	PAGE
32. Photograph and sketch of large scale trough-shaped cross-bedding	59
33. Photograph of a levee exposure downstream of Payan . . .	60
34. Photograph of a gravel lag being covered by a sand at waning flow	64
35. Sketch of an idealized sequence of a mid-channel bar deposit.	66
36. Sketch of an idealized fining upward sequence of a point bar deposit.	66
37. Sketch illustrating the textural variations on Mid-channel bar 1, downstream of Payan	73
38. Plot of textural variations for mid-channel bar surface samples from Aurora to the mouth of the Rio Magui.	75
39. Plot of textural variations for point bar trench samples from Aurora to the mouth of the Rio Magui. . . .	77
40. Plot of textural variations for trench samples of side bars from Aurora to the mouth of the Rio Magui	78
41. Photograph of a thin leaf mat lamination typical of large mid-channel bars along the study area	82
42. Photograph of large leaf mat accumulations typical of point and side bars of the Rio Magui.	84
43. Photograph of small wood debris typical of point and side bars along the Rio Magui.	85
44. Photograph of large wood debris on Side bar 11	86
45. Photograph of large wood debris exposed along the banks of the present river channel	86
46. Photograph of small wood debris on Rio Magui levees. . .	88
47. Photograph of bank collapse due to undercutting by flood waters.	88
48. Sketch depicting examples of patterns of flow around obstacles and features of different shapes with respect to their location along Rio Magui channel bars	90

FIGURE	PAGE
49. Photograph of helical flows on the surface of the Rio Magui at high flow conditions.	92
50. Location map of levee samples and major tributaries in the study area.	95
51. Plot of the percentage of sand/mud for each of the 25 levee samples	97
52. Plot of the percentage of sand/mud versus mean grain size (ϕ) for each of the 25 levee samples. . . .	98
53. Plot of mean grain size (ϕ) versus downstream distance (KM) from Payan for each of the levee samples	100
54. Longitudinal profile for the Rio Magui from Payan to the mouth of the Rio Magui showing average stream gradients and major tributary junctions	102
55. Photograph of typical composition of older terraces which deflect the course of the Rio Magui.	104
56. Plot of sorting versus downstream distance from Payan	106
57. Location map of the five floodplain traverses along the Rio Magui.	114
58. Cross-section of the five floodplain traverses along the Rio Magui.	117
59. Photograph of a wide backswamp along the Rio Magui at bank-full flow.	119
60. Photograph of dendritic lakes common to the Rio Magui floodplain from the junction of the Rio Guañambi downstream to the mouth of the Rio Magui. . .	119
61. Photograph of an irregular lake representative of the segment of the Rio Magui located around the town of Payan	120
62. Photograph of a bank exposure near Payan at less than 1/4-bank-full stage	122

LIST OF PLATES

PLATE

- I. BATHYMETRIC MAP OF THE PAYAN QUADRANGLE
- II. BATHYMETRIC MAP OF THE AGUA DERECHIO QUADRANGLE
- III. BATHYMETRIC MAP OF THE HORSESHOE MEANDER QUADRANGLE
- IV. BATHYMETRIC MAP OF THE GUANAMBI QUADRANGLE
- V. BATHYMETRIC MAP OF THE ESTERO SECO QUADRANGLE
- VI. BATHYMETRIC MAP OF THE BOCA MAGUI QUADRANGLE

CHAPTER I

INTRODUCTION

A. Scope of Thesis

The overall objective of this research is to document the modern depositional processes active in a tropical river system and to develop a sedimentologic model for that river. Because little work has been performed on modern river systems in tropical regions, this research may also help to determine if fluvial depositional processes behave differently in varying climatic regions. In order to document the processes affecting deposition along the Rio Magui, the proposed research must include a sedimentologic, hydrologic and morphologic examination of the river segment to be studied.

B. Location and Setting of Study Area

The study area includes the channel and floodplain of the Rio Magui from its mouth to approximately 40 km upstream near the village of Aurora. The study area lies in a tropical rain forest adjacent to the foothills of the Andes Mountains. Payan, the largest village on the Rio Magui, is located 75 km east of the coastal port of Tumaco in S. W. Colombia, South America (Figure 1).

C. Prior Research in Study Area

Isenor (1941) provided the first scientific study of the Rio Magui area by drilling several boreholes to depths up to 16.8 meters along a series of transects across the Rio Magui. Recent descriptive papers on the sedimentologic character of terrace gravels and detailed section descriptions include those of Darby (1976) and Ortiz (1982).

Other investigations by Darby have contributed greatly to a better understanding of the geologic setting within the Payan mining district (Darby, 1982; 1983a; 1983b). Darby and Whittecar (1984a; 1984b) provide a detailed assessment of the effects of the proposed mining upon the environment; and a detailed evaluation assessing the amount of placer gold recoverable from surficial sand and gravel deposits within the Payan mining district. Whittecar and others (1984) describe the changes of Quaternary fluvial systems in a high-relief humid tropical environment.

D. Importance of Research

Few studies exist on the hydrology and deposition of tropical rivers. As the following articles suggest, the principal interest of researchers has been upon the study and prediction of erosion and sedimentation in tropical rivers, especially in respect to monitoring sediment loss (Dunne and Dietrich, 1982) and measuring suspended loads (Wood, 1977). Gupta (1975) analyzed stream characteristics in an environment of seasonal flow where he described channel form and stream behavior in the seasonal tropics of Eastern Jamaica. Gupta compiled a sequence of events during flood stage based on field observations and historical information. Wood (1977), who studied suspended sediments with seasonal flow and large floods, established a general suspended-sediment-concentration-to-discharge relationship for the Hope River in Eastern Jamaica. Wood pointed out that different values of suspended concentrations for the same discharge indicate that a condition of hysteresis exists in the suspended sediment concentration and discharge relationship. The dearth of information concerning tropical streams indicates the need for more detailed descriptions of tropical river

processes.

In order to ascertain if fluvial depositional processes behave differently in varying climatic regimes, it will be necessary to delineate the nature and morphology of the present day Rio Magui and compare these results with well-studied river systems in other climates that exhibit similar hydrologic and sedimentologic characteristics. Numerous morphologic and sedimentologic parameters (e.g., width-depth ratios, channel slopes, sinuosity) have been described for streams in humid and semi-arid areas in temperate regions. For example, Visher (1956) examined fluvial processes as interpreted from ancient and recent fluvial deposits and found that specific sedimentary structures are directly related to sediment transport and the dynamics of open-channel flow. Baker and Penteado-Orellana (1978) examined a river that drained a relatively low relief basin containing semi-arid climates. A comparison of temperate-river features reported in these and other studies with tropical-river measurements taken from the Rio Magui may suggest what if any geomorphic differences may exist.

The documentation of the sedimentary structures found in the Rio Magui will be the basis for comparison between the present day Rio Magui and the older river system that deposited gold bearing sands and conglomerates in terraces now found along the Rio Magui. These data will be significant to the on-going studies of the depositional environment of these older, gold-bearing sands and conglomerates.

CHAPTER II

RIVER HYDROLOGY

In this chapter hydrologic variables such as suspended sediment concentrations, discharge and precipitation are documented in order to better understand the processes of suspended sediment transport during a flood.

A. Methodology

Several hydrologic parameters such as discharge, stage height, and suspended sediment concentrations were measured on the Rio Magui near Payan. In order to measure the river height, a 10-meter bamboo pole was marked in increments of 0.20 meters, placed in the channel (at low water flow), and tied-off with guide wires. This stage pole replaced a similar gauge constructed during the previous year and used to gather nine months of river height data (Darby, 1983a). Planetable-and-alidade survey data indicate that the elevations of the 1983 stage pole were within 5 cm of the elevations on the 1982 gauge. Discharge measurements were obtained by the velocity area method utilizing a price meter suspended on a steel cable from a small motor-boat. Measurements were taken across the river at the Payan gauging station at 4-meter intervals. For further information regarding the exact mechanics of discharge measurement readings, see Smith and Stopp (1978).

Concentrations of suspended sediments were measured from samples taken daily in the river channel thalweg at a depth of 0.6 times the total river depth at the time of measurement. Samples were taken in

a plastic bottle attached to a 5-meter bamboo pole. Known volumes of each sample were drawn through pre-weighed Gelman type A-E glass fiber filter papers by a hand-pump vacuum system. The filter papers were dried and carefully packed for eventual shipment to the laboratory in Norfolk, Virginia.

B. Results

1. Discharge and Rainfall Records

Daily flow measurements indicate that during periods between rainfall, the Rio Magui sustains a constant baseflow. Additionally, the river has a quick response time to precipitation and experiences a broad range of discharge. The average discharge of the Rio Magui from August 1982 through August 1983 was $25\text{m}^3/\text{sec}$ (Darby and Whittecar, 1984a). Discharge along the Rio Magui typically exceeded $5\text{m}^3/\text{sec}$ and on 13 separate occasions was greater than bank-full flow ($325\text{m}^3/\text{sec}$) (Figure 2). Discharge-stage relationships were established by a rating curve, (Figure 3) generated from 14 discharge measurements taken at Payan. Floods typically crest at Payan within 12 hours after sustained downpours, which were widespread up-valley from Payan. This brief response time for the moderate-size Rio Magui drainage basin (328 km^2) is attributed to short and steep valley slopes, abundance of clay-rich soils and the high drainage density in the Rio Magui tributary system (Darby and Whittecar, 1984a).

2. Suspended Sediment Concentrations

Darby and Whittecar (1984a) note that the concentration of suspended sediments in the Rio Magui at Payan varied daily (Figure 4). Typically, daily flows contained 3 to 100 mg/l of suspended sediments,

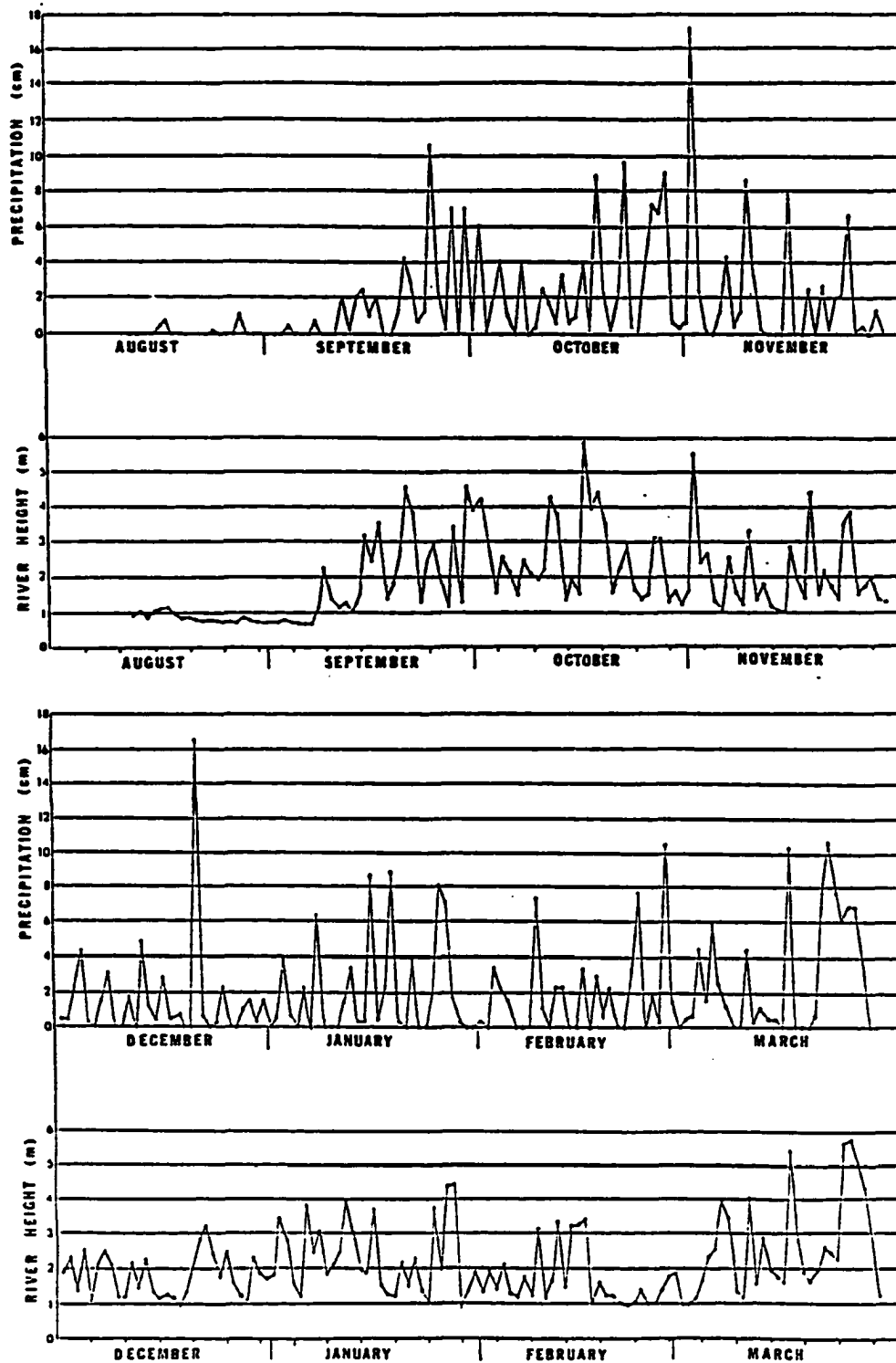


Figure 2. Plot of rainfall compared to river height measured at Payan for one year beginning August 8, 1982 (From Darby and Whittecar, 1984a).

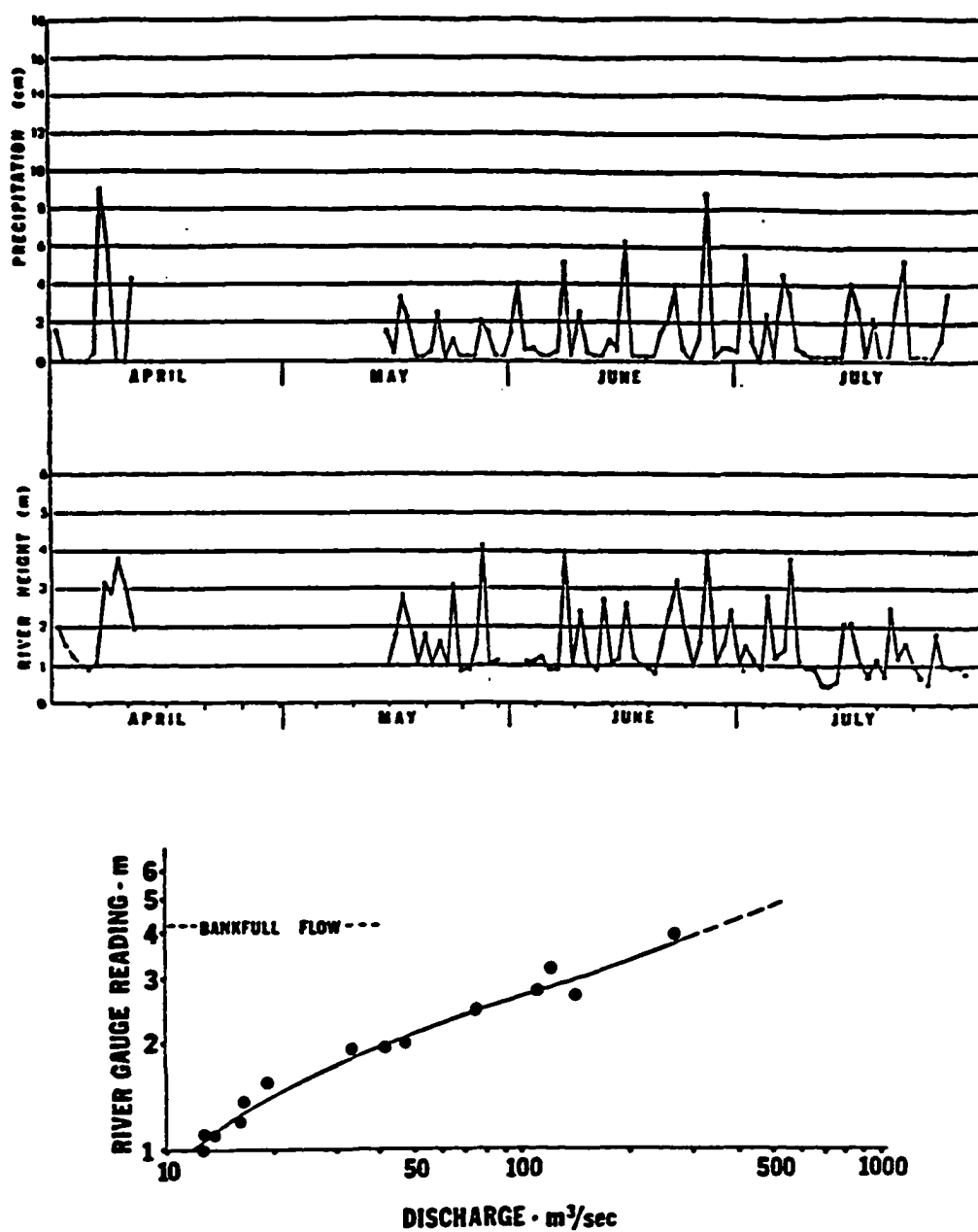


Figure 3. Rating curve for the Rio Magui at Payan gauging station (from Darby and Whittecar, 1984a).

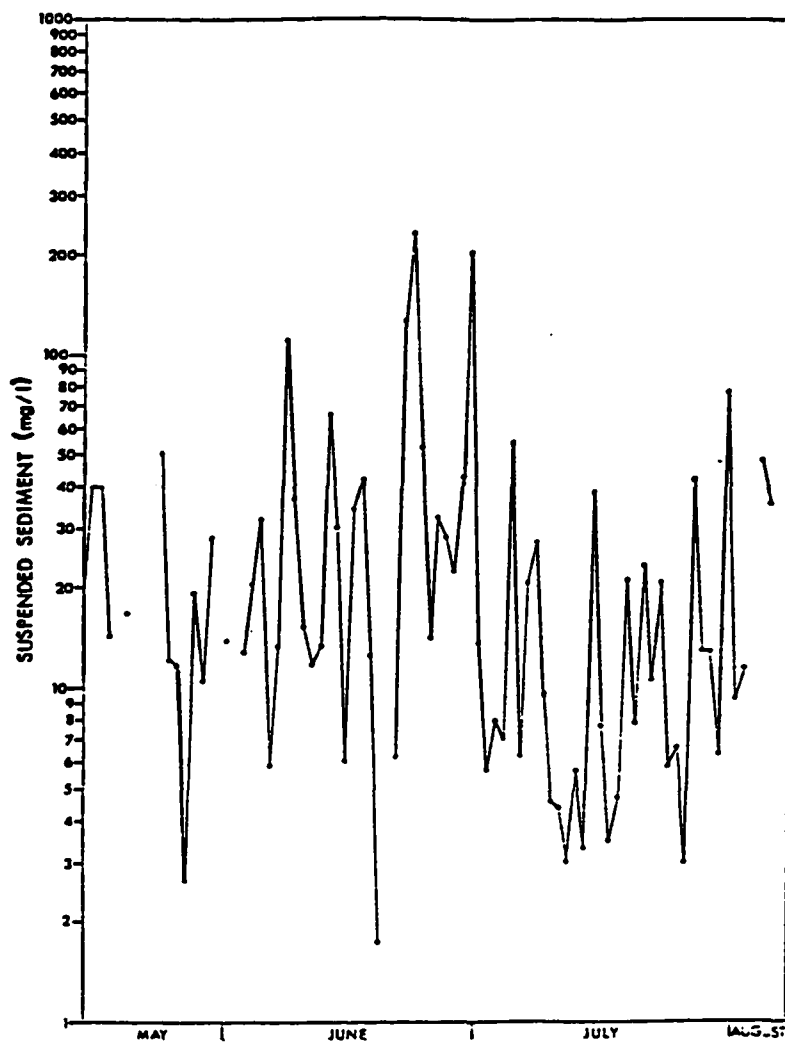


Figure 4. Plot of daily suspended sediment in the Rio Magui at Payan for the summer of 1983. Samples were collected in the thalweg at a depth of 0.6 times the total river depth at the time (from Darby and Whittecar, 1984a).

averaging approximately 18 mg/l per day (Figure 4). Figure 5 illustrates the relationship between peak discharge and concentrations of suspended sediments for one moderate-sized flood event. Moments of highest discharge typically are associated with highest concentrations of suspended sediments although not all high discharges necessarily have large suspended sediment concentrations (Darby and Whittecar, 1984a). Figure 6 illustrates the relationship of discharge and suspended sediment concentration for a single flood event. This plot indicates a pronounced hysteresis for a single flood event. These data may indicate processes of sediment movement active during the flood peak.

C. Discussion

Richards (1982) discusses how hysteresis in the suspended sediment concentration variation during a single storm floodwave reflects a change in supply between rising and falling flood stages. In small catchments, in particular, fine-grained sediment input from wash load continues as rain and runoff occur early in the flood but diminishes as the flood attains its peak. Typically, wash load is derived from bank erosion (Carson, et. al., 1973) or saturated from overland flow close to the channel margins (Bogen, 1980). Concentrations of relatively coarse-grained suspended sediments (e.g., sand carried as bed-load during non-peak flows) often reach their maximum during periods of greatest discharge (Richards, 1982).

Given the very slight skewness of suspended sediment concentrations towards the rising limb, (Figure 5) it is concluded that wash load (fine-grained sediments) and relatively coarse-grained suspended

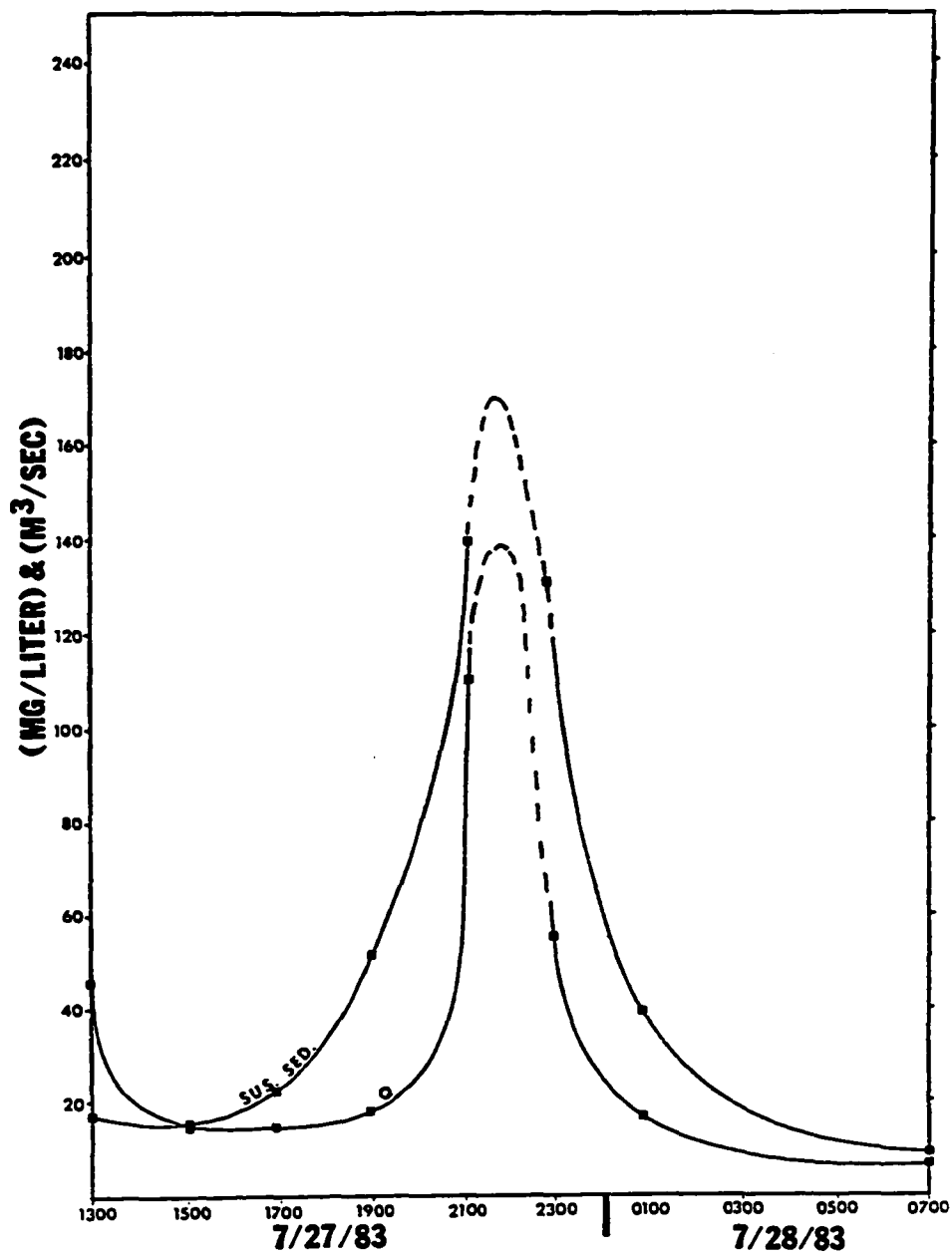


Figure 5. Plot of suspended sediment concentration and discharge for a single flood event.

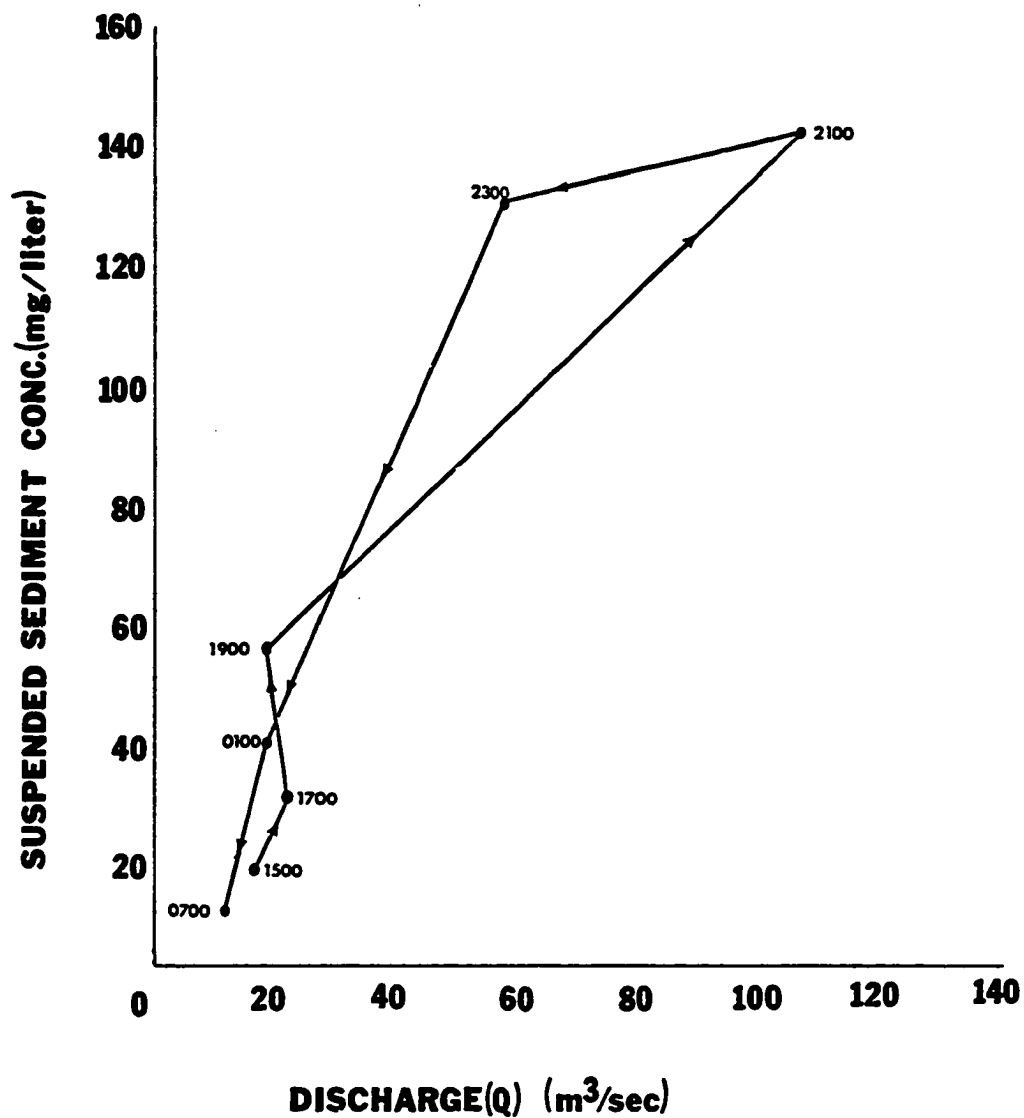


Figure 6. Plot of discharge (Q) and suspended sediment concentrations (SS) for one flood event. Time is in hours starting at 1500 hours. Note that the plot is non-linear due to the hysteresis effects caused by the flood peak.

sediments account for the occurrence of suspended sediment observed in the Rio Magui. Each individual flood may contain various quantities of suspended sediments due to such variables as storm intensity, duration and spatial distribution of storms and precipitation.

CHAPTER III

STREAM BATHYMETRY AND CHANNEL MORPHOLOGY

The purpose of this section is to describe and interpret the bathymetry and channel morphology of the Rio Magui. Discussions regarding the river's sinuosity, meander wavelength, radii of curvature, structural control and migration will prove helpful in determining the depositional processes active along the Rio Magui.

A. Methodology

Bathymetric profiles were constructed by attaching an Apelco Ranger 400 depth finder to a small motorboat and traversing straight-line segments across the river between points of known elevation. The difference in elevation between the river level and the levee tops was measured at each end point using a staff. Relative depth data were compiled from the depth finder's strip chart and converted to elevations for contouring at one-meter intervals. If commercial mining begins, at Payan, these bathymetric maps can be used as base line data to establish how much change occurs in channel morphology, size, location, and spatial distribution of pool-and-channel sequences and bars.

Planimetric base maps were constructed by re-photographing aerial photographs of the study area onto 35 mm slide film. These slides were projected to proper scale (1:2500) in order to trace the location of the channel and accompanying topographic features onto acetate field sheets. Because the aerial photographs were 20 years old, detailed topographic surveying of the river by plane table and

alidade was deemed necessary to "update" the location of the river channel.

B. Results

1. Bathymetry and Other Map Features

It is possible that future growth of channel bars induced by the discharge of mine tailings into the river could influence the navigability of the river (Darby and Whittecar, 1984b); therefore the size, location and spatial distribution of large pools and channel bars in the Rio Magui were mapped using bathymetric data. The accompanying set of bathymetric maps (Plates 1-6) spanning the Payan area downstream to the mouth of the Rio Magui (approximately 19 km) are based on bathymetric profiles compiled during May through August of 1983.

Other map features include the flow direction, location of major tributaries adjoining the Rio Magui, location and shape of mid-channel bars, and the position of older terrace edges in close proximity to the current river, and location of lakes and lagoons near the Rio Magui. Additional cultural information included on the bathymetric maps is significant because it represents the first known compilation of data regarding location of schools, mine sites, native pile dwellings, villages and names of rivers and lakes along the Rio Magui. For a more complete explanation of cultural patterns, work styles and living conditions in southwest Colombia, see West (1957). One feature detectable only by construction of the bathymetric maps is a river mouth bar which splits the thalweg. During low water conditions (1.0 meter above channel bottom) all river channel bars

are emergent with the exception of this submerged bar at the mouth of the Rio Magui (Plate 6).

2. Channel Morphology

In order to determine the nature of the sinuosity of the Rio Magui, two equations introduced by Mueller (1968) were used to calculate hydraulic sinuosity (HSI) and topographic sinuosity (TSI). These two equations attempt to define the components of sinuosity for the river from Payan to the mouth of the Rio Magui:

$$\text{Hydraulic sinuosity (HSI)} = \frac{100(\text{TS}-\text{VS})}{(\text{TS}-1)}$$

and

$$\text{Topographic sinuosity (TSI)} = \frac{100(\text{VS}-1)}{(\text{TS}-1)}$$

Figure 7 shows the sinuous channel of the Rio Magui following a meandering valley axis; several variables exist for the above two equations, total sinuosity (TS) is channel length divided by air distance (C/A), and valley distance (VS) is valley length divided by air distance (V/A) (Richards, 1982). Channel length (20.4 km), air distance (13.8 km) and valley distance (15.5 km) were calculated from the bathymetric maps (Plates 1-6) of the Rio Magui. The hydraulic sinuosity (HSI) is calculated to be 74.46%; the topographic sinuosity (TSI) 25.54%.

Thalweg depth in sinuous versus meandering reaches along the Rio Magui varies markedly. In straight segments of the river an alternating sequence of shallow pools attain a maximum depth of one to two meters. Meander loops display deeper pools, typically three to six meters in depth. This variation is due to greater velocities and

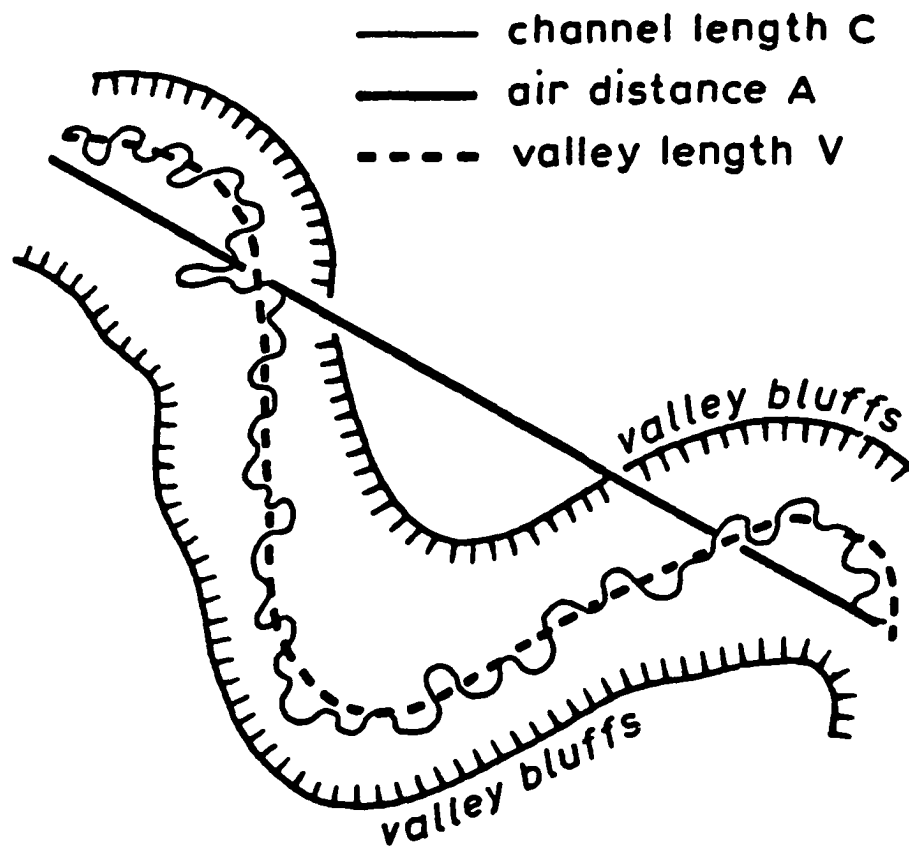


Figure 7. Sketch of hydraulic and topographic sinuosity (after Richards, 1982).

subsequent channel scouring in meander bends.

C. Discussion

The common tendency of rivers to adopt sinuous or meandering courses has been the subject of a large number of studies (see Davies and Tinker, 1984). Many contrasting views exist about the geological reason for various channel shapes. Several workers believe that random interactions among many processes and environmental factors directly contribute to channel shape (Thakur and Scheidegger, 1968, 1970; Ghosh and Scheidegger, 1971; Wallis, 1978). Other workers believe that meander formation is not an essentially random process but controlled by reversals of secondary circulation (Ferguson, 1976; Davies and Tinker, 1984).

As shown in Figure 8, the Rio Magui exhibits a concave-upward longitudinal profile with a major break in slope approximately 10 km downstream of Payan. This variation in slope may be attributed to the influx of sediment from the Rio Guañambi (see Plate 4) and will be discussed further in the section regarding levee environments. Upstream of the Rio Guañambi, river gradient at bankfull discharge ranges between 1 and 3 m/km; downstream of the Rio Estero Seco, river gradients are reduced, typically less than 0.5 m/km (Darby and Whittecar, 1984a).

Generally, the channel width increases from Payan downstream to the mouth of the Rio Magui as do pool-to-pool distances, radii of curvature in bends, and meander wavelength similar to meandering rivers in other regions (Figure 9). Lane (1957) and Leopold and Wolman (1957) indicate that meandering and braided streams develop

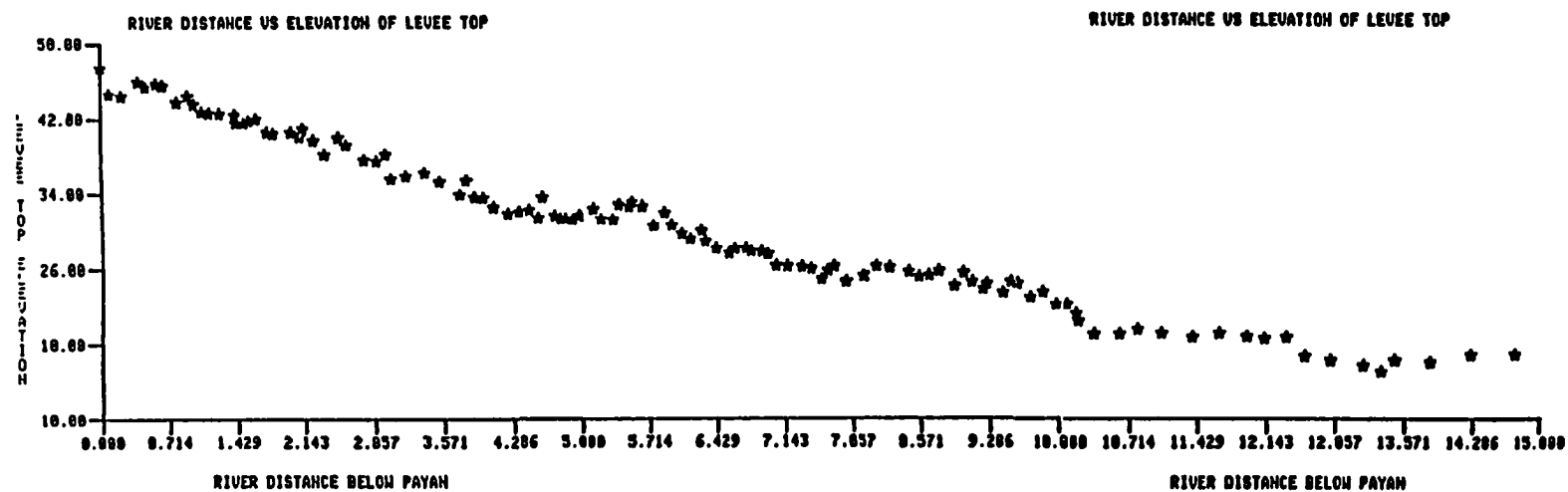


Figure 8. Longitudinal profile of the Rio Magui levees between Payan and the Rio Patia. Break in slope at approximately 10 kilometers possibly due to tributary influx. Other irregularities are due to local erosion and deposition on the river banks. (Modified after Darby and Whittecar, 1984a).

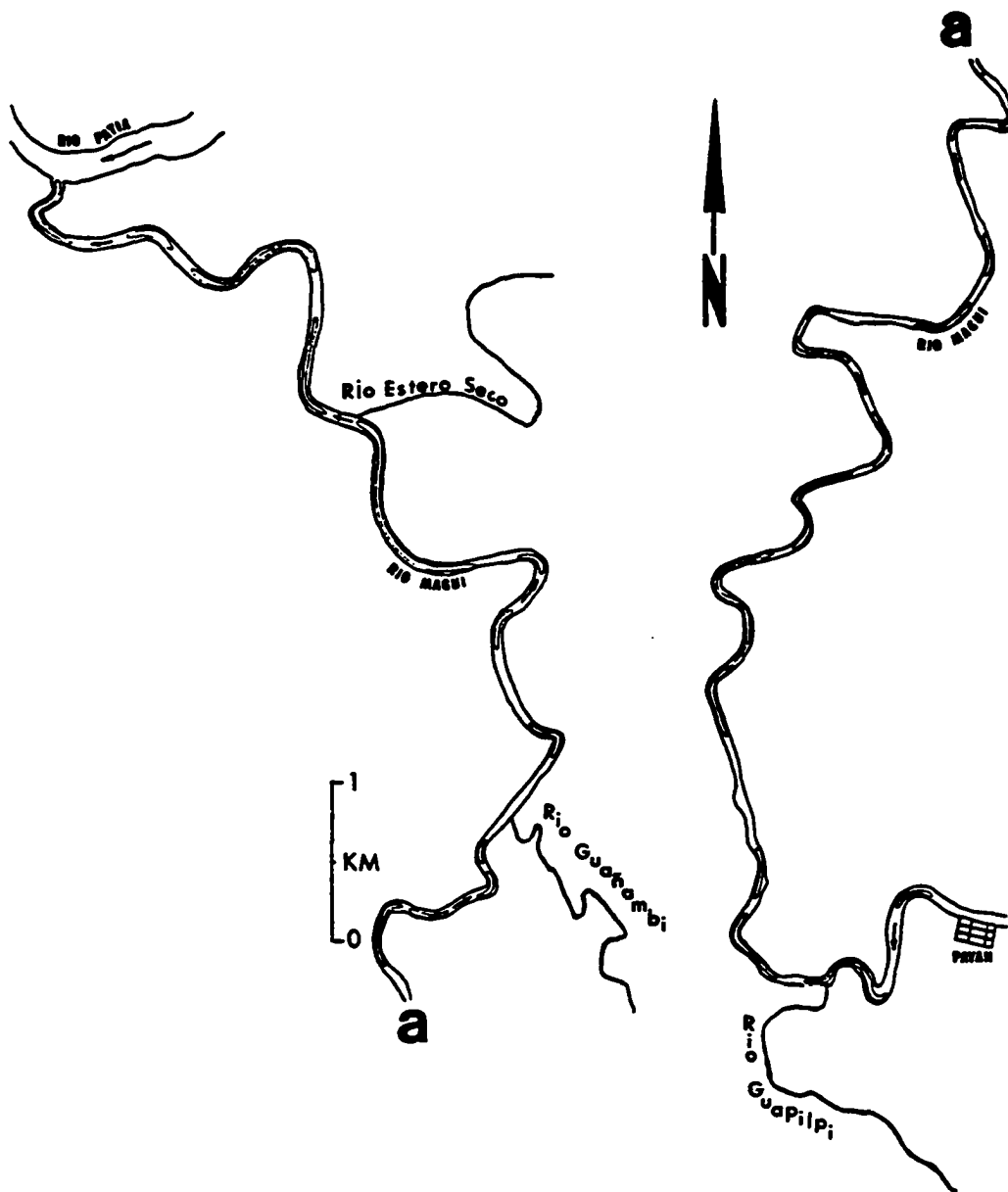


Figure 9. Map of the Rio Magui from Payan to the mouth of the Rio Patia showing the extent of river pools and shape of meanders. (Modified after Darby and Whittecar, 1984a).

under different ranges of hydrologic parameters specifically, slope and discharge. Figure 10 displays how the Rio Magui has an excessively steep slope for a stable, supposedly "meandering" stream. Rivers which plot on Figure 10 in the zone with braided rivers while their relatively low sinuosity (1.3) indicates a distinctive meandering character, may change their shape rapidly to a braided stream if sufficiently disturbed (Darby and Whittecar, 1984a). However, Darby and Whittecar (1984a) noted that most of the meanders on the Rio Magui form by deflection where the stream encounters the valley wall made of terrace gravels resistant to erosion; they believe therefore, that a true measure of sinuosity for the Rio Magui would disregard the numerous tight meanders and concentrate upon the broad open bends (Figure 11). For these reasons Darby and Whittecar conclude that as a whole, the Rio Magui is more "straight" than meandering and presently flows in a channel which is relatively stable morphologically.

An attempt to define the components of sinuosity for the Rio Magui using techniques outlined by Mueller (1968) resulted in a hydraulic sinuosity of 74.46% and a topographic sinuosity of 25.54%. Because the hydraulic sinuosity is significantly greater than the topographic sinuosity, it appears that the Rio Magui is actively meandering due to internal hydraulic processes more than believed by Darby and Whittecar (1984a) and is controlled to a lesser extent by topographic and environmental controls.

Langbein and Leopold (1966) describe how the thalweg or deepest part of the channel hugs the outside of meander loops close to the concave bank of the channel. In both meandering and straight stretches of the Rio Magui, the thalweg meanders from one side to the

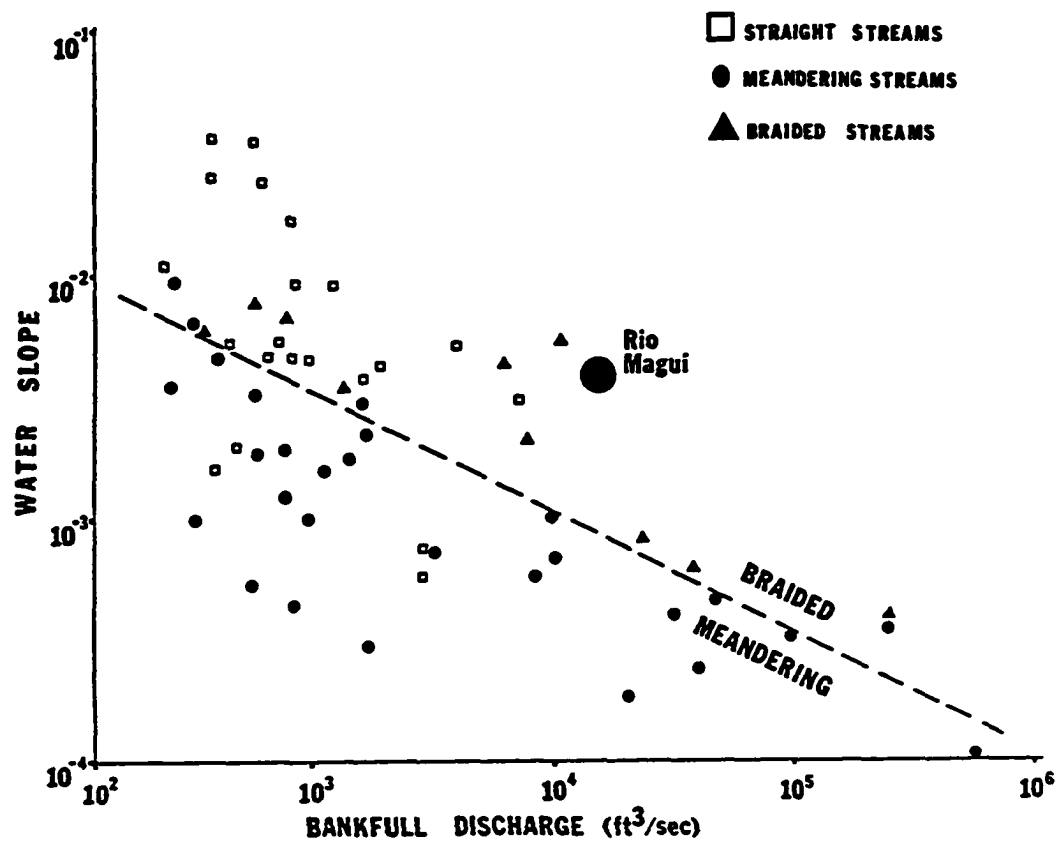


Figure 10. Plot of river slope versus bankfull discharge for meandering and braided streams. (Modified after Darby and Whittecar, 1984a).

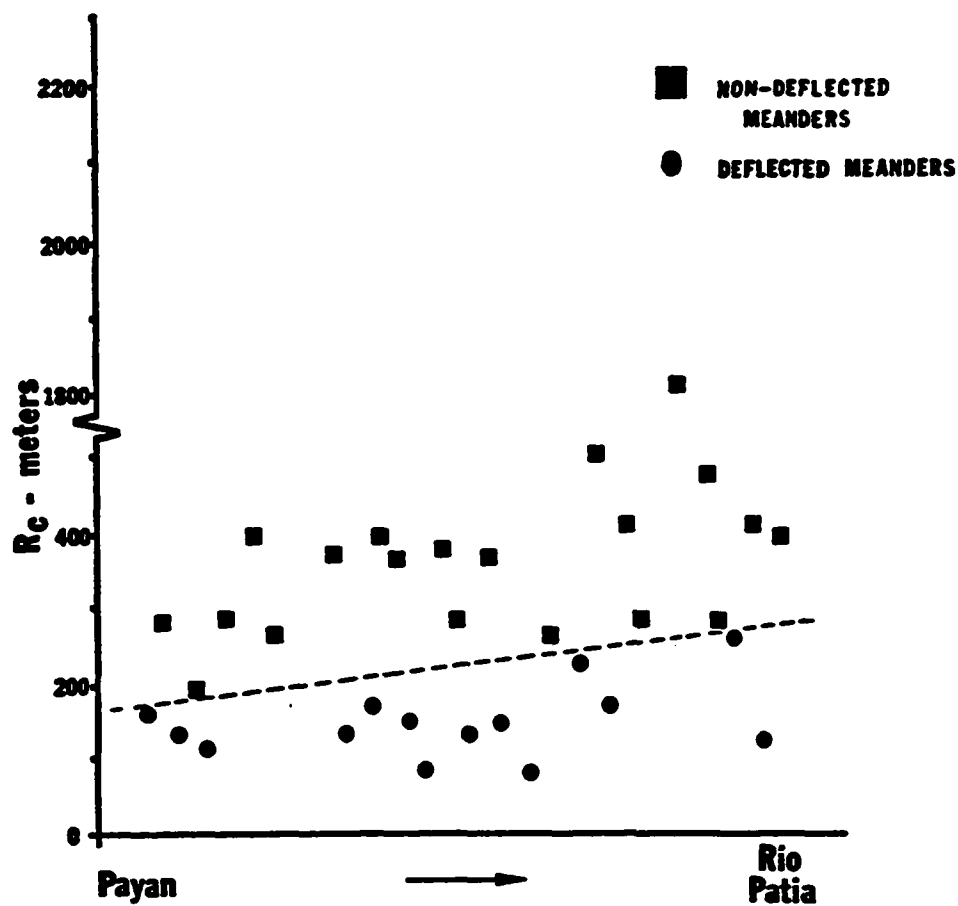


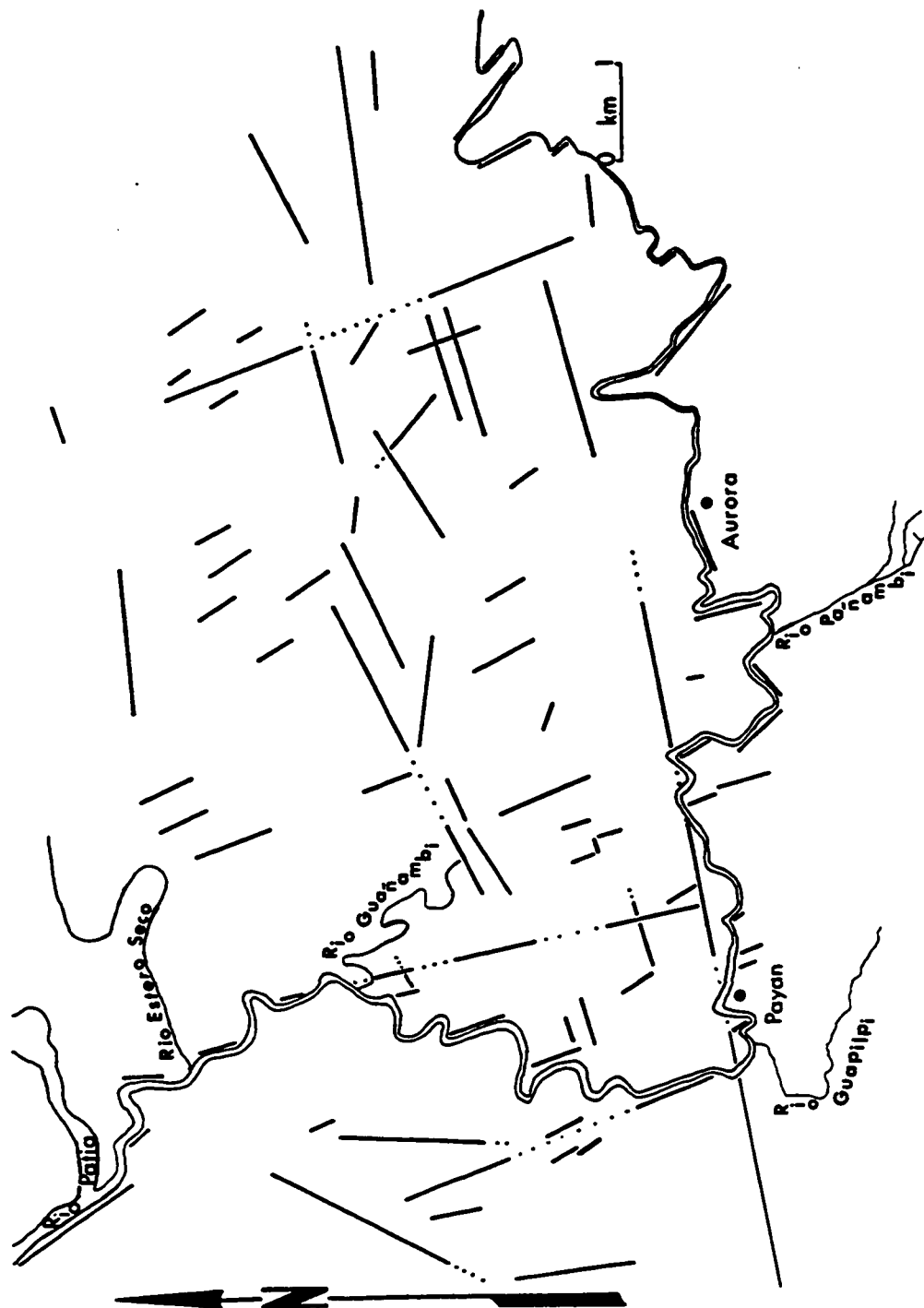
Figure 11. Plot of radius of curvature (R_c) for individual meanders on the Rio Magui between Payan and the Rio Patia. The dotted line separates values from meanders which are deflected by terraces from those meanders which are not deflected. (Modified after Darby and Whittecar, 1984a).

other (see straight stretch on Plate 2). Several relatively straight stretches exist along the Rio Magui (see Plates 1-6), perhaps the most obvious being the straight segment on the Agua Derecho Quadrangle (see Plate 2) which is 13 times as long as it is wide. Richards (1982) discusses the rarity of uniform, straight natural channels longer than ten channel widths. Langbein and Leopold (1966) suggest that "meandering" is a more probable equilibrium shape than "straight" due to the variability of bank materials and the influence of bank vegetation associated with random bank collapse.

One possible cause for straight reaches along the Rio Magui may be structural control by joints or faults in bedrock transmitted up through Quaternary alluvium. Figure 12 displays all major lineaments (streams, terrace edges) associated with the Rio Magui and surrounding vicinities as plotted from a radar image of S. W. Colombia. This map suggests two major lineament orientations exist: N20W and N75E. Although no faults were seen in the field area, the lineament pattern may reflect regional tectonic stresses along major Andean faults (Arango and Ponce, 1982).

A meandering channel system is inherently mobile as various rates of erosion in neighboring meanders lead to periodic formation of chute cut-offs and neck cut-offs (Fisk, 1947). Chute cut-offs are low-angle meander cut-offs (Figure 13). A chute cut-off is actively forming approximately 1 km upstream of Payan along a portion of the Rio Magui not documented on the accompanying set of bathymetric maps (Plates 1-6). Two neck cut-offs are recognized along the river from Payan to the mouth of the Rio Magui. The first is located approximately 1 km downstream of Payan (see Plate 3) and the second is located on the

Figure 12. Inferred lineament control of topographic elements in the Rio Magui area as mapped from radar imagery of S. W. Colombia. Solid lines are lineaments, dotted lines are inferred. Two orientations are recognized; a primary NE/SW orientation and a secondary NW/SE orientation. The majority of these lineaments seem to control rectilinear drainage segments.



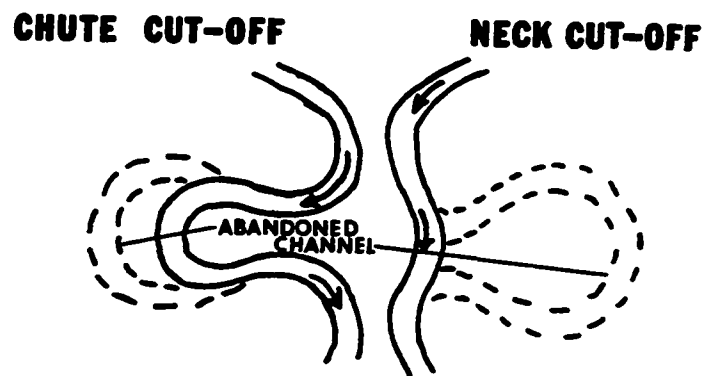


Figure 13. Sketch depicting modes of channel migration. Left figure: chute cut-off, right figure: neck cut-off. (Modified after Allen, 1965).

Horseshoe Meander Quadrangle (see Plate 2) approximately 7 km downstream of Payan. During overbank flows, a portion of the river may travel across the floodplain, by-passing the meander, and eroding chutes or deepening pre-existing swales. As the cut-offs gradually take an increased proportion of the discharge with successive floods, flow in the main channel is reduced resulting in gradual filling by bed load. Later, silts and clays carried overbank by floods fill the abandoned meander. An excellent example of an abandoned meander is shown on the Payan Quadrangle (Plate 1) near the mouth of the Rio Guapilpi.

CHAPTER IV

CHANNEL BAR MORPHOLOGY

The following discussion deals with the morphology of channel bars within the Rio Magui; descriptions will be based on data presented in Table 1. The three major types of channel bars (mid-channel, point and side) vary in terms of length, width, height topography and relief (Figure 14), outline (Figure 15) and the presence or absence of vegetation.

A. Methodology

Channel bar lengths and widths for every major bar along the 40 km study area were measured with a metric tape; bar heights were ascertained with a Brunton compass and pocket alidade. Additionally, oblique aerial photographs taken by ODU personnel from a small helicopter hovering approximately 100 meters above the river proved helpful in distinguishing channel bar shapes.

B. Results

1. Mid-channel Bars

Mid-channel bars typically occur approximately 200 meters downstream of the axial bend of a meander along the Rio Magui, but can also exist in relatively straight segments of the river. Mid-channel bars represent the largest of the three channel bar types examined in the study area, with an average length of 95.3 meters, average width of 27.9 meters, and an average height of 1.6 meters (n=11). Mid-channel bars display a marked decrease in length, width and height downstream. As seen from Figure 16, the length of mid-channel bars decreases uniformly from the village of Aurora downstream

Table 1. Characteristics of river channel bars within the Rio Magui. All dimensions are in meters. Cross-sectional and plan-view shapes described in Figures 15 and 16. Bar notation as follows: MCB (mid-channel bar), PB (point bar), SB (Side Bar).

Bar	Length	Width	Height	Lon. X-sec.	Lat. X-sec.	Planar outline	Vegetated	Stage Flooded
MCDA1	113.9	38.2	1.0	Convex	Flat-topped	Diamond	No	3/4 Bank-Full
MCDA2	30.3	18.2	1.5	Convex	Domed	Elliptical	Yes	Bank-Full
MCBA3	100.0	26.4	1.5	Convex	Domed	Elliptical	Yes	Bank-Full
MCBA4	85.0	21.0	1.5	Convex	Domed	Teardrop	Yes	Bank-Full
MCBA6	151.0	57.0	4.0	Domed	Undulatory	Tooth	Yes	Never
MCB1	270.0	30.0	3.0	Convex	Domed	Elliptical	Yes	Bank-Full
MCB2	72.0	24.0	1.0	Convex	Flat-topped	L-Shaped	No	3/4 Bank-Full
MCB3	81.5	21.0	1.0	Convex	Flat-topped	Teardrop	No	3/4 Bank-Full
MCB4	54.0	29.0	1.0	Convex	Flat-topped	Tooth	No	3/4 Bank-Full
MCB5	30.0	9.4	1.0	Convex	Convex	Elliptical	No	1/2 Bank-Full
MCB6	60.6	13.6	2.0	Convex	Domed	Elliptical	Yes	Bank-Full
RFMCB1	333.0	121.0	2.0	Convex	Undulatory	Tooth	Yes	Never
RFMCB2	159.0	48.5	2.0	Convex	Undulatory	Tooth	Yes	Never
PBA1	60.6	19.7	1.0	Convex	Convex	Lunate(a)	No	3/4 Bank-Full
PB1	50.0	40.0	1.0	Convex	Inclined	Lunate(a)	No	3/4 Bank-Full
PB4	45.5	6.4	1.0	Convex	Inclined	Lunate(a)	No	3/4 Bank-Full
PB5	49.0	4.5	1.0	Convex	Inclined	Lunate(a)	No	3/4 Bank-Full
PB6	30.0	7.8	1.0	Convex	Inclined	Lunate(a)	No	3/4 Bank-Full
PB7	60.6	7.0	1.8	Convex	Inclined	Lunate(a)	No	3/4 Bank-Full
SBA1	75.0	13.0	4.0	Convex	Flat-topped	D-Shaped	No	Bank-Full
SBA1'	121.2	22.7	1.0	Convex	Inclined	D-Shaped	No	3/4 Bank-Full
SBA4'	90.9	57.0	1.5	Convex	Inclined	D-Shaped	No	3/4 Bank-Full
SBA5	15.7	4.8	1.0	Convex	Inclined	D-Shaped	No	1/2 Bank-Full
SB1	51.0	9.0	1.5	Convex	Inclined	D-Shaped	No	1/2 Bank-Full
SB2	30.0	11.0	1.0	Convex	Inclined	D-Shaped	No	1/2 Bank-Full
SB3	61.0	10.0	1.0	Convex	Inclined	D-Shaped	No	1/2 Bank-Full
SB4	58.0	7.0	2.0	Convex	Inclined	D-Shaped	No	1/2 Bank-Full
SB5	30.0	3.3	2.0	Convex	Inclined	D-Shaped	No	1/2 Bank-Full
SB6	54.0	7.0	1.0	Convex	Inclined	D-Shaped	No	1/2 Bank-Full
SB7	60.6	3.6	2.5	Convex	Inclined	D-Shaped	Yes	3/4 Bank-Full
SB8	64.0	7.6	2.5	Convex	Inclined	D-Shaped	Yes	3/4 Bank-Full
SB9	60.6	12.7	1.5	Convex	Inclined	D-Shaped	No	1/2 Bank-Full
SB10	60.6	6.4	1.5	Convex	Inclined	D-Shaped	No	3/4 Bank-Full
SB11	50.3	8.2	1.0	Convex	Inclined	D-Shaped	No	3/4 Bank-Full

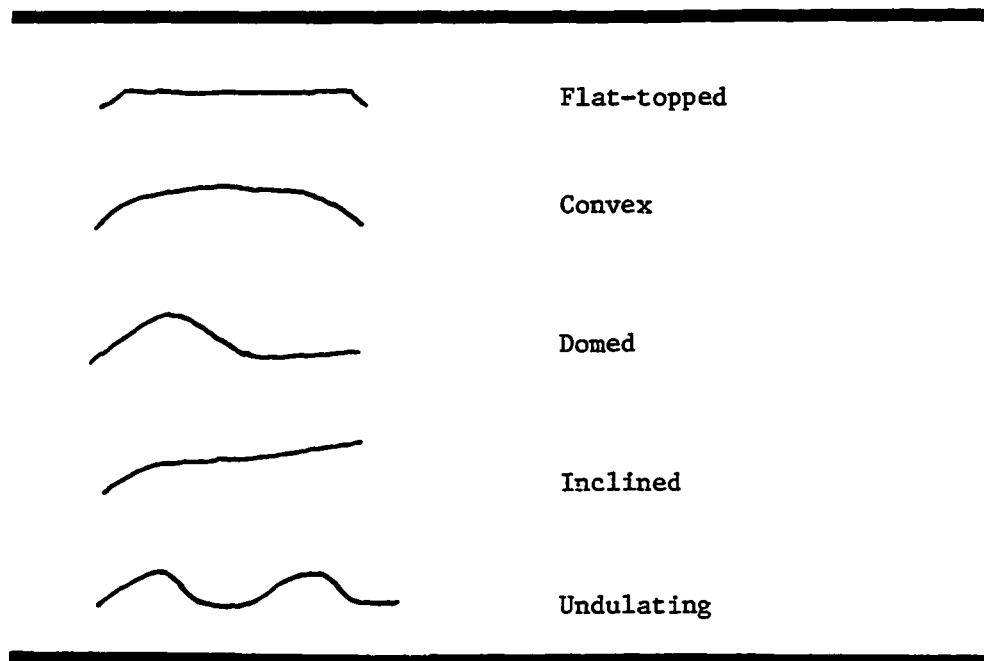


Figure 14. Cross-sectional (longitudinal and lateral) view of surface topography on channel bars within the Rio Magui.

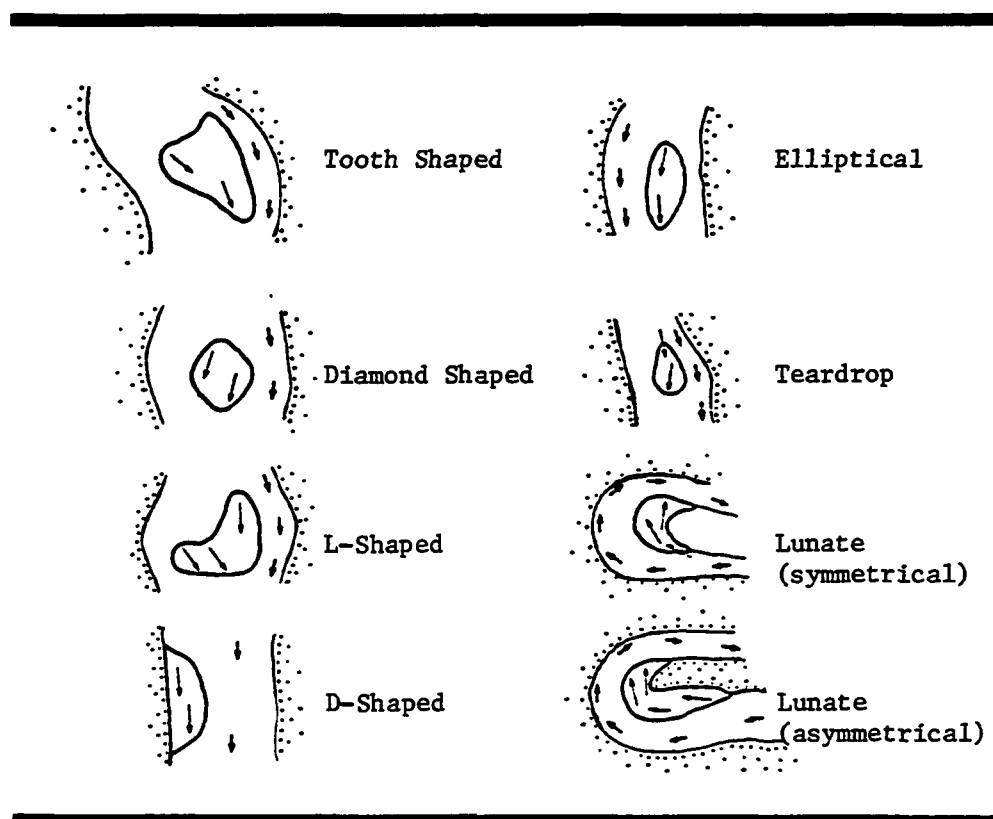


Figure 15. Sketch depicting planar view of shape and configuration of river channel bars with respect to channel walls within the Rio Magui. Short arrows show thalweg location at 1/2-bank-full flow, longer arrows show flow over the bar at 3/4-bank-full flow.

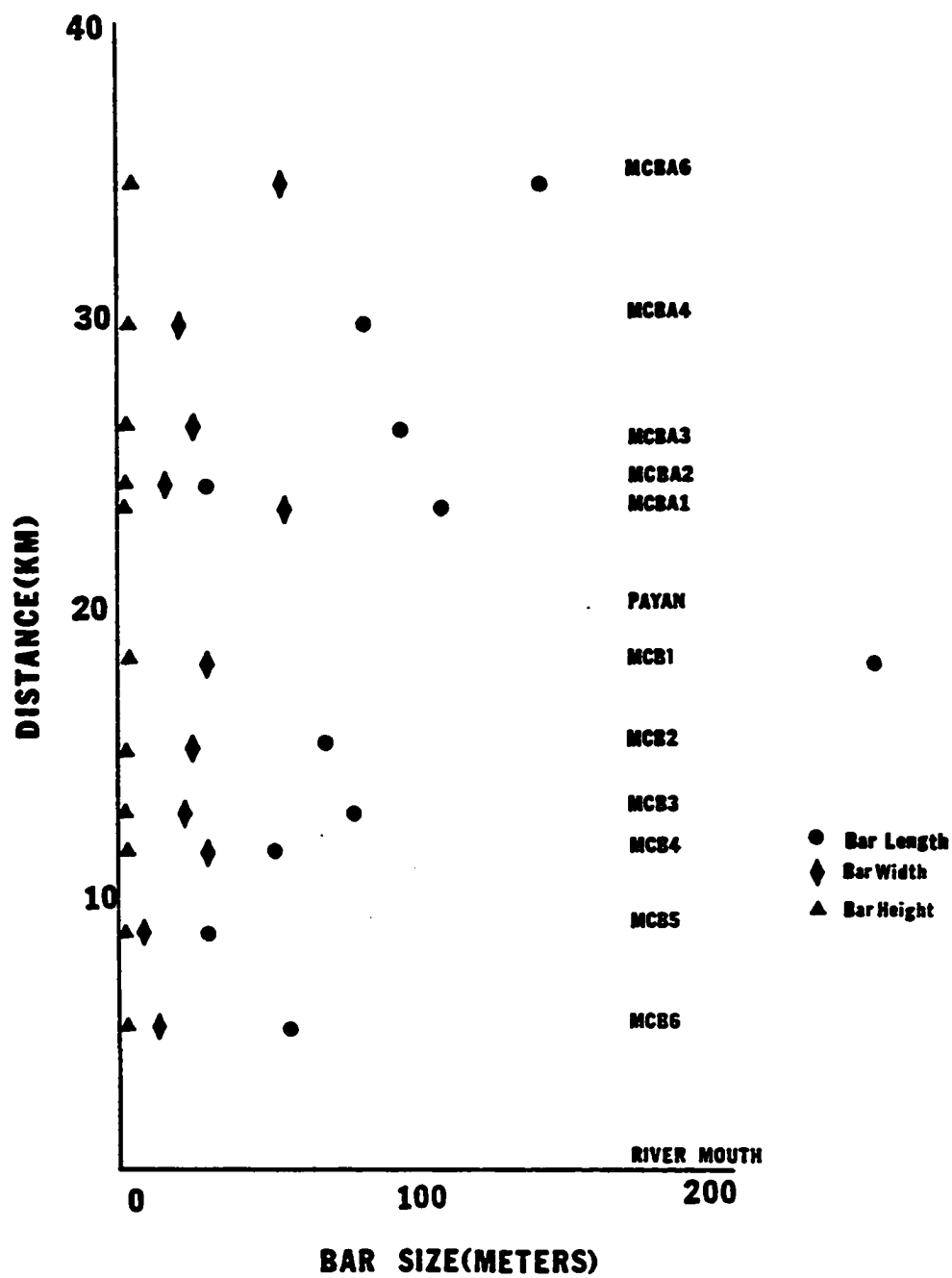


Figure 16. Plot of size characteristics for all mid-channel bars along the Rio Magui.

to the mouth of the Rio Magui with the exception of Mid-channel bar 1. Width and height characteristics of mid-channel bars uniformly decrease downstream. All mid-channel bars have a convex longitudinal cross-sectional profile. Many mid-channel bars are flat-topped and dome-shaped in lateral cross-section and very rarely undulatory and convex. Mid-channel bars exhibit a wide variety of shapes (Figure 15) in planar view. Many of these bars are elliptical and tooth-shaped, a few are teardrop-shaped and one example exists of both a diamond-and L-shaped bar.

Vegetation consisting primarily of low-lying grasses, reeds and short trees approximately 3 meters tall covers the middle to downstream portion of most mid-channel bars (Figure 17). This vegetation usually remains emergent at 3/4-bank-full stage, only to become submerged at near bank-full flow conditions. Three bars along the Rio Magui display vegetation which is always emergent.

2. Point Bars

The sediment body enclosed by the meander loop is termed the point-bar. It has an essentially horizontal upper surface at about the level of the surrounding floodplain and slopes gradually along its channel margin, towards the thalweg (Reading, 1978). Point bars represent the shortest river channel bar on the Rio Magui, attaining an average length of 49.2 meters, average width of 14.2 meters, and an average height of 1.1 meters ($n=7$). Point bar length generally decreases downstream (Figure 18); however, point bar 7 which is located nearest to the mouth of the Rio Magui is equally as long as point bar A1 upstream of Payan, which coincidentally is one of the longest point



Figure 17. Photograph of Mid-channel Bar 1, 1 km downstream of the village of Payan in a transitional form. A narrow chute towards the extreme right of the photograph is slowly aggrading and will eventually fill-in and form a side bar. Flow is from background to foreground, and river height is approximately 1/2-bank-full. Vegetation in the middle of the bar is approximately 3 meters high. Pig for scale (crossing river).

bars documented along the study area. Point bar width decreases from 2 kilometers upstream of Payan to several kilometers downstream of Payan and then begins to increase towards the mouth of the Rio Magui. Point bar height remains relatively unchanged from all localities with the exception of point bar 7 (located nearest to the river mouth) which is somewhat higher in elevation. All point bars have a convex longitudinal cross-sectional profile. Most point bars have an inclined lateral profile although one bar does display a convex lateral cross-sectional profile. The most frequent shape and configuration of these point bars as seen in planar view is an asymmetrical lunate shape, which contains little or no vegetation (Figure 19). Most point bars are emergent at 1/2-bank-full stage and become flooded at 3/4 or greater bank-full flow.

3. Side Bars

Side bars along the Rio Magui occur primarily on the downstream convex side of meanders but can also exist along straight segments of the river. As described on other rivers by Reading (1978) and Collinson (1970), side bars along the Rio Magui develop on the inside of the thalweg where it meanders within the confines of a straight channel, in contrast to point bars which occur along the meander loops. Side bars within the Rio Magui attain an average length of 58.6 meters, average width of 12.1 meters, and an average height of 1.6 meters (n=16). Length and width characteristics generally decrease downstream for all side bars (Figure 20), although bar height tends to increase with downstream direction. All side bars along the Rio Magui display a convex longitudinal profile, an inclined, lateral cross-

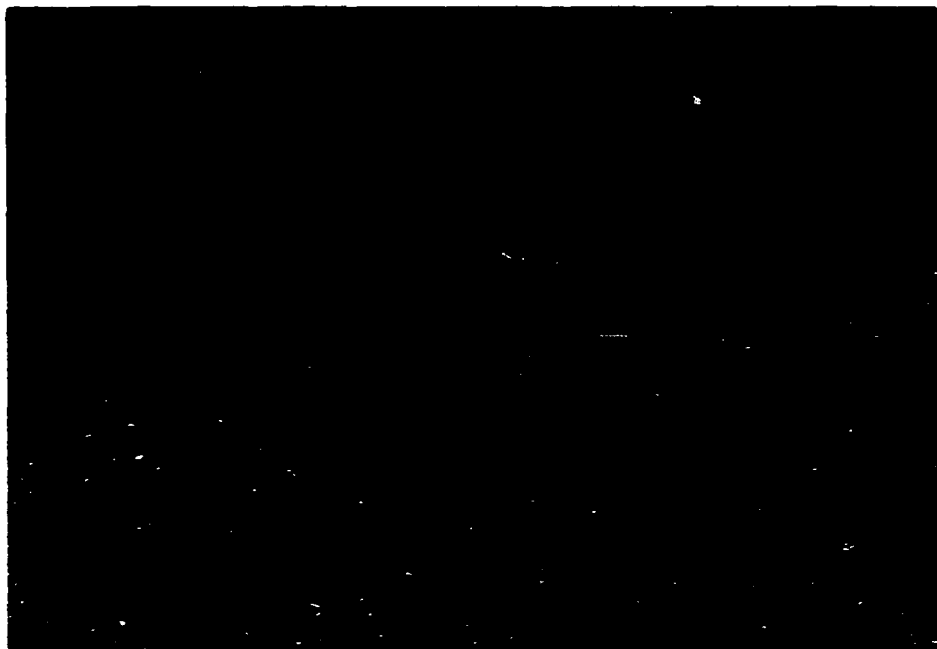


Figure 19. Photograph of Point Bar 1 approximately 1 km downstream of the village of Payan. This bar is laterally inclined (left to right) and displays a gravel lag which was covered by sand at waning flow. Flow is low (less than 1/4-bank-full stage); flow is from left to right. Note the lack of vegetation characteristic of all point bars of the Rio Magui.

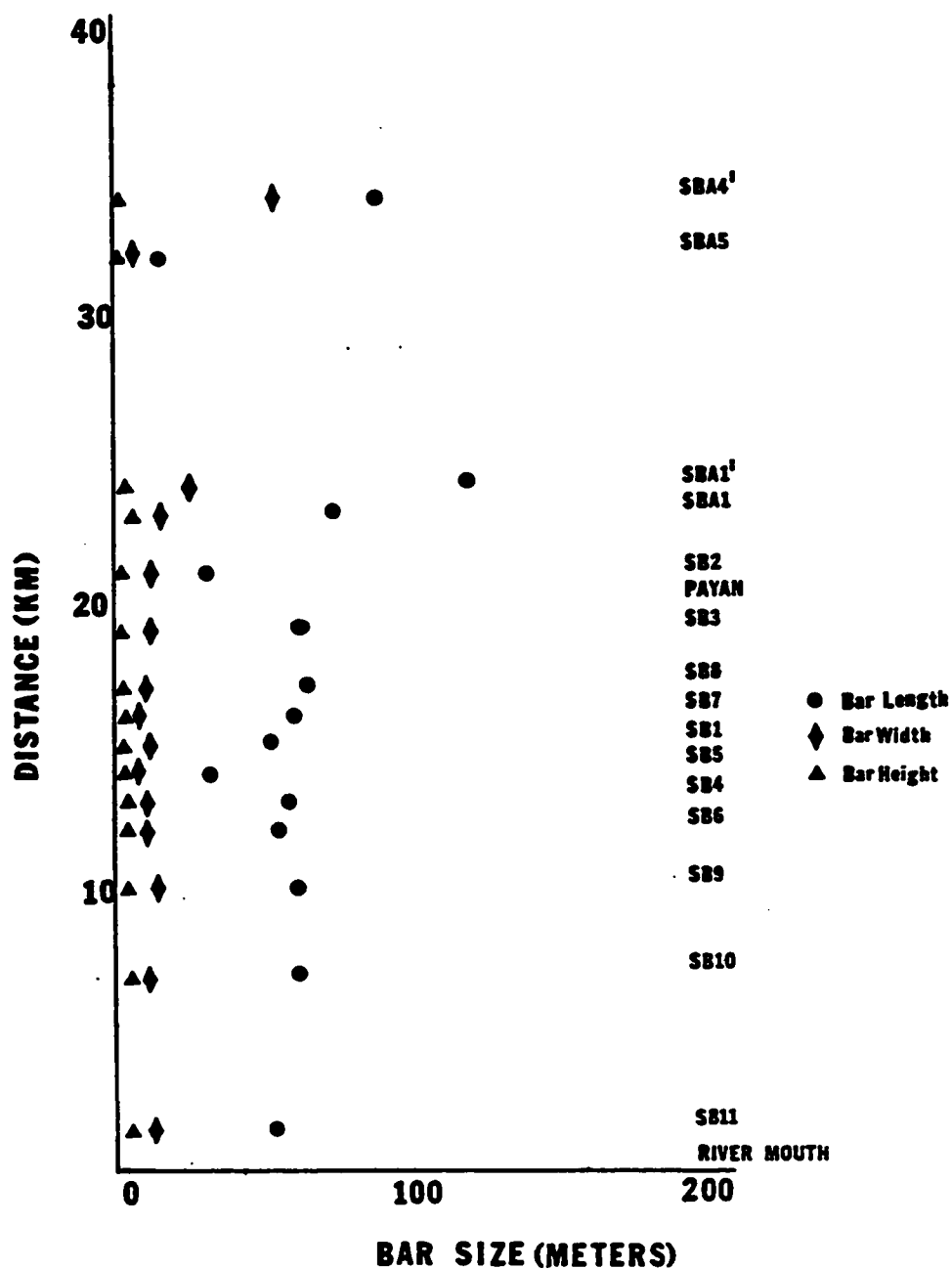


Figure 20. Plot of size characteristics of all side bars along the Rio Magui.

sectional profile, and are D-shaped in plan view. Little or no vegetation grows directly on the surface (Figure 21). Because side bars hug bank edges, the canopy of the surrounding jungle may overlap the side bars which suggests a false impression of vegetation growing on the bar. Side bars are normally emergent at low water conditions (1/4-bank-full stage) up through 1/2-bank-full flow although some larger side bars are emergent up through 3/4-bank-full flow.

C. Discussion

In order to better understand why channel bars form, it is essential to determine the flow patterns under which material is actively transported and subsequently deposited. The growth and development of mid-channel bars is closely tied to the formation of coarse-grained riffles by secondary circulation patterns (Figure 22) (Richards, 1982). During high-flow conditions, riffles form at points of divergent surface flow. At depth, this flow pattern converges and aggrades sediment in a submerged mound in the center of the channel. During low-flow conditions the riffles become coarse-grained obstacles which the river must cross; at riffles rivers usually display rapid, shallow flow with a steep water surface gradient and resemble a broad-crested weir (Richards, 1978) which dams the flow back into the upstream pool.

Under low-flow conditions, pools are slow-forming deep areas that display a gentle surface slope and sandy beds (Richards, 1982). During high-flow conditions, however, pools are formed by scouring on the bed by convergent flow cells. At the water's surface, floating material such as leaves and wood debris can collect in the shallow mid-channel depression where convergent flow meets and descends; at depth, high

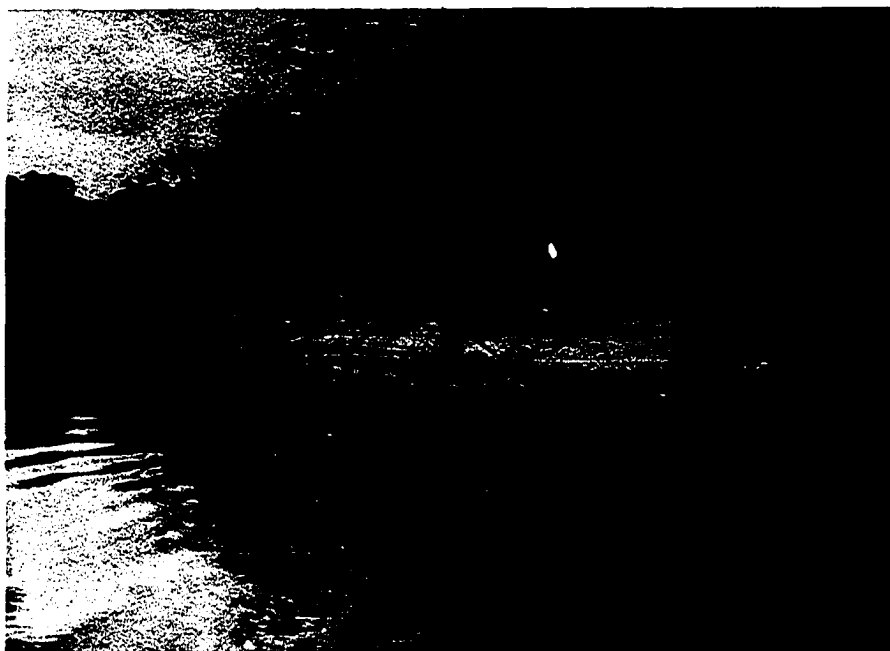


Figure 21. Photograph of Side Bar 9 approximately 8 km downstream of the village of Payan. Flow is from foreground to background at approximately 1/2-bank-full stage. Lateral water marks on the side bar were formed by winnowing during declining flow levels. Note the apparent lack of vegetation that is characteristic of nearly all side bars along the Rio Magui. Villager in dug-out canoe for scale.

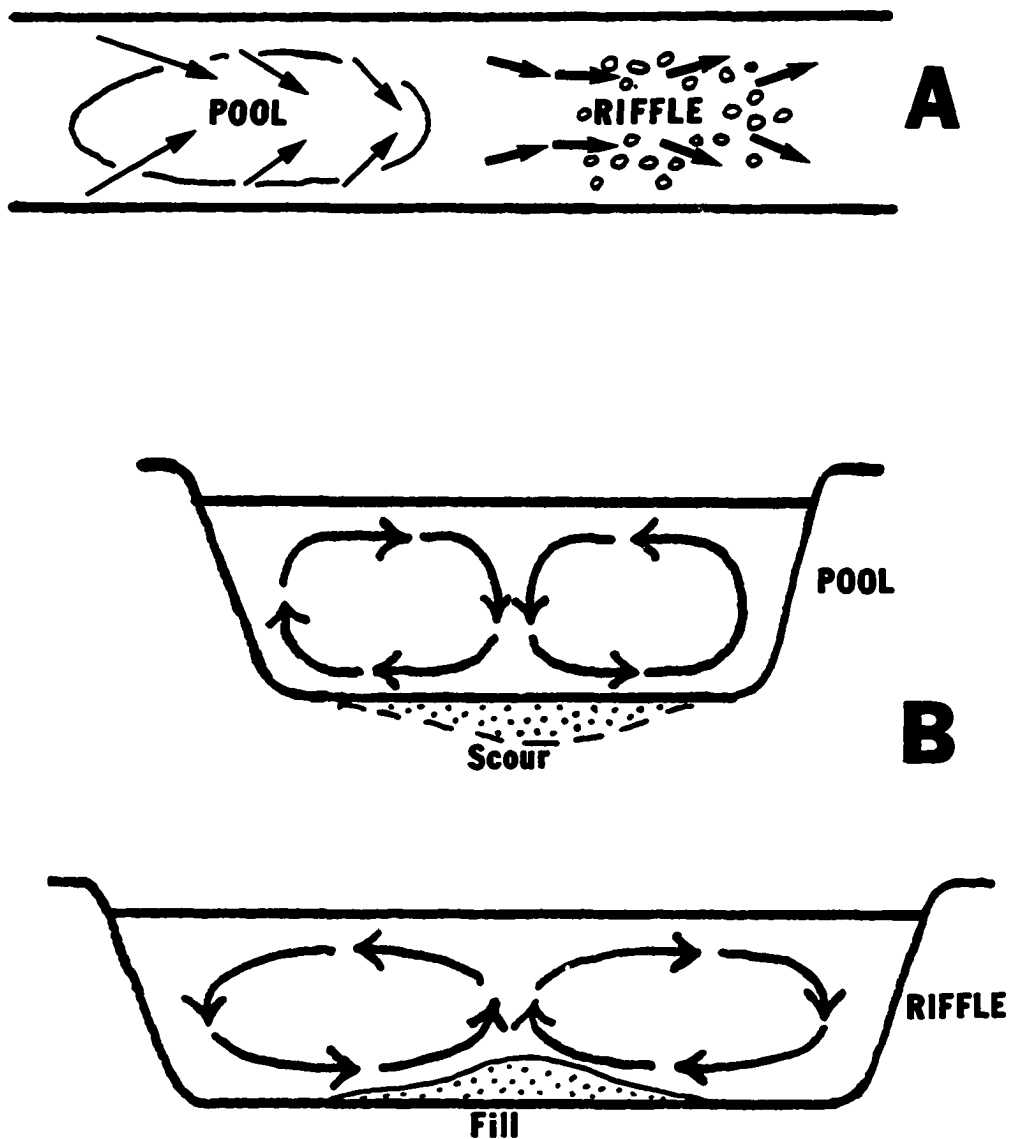


Figure 22. A. Plan view of surface flow in pools and riffles, in a straight reach of a stream. B. Cross-sectional view of symmetric secondary circulation patterns in a pool and riffle (modified after Richards, 1982).

discharge flow diverges, scours and can remove most sediment transported by the stream except for a coarse gravel lag which is eventually buried by sand during waning- and low-flow conditions (Hack, 1957; Lisle, 1979).

The amount of sediment available for transport is a direct function of the flood magnitude—higher discharges yield greater transport of bed-load material (Leopold et. al., 1964). In most streams, riffles form from pebbles and cobbles eroded from or transported across pools during high-flow periods. Particles may be transported off of riffles onto bars downstream but the position of the riffle will not change until the secondary circulation cells migrate. In reaches where the rate of accumulation of particles exceeds the rate of removal, the riffle may develop into a mid-channel bar.

As mentioned earlier, channel bars along the Rio Magui exhibit a variety of sizes and shapes. Because of lower flow velocities towards the mouth of the Rio Magui, less coarse-grained material is transported and subsequently deposited, which may account for the general decrease in size characteristics of all channel bars with downstream distance. Unfortunately, little data is available which might offer an explanation for the diverse bar shapes which exist for the Rio Magui channel bars. It appears that the specific shape of a channel bar is dependent upon the extent and influence of pools and riffles, and patterns of secondary circulation in progress during various stages of high-flow conditions. Thus, the morphologic outline of channel bars along the Rio Magui appears to be an on-going ever-changing process.

CHAPTER V

CHANNEL BAR SEDIMENTARY STRUCTURES

Two classes of sedimentary structures will be discussed in this thesis: 1) Sand waves and ripples visible on the surface of channel bars and 2) Cross-bedding seen on cleaned walls of bar trenches and levee cuts. The following discussion will describe ripples and sand waves characteristics of channel bars along the Rio Magui. Low-velocity conditions will be discussed first by citing examples from other authors and including photographs and illustrations depicting the bedding on channel bars of the Rio Magui. This organizational scheme will also be employed to discuss medium- and high-flow conditions.

Specific identifying labels are given in figure captions to indicate where each feature occurs (an example is SB3, which stands for Side Bar no. 3). Figure 23 illustrates the location of specific bars discussed in this thesis.

A. Methodology

Channel bars along the Rio Magui were trenched whenever water levels permitted. Trenches on large channel bars with low water tables were generally 2 meters long, 1 meter wide, and 1 meter deep. Field notes, sketches and photographs detailed the structures exposed in vertical trench walls for subsequent depositional interpretations.

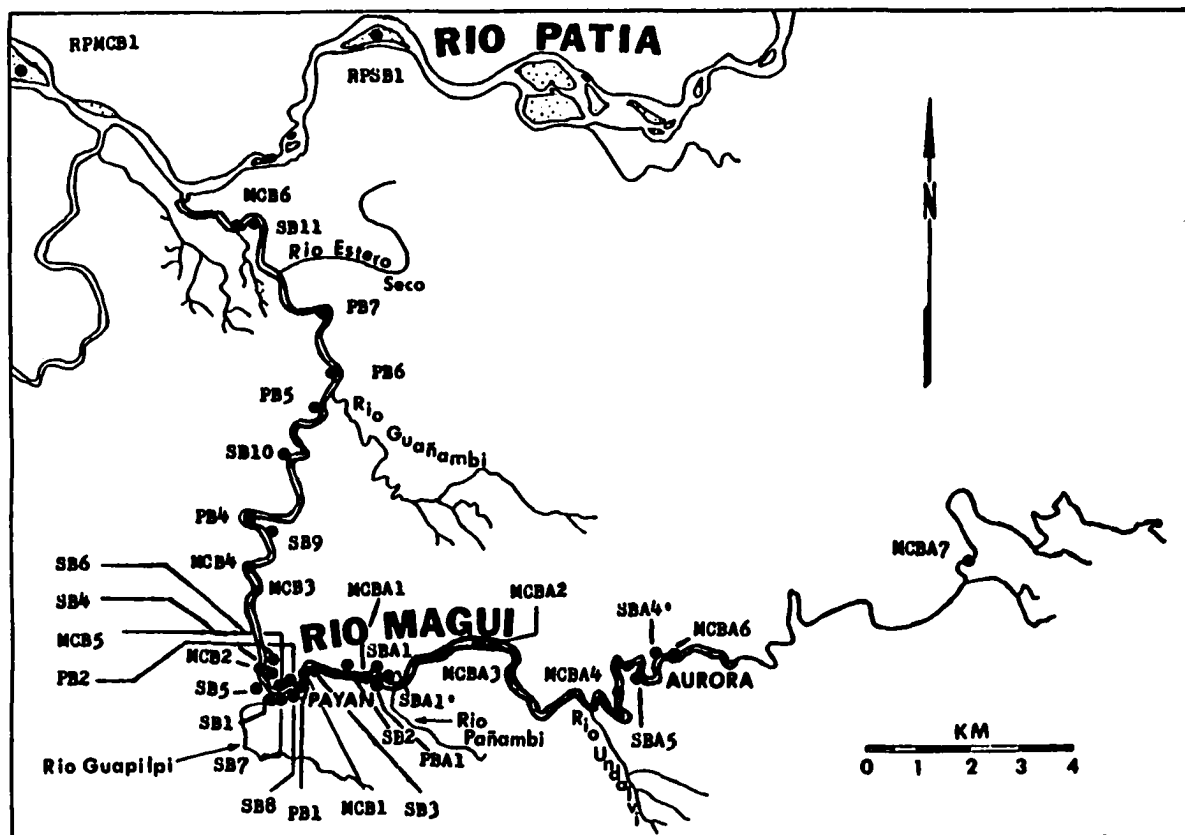


Figure 23. Map showing location of mid-channel, side and point bars examined in the study area.

B. Results

1. Surface Features

Straight-crested ripples exhibit linear parallel crests typically 40-50 cm in length (Figure 24). Average grain size of the sand comprising straight-crested ripples is 2.5 ϕ but can range from 2 to 3 ϕ . Straight-crested ripples are typically found on the downstream portion of channel bars and form at low velocity conditions during the waning stages of high flow (Harms, 1969).

Many bars exhibit current ripples known as undulatory ripples (Figure 25). These ripples are small bedforms typically 35-40 cm in length with gentle upstream slopes and steep downstream slopes (Raudkivi, 1963). Grain size of the sand comprising these ripples is 2.5 ϕ but can be slightly finer or coarser. Undulatory ripples are formed on the middle to downstream portion of all types of river channel bars. These ripples form at velocities ranging between low-energy (as required for straight-crested ripples) and higher energy (as required for lingoid and lunate ripples) flow conditions (Reineck and Singh, 1975).

A distinctive type of current ripple present on the surface of the river bars of the Rio Magui is lingoid ripples (Figure 26). Lingoid ripples display discontinuous, highly sinuous crests exhibiting a three-dimensional outline and tongue-shaped appearance whose horns point into the current (Gary, et. al., 1972). Usually these ripples have asymmetrical profiles (Collinson and Thompson, 1982), exhibit steep, concave-upwards lee faces and more gently sloping convex-upwards stoss sides, indicative of unidirectional currents.

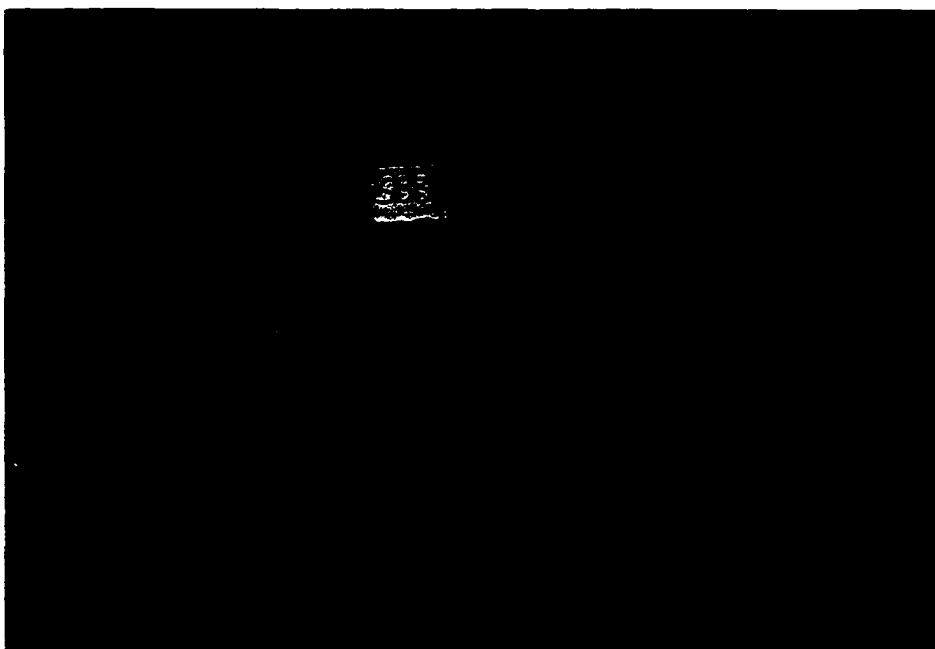


Figure 24a. Photograph of sandwave and ripples on central portion of Side bar 3. Sand waves indicative of high-flow conditions originating from the top left to the bottom right. As flow velocity diminishes, a change in flow direction forms the straight-crested ripples which line the crests and troughs of the sand waves. The flow direction which formed the straight-crested ripples is from bottom left to top right. As flow velocity continues to subside, muds are deposited in the troughs of the straight-crested ripples. Scale is extended to 43 cm.

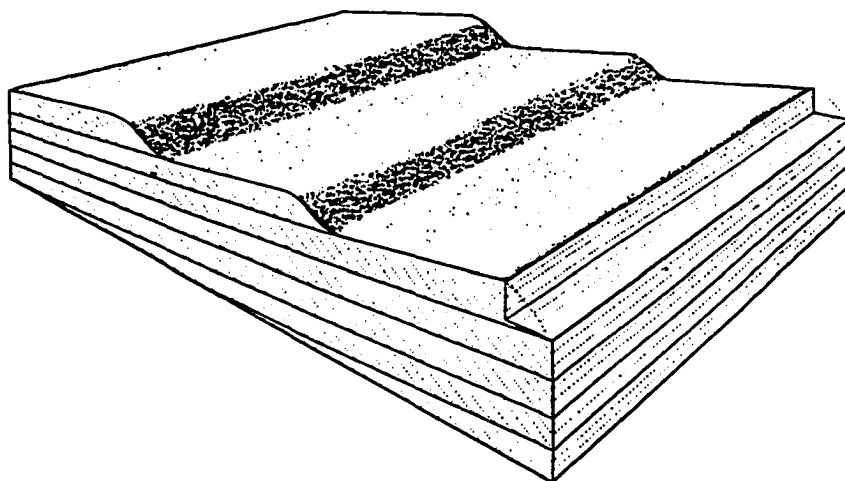


Figure 24b. Block diagram showing cross-bedding produced by migration of straight-crested ripples. The cross-bedded units are planar in character (from Reineck and Singh, 1975).

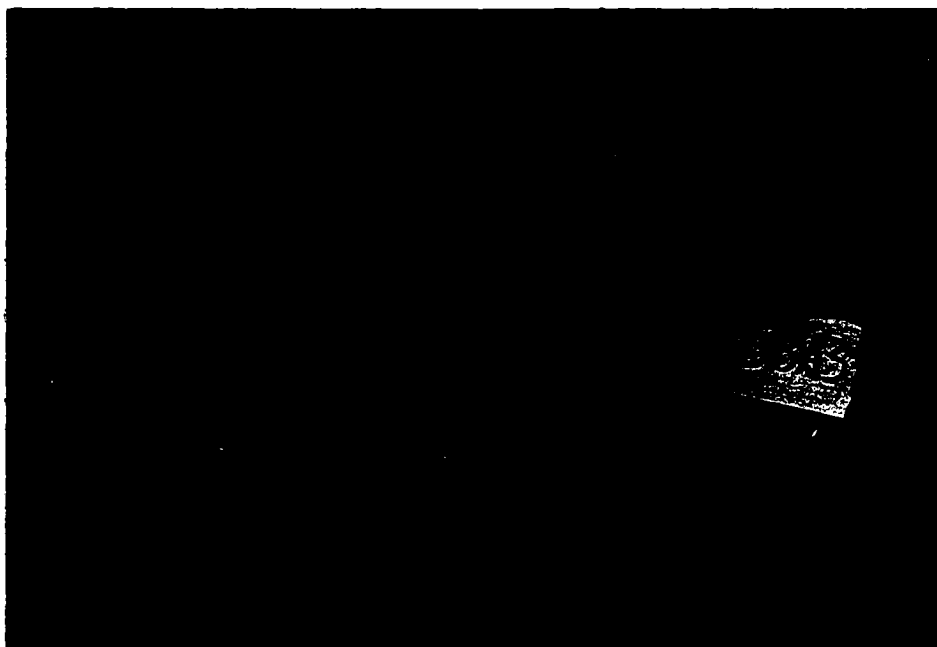


Figure 25a. Undulatory ripples on the upstream portion of Side bar A3 representing transitional forms between straight-crested and lingoid ripples. Flow is from bottom to top. Bamboo stick in background is 40 cm long.

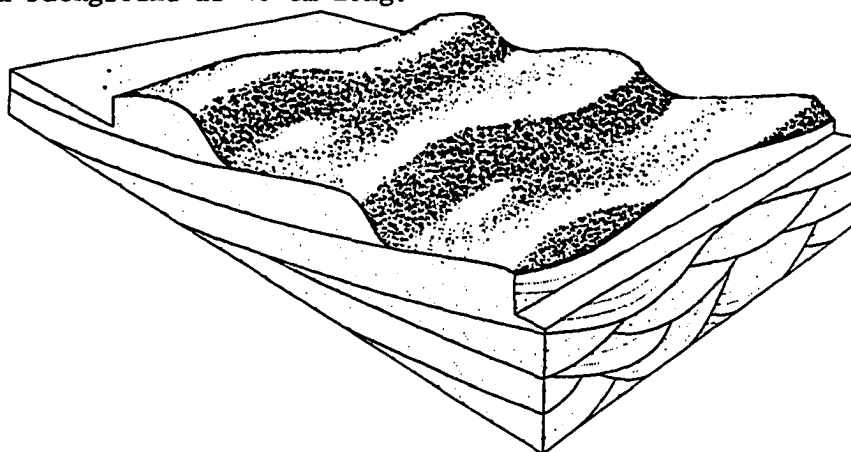


Figure 25b. Block diagram showing cross-bedding produced by migration of undulatory ripples. The cross-bedded units are weakly festoon-shaped. In the front view the lower units are strongly trough-shaped (from Reineck and Singh, 1975).

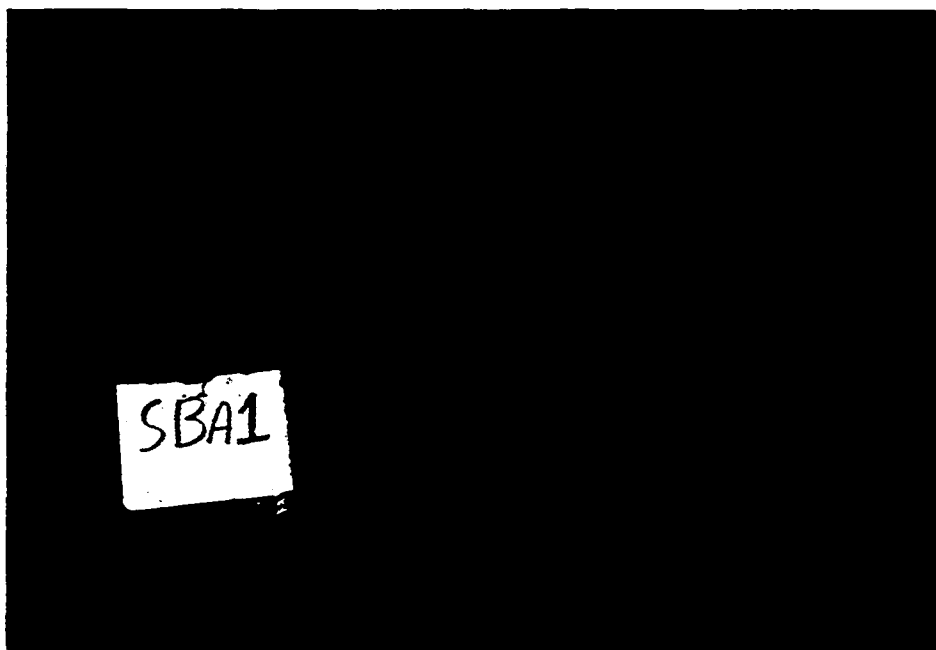


Figure 26a. Lingoid ripples on the downstream portion of Side bar A1. Note the accumulation of heavy minerals lining the top of the crests. Flow direction is from bottom right to top left. Hand lens for scale.

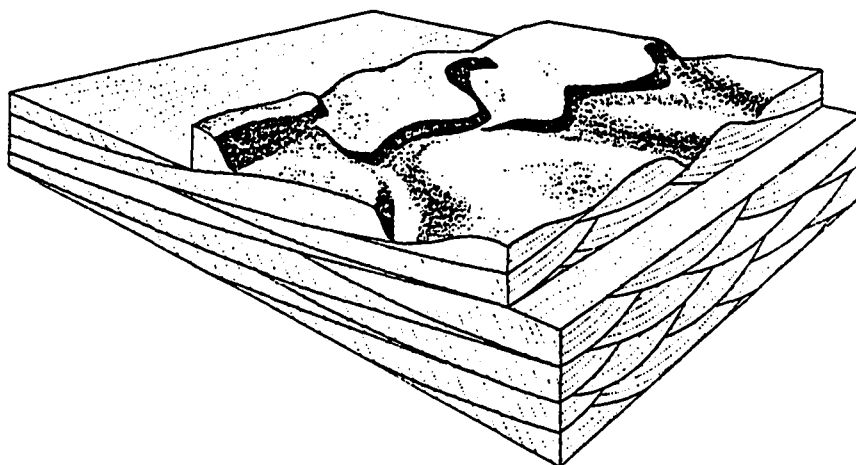


Figure 26b. Block diagram showing cross-bedding produced as a result of migrating lingoid ripples. Cross-bedded units are strongly festoon-shaped (from Reineck and Singh, 1975).

Typically these lingoid ripples are 40 cm long from horn to horn. Average estimated grain size of the sand comprising the lingoid ripples is 2Ø but can range between 1.5Ø-2.5Ø. Lingoid ripples are often found on the mid-to-downstream portion of channel bars and produced at velocities higher than that needed to produce straight-crested or undulatory small ripples (Reineck, 1963). Reineck and Singh (1975) state that it is unclear under what conditions lingoid ripples are replaced by lunate ripples and discuss the difficulty in distinguishing lingoid ripples from lunate ripples which also produce similar types of cross-bedding (festoon-shaped trough cross beds). Allen (1963) and Tanner (1960) both indicate that the only distinction between lingoid and lunate ripples is the topographic form of the ripple crests. Conybeare and Crook (1968) explain that lunate ripples have horns which point downstream in contrast to the lingoid ripples described earlier.

Several large surface structures exist on channel bars of the Rio Magui. Sand waves are relatively straight to sinuous large bed-forms containing uniform scours in their troughs, typically spaced 5-100 meters apart (Harms et. al., 1975). The sand wave detailed previously in Figure 24a extends to 2.5 meters in length and approximately 0.75 meters in width. The average crest to crest distance for sand waves is 1.5 meters. Average grain size of the sand comprising sand waves on the Rio Magui is 1.5Ø but can range from 1.0-2.0Ø. Sand waves are typically located in the mid-to-downstream portion of all types of channel bars on the Rio Magui, and develop at relatively high flow conditions. Harms et. al., (1975) suggest that sand waves form between 35 and 75 cms-1, before maximum river flow. As

flow conditions diminish along the Rio Magui, smaller straight-crested ripples form in the troughs and on the crest tops of the sand waves, perpendicular to the previous high-stage which initially formed the sand waves. Harms and Fahnestock (1965) and Collinson and Thompson, (1982) describe similar examples where changes in flow direction superimpose small scale ripples on top of larger, previously formed megaripples. It is equally interesting to note the presence of cracked mud drapes (Figure 24a) that form during waning moments of the flow, lining the troughs of the straight-crested ripples.

Lunate megaripples are another large surface feature found in channel bars of the Rio Magui (Figure 27). These ripples are often termed D-shaped megaripples because they fail to exhibit continuous crests (Hantzschell, 1938). Lunate megaripples on the Rio Magui often exceed one meter in length, 0.75 meters in width, and have an average crest to crest distance of 0.8 meters. Average grain size of the sand comprising the lunate megaripples is 1.5 ϕ but can range from 1.0-2.0 ϕ . As with most of the previously described ripples, lunate megaripples are found on the middle to downstream portion of channel bars. Little specific information exists in the literature describing flow velocities for lunate megaripples. Reineck and Singh (1975) do state however that lunate megaripples form at higher velocities than straight-crested ripples.

All of the previously mentioned sedimentary structures form on the middle to downstream portion of the channel bars. The coarse, cobbly texture of the upstream portions of the majority of the channel bars tends to inhibit ripple or megaripple formation.



Figure 27a. Lunate megaripples on the downstream portion of Mid-channel bar A4. Flow direction is from right to left. Scale is extended to 1 meter.

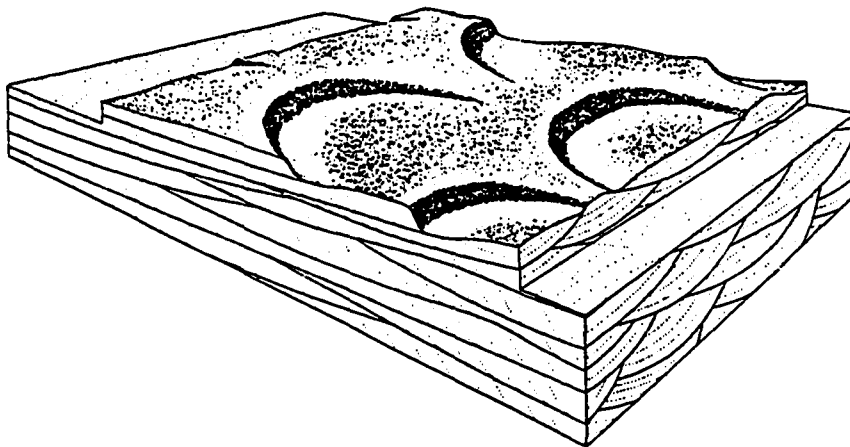


Figure 27b. Block diagram showing cross-bedding produced by migration of lunate megaripples (from Reineck and Singh, 1975).

One final surface feature commonly seen on the edges of channel bars is the concentration of heavy minerals winnowed by waning flows (Figure 28).

Much information exists in the literature regarding the depositional processes for heavy mineral laminations in a marine environment (Blatt et. al., 1980; Clifton, 1969; Ljunggren and Sunborg, 1968). Surprisingly, little data exist for these processes active in a fluvial environment.

Heavy mineral laminations accumulate on the edges of all types of channel bars along the Rio Magui. As flow decreases during the waning stages of a flood, high density minerals are winnowed out by the removal of the light minerals along surficial bar sediments and form thin laminations along the water line of a channel bar. Sediment accumulations called sand shadows consisting of heavy minerals immediately downcurrent of large clasts are common along the surface of many channel bars.

2. Cross-Bedding

Two major classifications of cross-bedding are recognized in the study area. The first is planar cross-bedding which is characterized by planar bounding surfaces as described by McKee and Weir (1953), and diagrammatically represented in Figure 29. The second major classification of cross-bedding is trough cross-bedding characterized by curved, trough-shaped bounding surfaces (Potter and Pettijohn, 1963), as shown in Figure 30.

Several specific types of cross-bedding are produced in the Rio Magui system, the most common being small ripple cross-



Figure 28. Winnowed concentration of heavy minerals along the edges of the downstream portion of Mid-channel bar 1. Flow direction is from bottom to top. Paper is 18 cm long for scale.

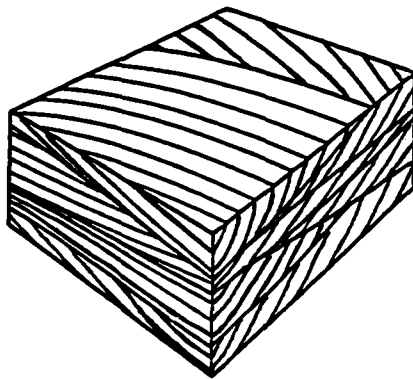


Figure 29a. Block diagram showing planar cross-bedding. Units are tabular to wedge-shaped; bedding surfaces are planar (from Reineck and Singh, 1975).

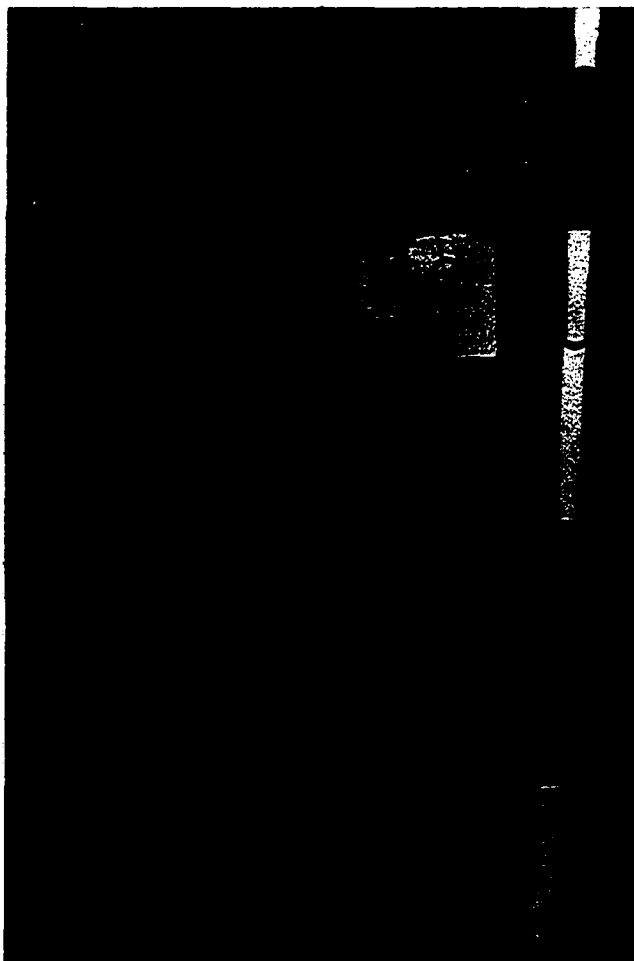


Figure 29b. Planar cross-bedding as seen in trench "B" of Side bar 9. Bedding is parallel to present flow of river and trench "B" is located on the downstream portion of the bar. The white segments of the scale are 20 cm in length.

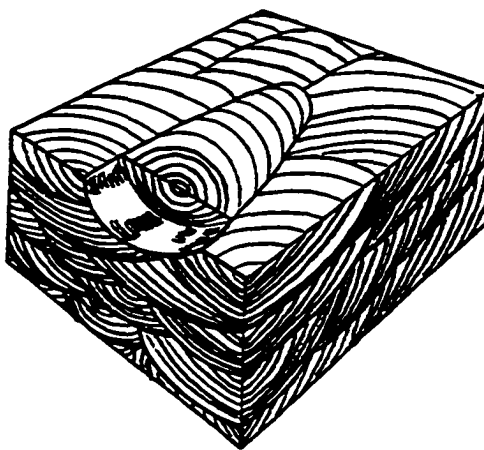


Figure 30a. Block diagram showing trough cross-bedding as seen in horizontal, transverse and longitudinal sections. Units are festoon-shaped. In transverse section troughs are well developed, with strongly curved bedding surfaces (from Pettijohn, 1957).

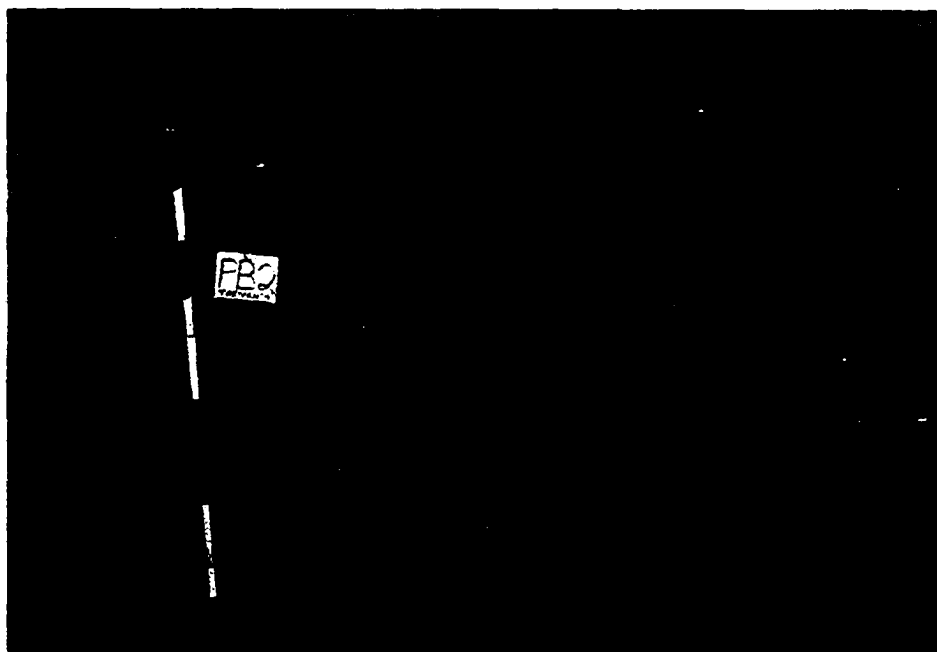


Figure 30b. Trough cross-bedding as seen in trench "A" of Point bar 2. Bedding is perpendicular to present flow of the river and trench "A" is located on the downstream portion of the bar. The white segments of the scale are 20 cm in length.

bedding (Figure 31). Reineck (1963) described upper point bars as typical localities to observe small ripple cross-bedding. Reineck states that usually this cross-bedding is festoon-shaped and formed by lingoid ripples but may be planar in nature (Figure 31) as formed by straight-crested ripples.

Cross-bedded units composed of foreset laminae produced as a result of migration of large current ripples are called megaripple bedding (Reineck and Singh, 1975). Figure 32 displays this variety of cross-bedding, common to all types of river channel bars of the Rio Magui. Megaripple bedding is primarily differentiated from small ripple bedding by its size (amplitude is greater than 4 cm) (Reineck, 1963).

Cross-bedding is generally absent in the levee exposures along the Rio Magui. A massive, homogeneous accumulation of mottled grey to brown mud appears in all levee exposures, although planar laminations of fine-to-very fine sand (2.5-3.5 ϕ) are exposed infrequently between the mottled, homogeneous muds (Figure 33).

3. Variations in Sedimentary Structures

Thus far, I have discussed what types of ripples exist along the Rio Magui channel bar surfaces and how they are represented in the form of cross-bedding as viewed from trench walls. At this point, I will document where specific sedimentary structures exist along the three main types of channel bars (mid-channel, point and side) with special consideration given to analyzing the change in structures within one channel bar and also with respect to downstream changes (if any) from bar to bar.

Mid-channel bars that could be studied along the Rio

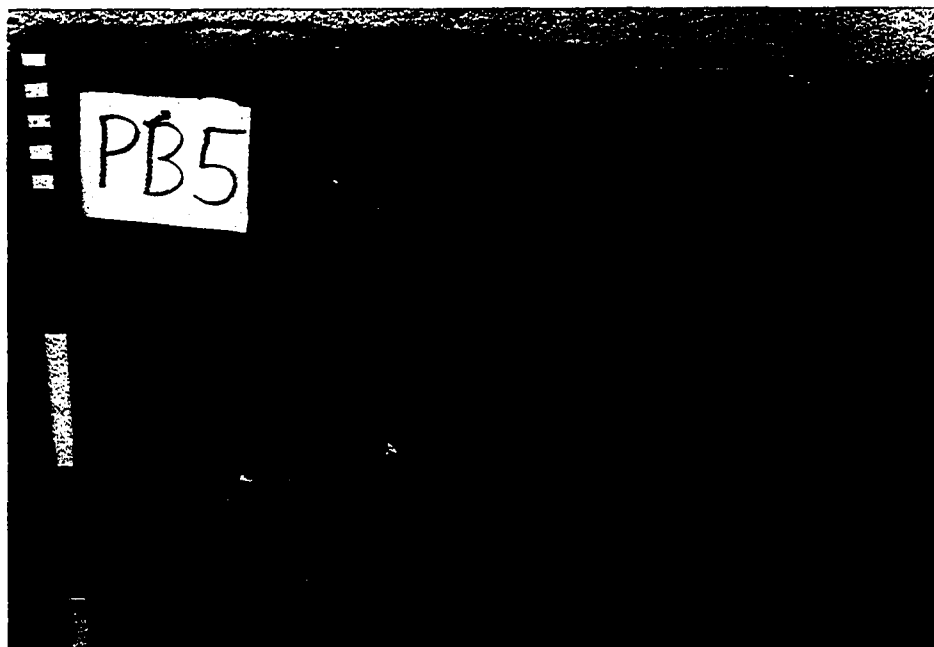


Figure 31a. Small ripple cross-bedding as seen in trench "B" of Point bar 5. Bedding is parallel to the present flow of the river and trench "B" is located on the downstream portion of bar. The white segments of the scale are 20 cm in length.

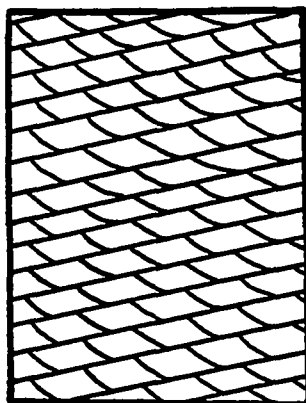


Figure 31b. Diagrammatic representation of small ripple cross-bedding (Modified after Blatt et. al., 1980).

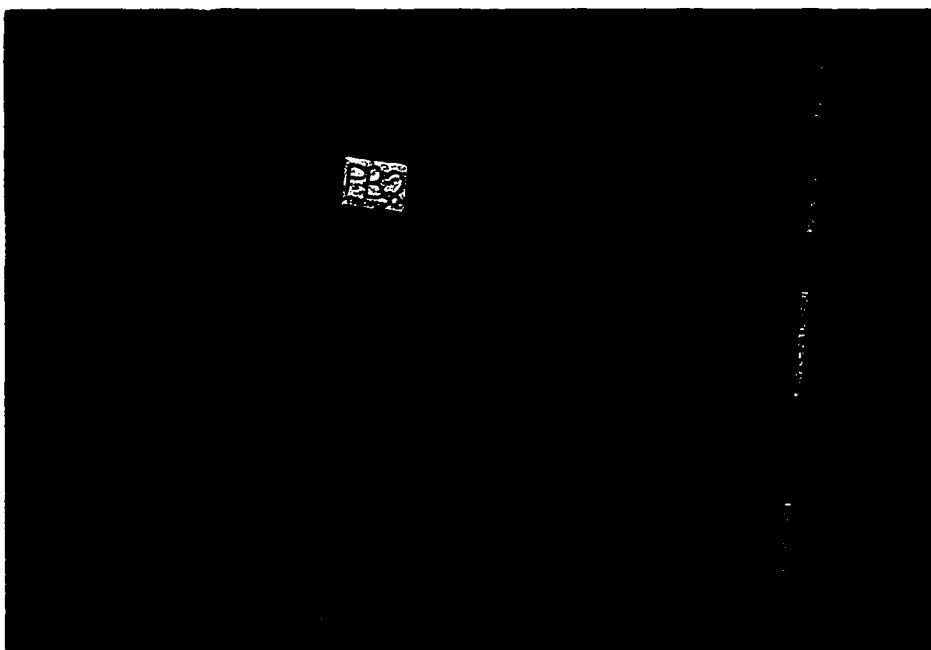


Figure 32a. Large scale trough-shaped festoon cross-bedding (far right) in trench "A" of Point bar 2. Also evident in this photograph are avalanche beds, cut and fill scour (far left) and reactivation surfaces. Bedding is perpendicular to the present flow of the river and trench "A" is located on the downstream portion of the bar. The white segments of the scale are 20 cm in length.

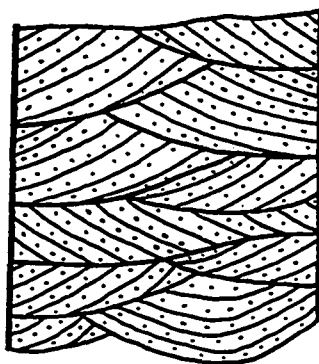


Figure 32b. Diagrammatic representation of large scale ripple (trough-shaped) cross-bedding (Modified after Doeglas, 1962).



Figure 33. Photograph of levee exposure downstream of Payan. Most levee sediments consist of homogeneous, mottled muds, but may occasionally contain planar lamination of fine sand and mud. The surface of the levee is 0.5 meters above the exposed sediments in the upper portion of the photograph. The white segment of the scale is 20 cm in length.

Magui were large, emergent at low water, and well-developed with pronounced topographic relief. Because small mid-channel bars are composed primarily of cobbles and pebbles in a sand matrix and have little topographic relief or extensive sand deposits, few surficial sedimentary structures exist there other than imbricated clasts; additional study of sedimentary structures in trenches on small mid-channel bars was inhibited due to an influx of the surrounding river water into any attempted trench. Point and side bars of all sizes could be examined with ease.

a). Intra-Bar Comparisons

Usually large mid-channel bars along the Rio Magui (e.g., MCB1) display a zone of imbricated cobbles and pebbles at the upstream end of the bar which gradually diminishes in abundance downstream and grades into coarse sand bodies; fine sands dominate near the downstream portion of the bar. Sand waves and lunate mega-ripples exist towards the downstream end with straight-crested, lingoid and undulatory ripples commonly present both within and adjacent to these larger surface features. An examination of the bar's trenches finds large scale troughs, mega-ripple, small ripple and planar cross-bedding frequently represented.

Representative point bars (e.g., PB2) usually have sedimentary structures similar to those found on mid-channel bars, with the general omission of lunate mega-ripples. A zone of imbricated pebbles at the upstream portion of the point bar gradually grades into coarse and medium-grained sands, and finally, towards the downstream end of the bar, fine-grained sands. Large scale surface ripples such as sand waves are occasionally represented on the mid-to-

downstream segments of a point bar. Smaller features such as straight-crested, lingoid and undulatory ripples are commonly found within and adjacent to the sand waves. An examination of point bar trenches generally reveals varieties of cross-bedding (e.g., large scale trough, mega-ripple, small ripple and planar cross-bedding) which are similar to those found in mid-channel bar trenches.

A representative side bar (e.g., SB1) consists of medium to predominantly fine-grained sand and displays small-scale surface features such as straight-crested, lingoid and undulatory ripples. Cross-bedding as expressed in side bar trenches also reflects small scale sedimentary structures such as small ripple and planar bedding. Large scale sedimentary structures are not represented on side bars.

All of the intra-bar variations in sedimentary structures described for mid-channel, point and side bars of the Rio Maguí exist with respect to upstream/downstream position along the channel bar (i.e., parallel to the river channel). Little change in sedimentary structures occur on bars perpendicular to the river channel.

b). Inter-Bar Comparisons

Only subtle variations in sedimentary structures exist between bars of similar type (mid-channel, point and side) along the Rio Maguí. Large mid-channel bars all display sand waves, straight-crested, undulatory and lingoid ripples. Cross-bedding on large mid-channel bars throughout the study area consistently shows mega-ripple, small ripple and planar forsets. Lunate mega-ripples and large scale trough cross-beds are generally absent but do appear

on two mid-channel bars (MCBA4 and MCB1). Imbricated cobbles and pebbles are characteristic of the upstream portions of mid-channel bars along the study area except on one bar (MCB6) located approximately 18 km downstream of Payan. This bar is the only mid-channel bar downstream of the junction of the Rio Guañambi and is located along a portion of the river which has a stream gradient of only 0.0004, apparently much too low to generate flood currents capable of transporting gravel. This decrease in channel slope downstream of the junction of the Rio Guañambi also coincides with the decline of gravels on channel bars towards the mouth of the Rio Magui. During waning flow conditions as the stream competency diminishes, gravels and other coarse-grained material are no longer transported. Sufficient velocities do exist, however, to transport and deposit sand over the tops of the previously deposited gravels. Many channel bars display textural surface changes due to "sieving" processes when medium- and coarse-grained sand are deposited on top of bar gravels as seen in Figure 34.

Point bars along the Rio Magui also display a zone of imbricated cobbles towards the upstream portions, along with sand waves, straight-crested, lingoid and undulatory ripples. Cross-bedding on point bars is nearly identical to mid-channel bar cross-bedding except for the absence of large-scale trough cross-sets. As with mid-channel bars, point bars display a decline of gravels with downstream transport, and ultimately consist of primarily sand near the river mouth. The relative abundance of sedimentary structures along point bars of the Rio Magui is generally quite similar from bar to bar.

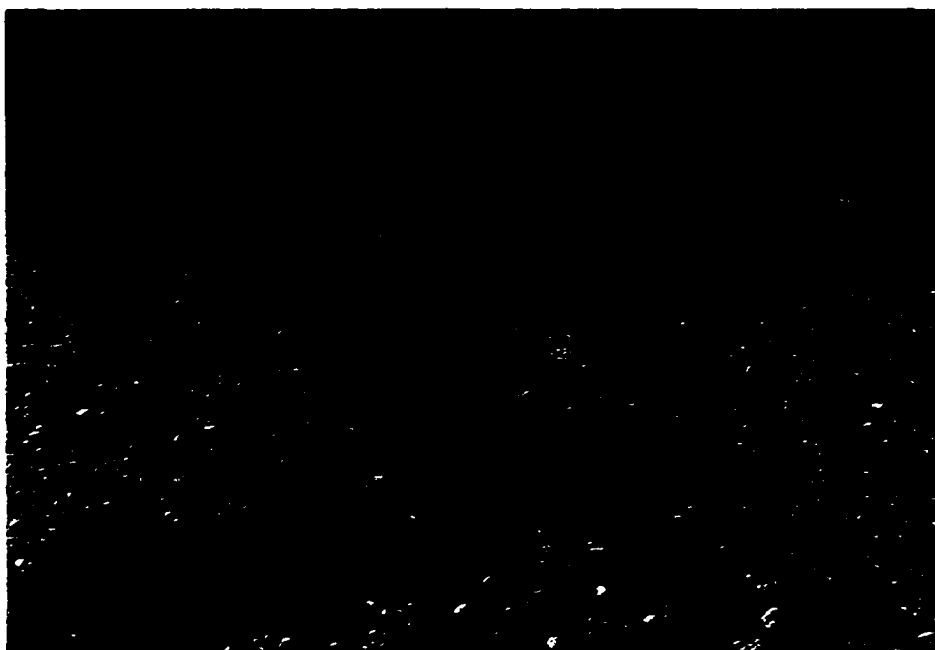


Figure 34. Photograph of a gravel lag being covered by a sand at waning flow in the middle portion of Point bar no. 1. Flow is from left to right. Paper is 18 cm long.

Side bars display surface structures and cross-bedding similar to those found on point bars. Mega-ripple, small ripple and planar forsets are commonly found while large-scale trough cross-bedding is characteristically absent. One apparent distinction between side bars and point bars is the general lack of gravel on the upstream segments of the side bar. Side bars nearly always are composed of fine-grained sand from one end to the other regardless of where the side bar is spatially located along the river. As with mid-channel and point bars, all side bars exhibit similar relative abundances of sedimentary structures in sand.

C. Discussion

Up to this point, I have documented what specific sedimentary structures and features exist along various channel bars of the Rio Magui. It is appropriate at this time to try and associate the type of sedimentary structures with particular depositional events.

Doeglas (1962) conceived of an ideal mid-channel bar sequence (Figure 35) very similar to that presented by Reineck and Singh (1975) for point bars. Doeglas (1962) associates the following sequence of events with specific sedimentary structures for a mid-channel bar. A basal zone of large-scale cross-bedding is formed by the lateral and downstream advance of mid-channel bars. These sediments which represent the coarsest material in the sequence are composed of cobbles and pebbles arranged in inclined layers. These sediments are transported during the high-flow conditions such as rapid turbulent or shooting flow conditions characteristic of upper flow regime and are deposited as river discharge drops. During lower-flow conditions, finer-grained sediments are deposited over

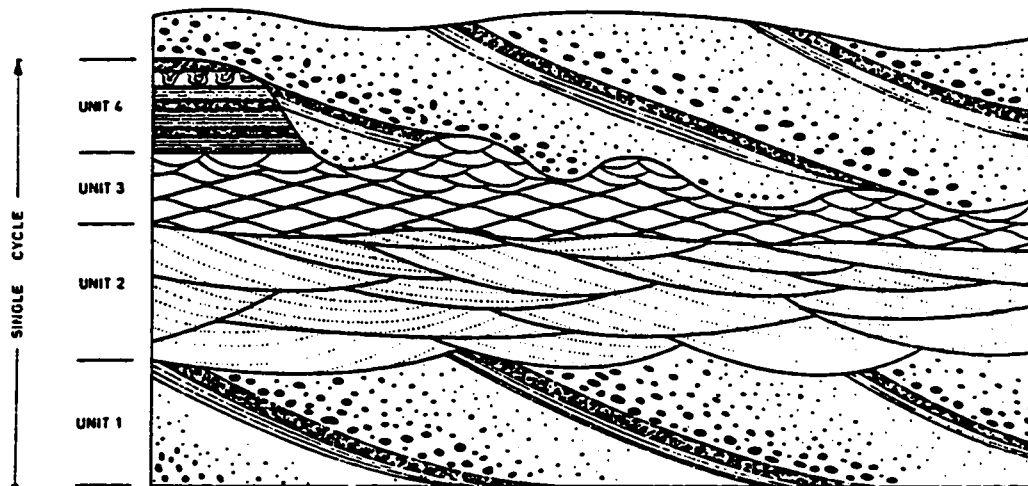


Figure 35. Sketch of an idealized sequence of a mid-channel bar deposit. Unit 1 - large-scale cross-bedding with pebbles; Unit 2 - megaripple bedding, medium sand; Unit 3 - small ripple bedding, fine sand; Unit 4 - fine sand and mud, horizontal bedding (Doeglas, 1962).

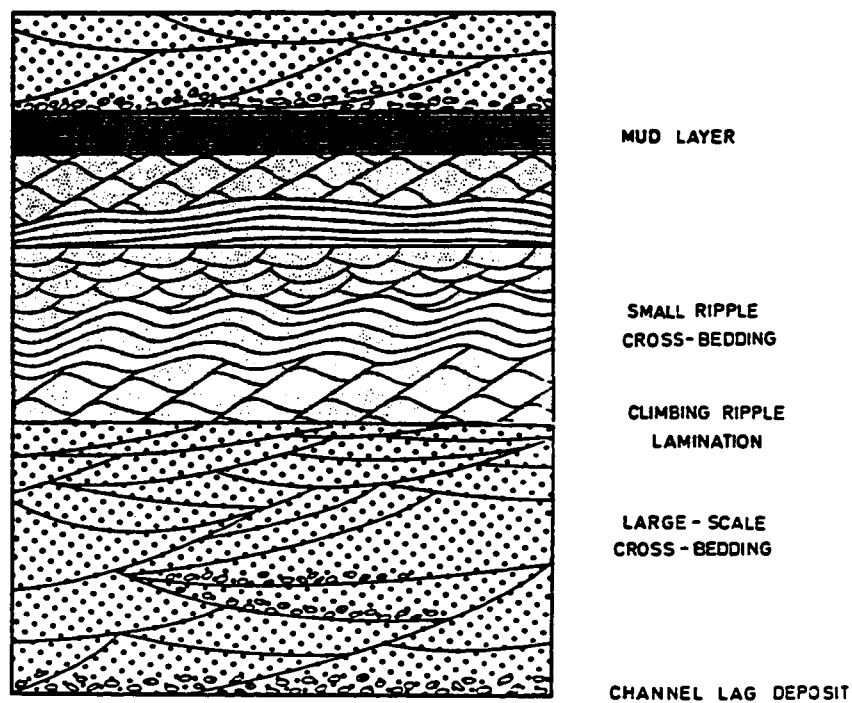


Figure 36. Sketch of an idealized fining upward sequence of a point bar deposit (Modified after Reineck and Singh, 1975).

the previously deposited cobbles and pebbles. Medium-grained sand with megaripple bedding is formed during high intensity, lower flow regime conditions. Following the zone of megaripple bedding, is a zone of small ripple cross-stratification formed during low-intensity, lower flow regime conditions. Topping the sequence is a zone of fine sand and mud deposited in horizontal layers formed originally by overbank flooding. Because this flood water contains a large amount of suspended sediments, the fines eventually settled-out of suspension and form horizontal laminations on top of the mid-channel bar.

Mid-channel bars along the Rio Magui are nearly identical to the sequence presented by Doeglas (1962). A basal zone of large scale cross-bedding is formed by lateral and downstream advance of the mid-channel bar. This zone of large-scale cross-bedding usually exhibits coarse-grained sand with sparse amounts of pebbles arranged in inclined layers. These sediments are characteristic of upper flow regime conditions of relatively low intensity and are deposited as river discharge drops following the peak of a flood. Somewhat lower flow conditions along the Rio Magui (high intensity of the low flow regime) deposit finer-grained sediments on top of the previously deposited pebbles and coarse sand in the form of megaripple bedding. Following the zone of megaripple bedding is a zone of fine-grained small ripple cross-stratification formed during low-intensity, low flow regime conditions. One difference between the Rio Magui mid-channel bar sequence and the idealized sequence of Doeglas (1962) is the general lack of horizontal mud laminations overlying the small ripple cross-bedding characteristics of Doeglas' sequence. The frequent recurrence of flooding typical of this tropical region could

scour the fine-grained rippled sequence deposited from a previous flood.

Reineck and Singh (1975) envision an ideal point bar sequence (Figure 36) as one which is dominated by large forset cross-bedding (megaripple bedding) in the lower part formed by a rapid decrease of discharge and velocity following the main passage of a flood. Overlying this zone is a sequence of small forset cross-bedding and small trough-fill cross-bedding formed as velocities diminish further. Ponding of suspended sediments as flow retreats is also common during this interval. Topping-off the sequence is a zone of parallel laminae which forms during near tranquil flow conditions.

Point bars along the Rio Magui offer a similar sequence of events to those described by Reineck and Singh (1975). Rio Magui point bar sequences are dominated by large scale cross-bedding in the lower part (Figure 32a) formed by a rapid decrease of discharge and velocity following the passage of a flood (low intensity), upper flow regime. As velocities diminish further, a sequence of small forset cross-bedding and small trough-fill cross-bedding forms as velocities continue to diminish (Figure 31a and 30b respectively). Further decrease of velocities during low intensity, low flow regime conditions results in ponding of suspended sediments.

Sedimentary structures found in Rio Magui side bars contain all of the features and characteristics of Rio Magui point bars. Occasionally side bars may exhibit planar laminations (Figure 29b) in place of large-scale cross-stratification. These planar laminae form during low intensity upper flow regime conditions following the peak of a flood. Other than this minor variation in sedimentary

structures, Rio Magui side bars and point bars are difficult to distinguish in cross-section. This striking similarity and lack of differentiation may indicate that the formative processes active along the Rio Magui point and side bars are very similar.

Apparently, the processes which form the three types of channel bars (mid-channel, point and side) along the Rio Magui are nearly identical due to the similar trends of sedimentary structures and features. Reineck and Singh (1975) recognize also that no well-defined differences exist between the sequence of mid-channel bar deposits and point bar deposits.

As with the uppermost layers of Rio Magui mid-channel bar sequences, the upper layers of horizontal bedding characteristic of Reineck and Singh's (1975) idealized point bar sequence is curiously absent. While no definitive explanation exists to adequately account for this feature, it is possible that the frequent flooding of the Rio Magui which appears to be characteristic of rivers in tropical climates, may tend to remove the previously deposited upper laminae of fine-grained material.

CHAPTER VI

TEXTURAL CHARACTERISTICS OF CHANNEL BARS

The purpose of this section is to document the textural variations of channel bars along the Rio Magui. Mean grain size and sorting trends for representative mid-channel, point and side bars will be examined along with textural variations and trends from bar-to-bar downstream.

A. Methodology

Approximately 51 channel bar samples were collected along the 40 km stretch from Aurora to the mouth of the Rio Magui. These samples, which represent both surface and trench wall grab samples, were shipped to the laboratory in Norfolk, Virginia, where each sample was sieved on the Ro-Tap for 45 minutes at half-phi intervals according to Folk's procedures (1974). Half-phi sieve intervals were used because of the broad range of grain sizes comprising the samples (e.g., 4.00 through -4.00). Weight percentages were used as input in the sediment size analysis program of Darby and Wobus (1976) which calculated mean grain size and sorting values.

B. Results

1. Intra-Bar Comparisons

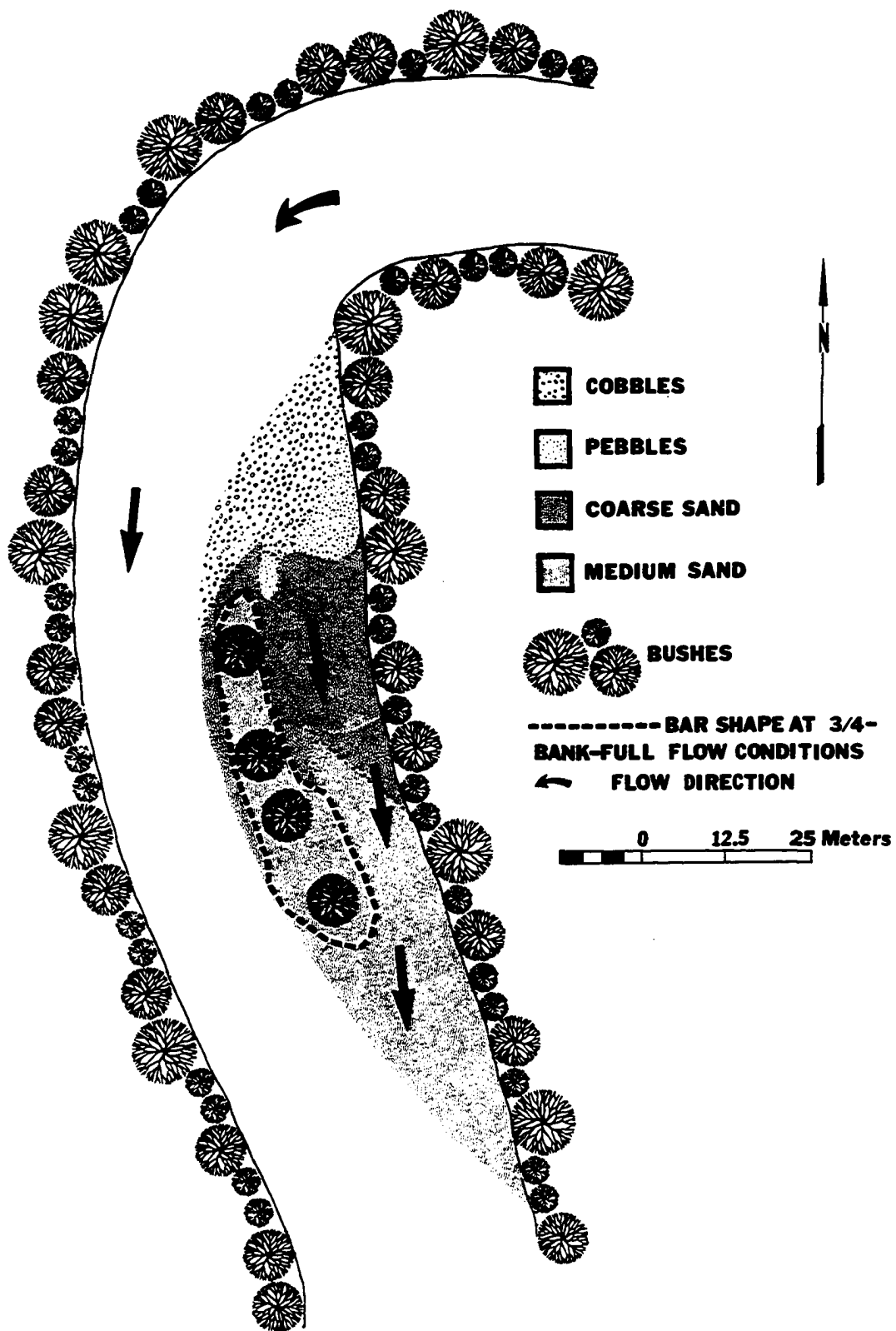
Surface and trench samples were collected from the surface of all Rio Magui channel bars. Surface samples consisted of approximately 20 kilograms of sand, pebbles, and sometimes cobbles present on the upstream segments of Rio Magui channel bars. To avoid bias, samples were collected at the same position on each bar. Trench samples

were taken from a trench wall approximately 25 cm from the top of each bar trench.

The majority of mid-channel bars characteristic of the Rio Magui display little topographic relief and are composed primarily of gravel intermixed with coarse-grained sand. One mid-channel bar (MCB2), representative of the 12-mid channel bars analyzed in this study, was examined for textural variations. This bar displays a poorly sorted pebble zone containing clasts up to 1 cm in diameter uniformly distributed throughout the entire bar. Pebbles on the upstream portion of this bar are typically 0.7 cm in diameter. Towards the mid-to-downstream portions of this bar the average pebble size decreases to 0.5 cm and greater amounts of coarse-grained sand is present between the pebbles.

Not all mid-channel bars along the Rio Magui are small, low-relief gravel bars. Of the 12 mid-channel bars recognized in the Rio Magui, four are large, vegetated islands which have considerable topographic relief, vegetative cover and diversity in the size of surface material (Figure 37). Bar MCB1 is a good case in point. MCB1 is located approximately 1 km downstream of Payan and is submerged only at near-bank-full stage. During low-flow conditions (1/4-bank-full flow or less) most of the bar is emergent as depicted in Figure 37. As the river rises, the swale or chute along the eastern portion of the mid-channel bar is initially breached and ultimately carries a very large portion of the flood waters. Because of these reasons, the bar resembles a traditional mid-channel bar only during high-flow conditions (3/4-bank-full or greater) and even then displays emergent shrubs and grass. During low flows, the bar

Figure 37. Sketch illustrating the textural variations on Mid-channel bar 1, downstream of Payan. This bar which is located slightly downstream of the channel meander is in transition from a mid-channel bar to a point bar. Arrows indicate flow direction over bar at 3/4-bank-full stage. As river height drops, flow is restricted to the main channel (west of the bar).



physically appears as a point bar.

During low-flow conditions, sampling of all portions of this bar is possible. Cobbles up to 15 cm in length are dominant on the upstream portion of the bar grading into either a poorly-sorted, small pebble zone or directly into a predominantly moderately-sorted coarse-grained sand accumulation. The mid-to-downstream segments of this bar consist primarily of moderately-sorted medium-grained sand.

On point bars, similar grain size trends are evident from trench samples. A representative point bar (PB2) chosen from the eight point bars analyzed in this study was examined for textural variations. PB2 contains poorly-sorted, coarse-grained sand on its upstream portions, moderately-sorted, medium-grained sand in the middle and moderately-sorted, fine-grained sand towards the downstream segment. Additionally, finer-grained material exists on the higher portions of the point bar near the channel bank compared to the lower segments of the point bar which generally have coarser-grained material.

Textural data from individual side bars, however, display less pronounced trends on individual bars. An analysis of a representative side bar (SB9) indicates a relatively uniform well-sorted, fine-grained sand with little downstream variation.

2. Inter-Bar Comparisons

Textural variations for mid-channel bar surface samples generally display decreasing mean grain size and perhaps decreased sorting trends with downstream distance (Figure 38). Samples from three sites (MCBA6, MCBA3 and MCBA4) however, plot off of these two trends. Closer examination of the area reveals that only the bars

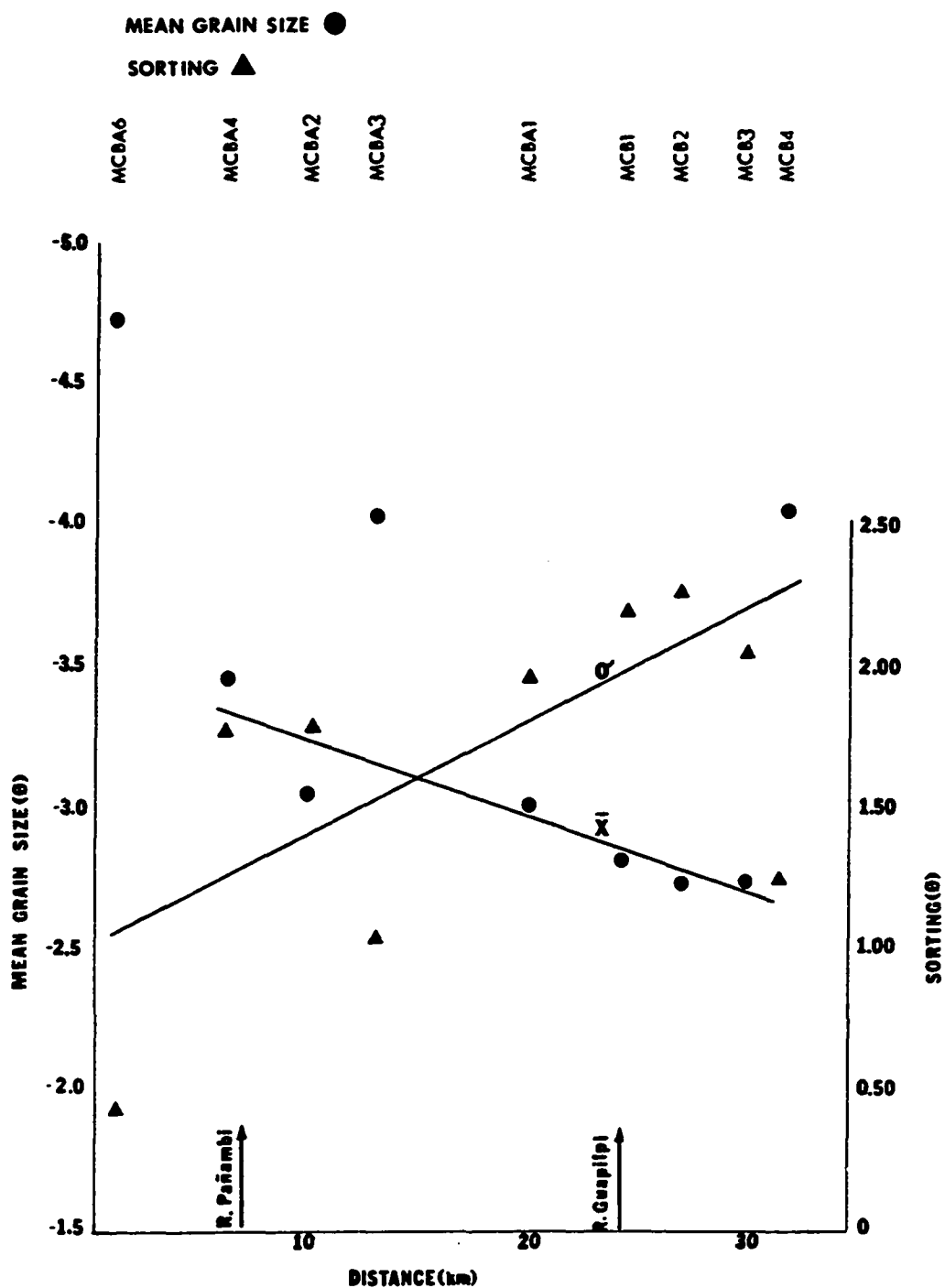


Figure 38. Plot of textural variations for mid-channel bar surface samples from Aurora to the mouth of the Rio Magui.

deposited within 50 meters downstream of mine creeks contain relatively coarse-grained gravels. These bars also contain gravels that are better sorted than other bar samples. Some concern did initially exist regarding the spatial distribution of bar samples with respect to "nearness" of terraces and smaller tributaries whereas the presence of these extrinsic variables could bias the samples. Fortunately, terraces and tributaries (other than mine creeks) do not appear to significantly influence the channel bar samples collected for this study because no spatial relationship exists between anomalous samples and terraces or tributary mouths along the river.

An analysis of point bar trench samples suggests a decrease in mean grain size and sorting with downstream distance (Figure 39). But because of the low number of such analysis and their occurrence only between 18 and 33 km downstream from Aurora, only a poorly defined trend was obtained.

Trench samples from side bars display two very gradual trends—an increase in mean grain size and very slight decrease in sorting (Figure 40). The small range of phi units for both the mean grain size and sorting and the relatively small number of samples available weakens an interpretation of these two apparent trends.

C. Discussion

Textural investigations are a dominant part of virtually all sedimentologic studies. Modern studies on the subject began with the formulation of a particle size scale of Wentworth (1922; based on Udden, 1914) and the utilization of logarithmic phi scale for grain size descriptions (Krumbein, 1934). Subsequent attempts to use sorting values to determine environments of deposition initially began

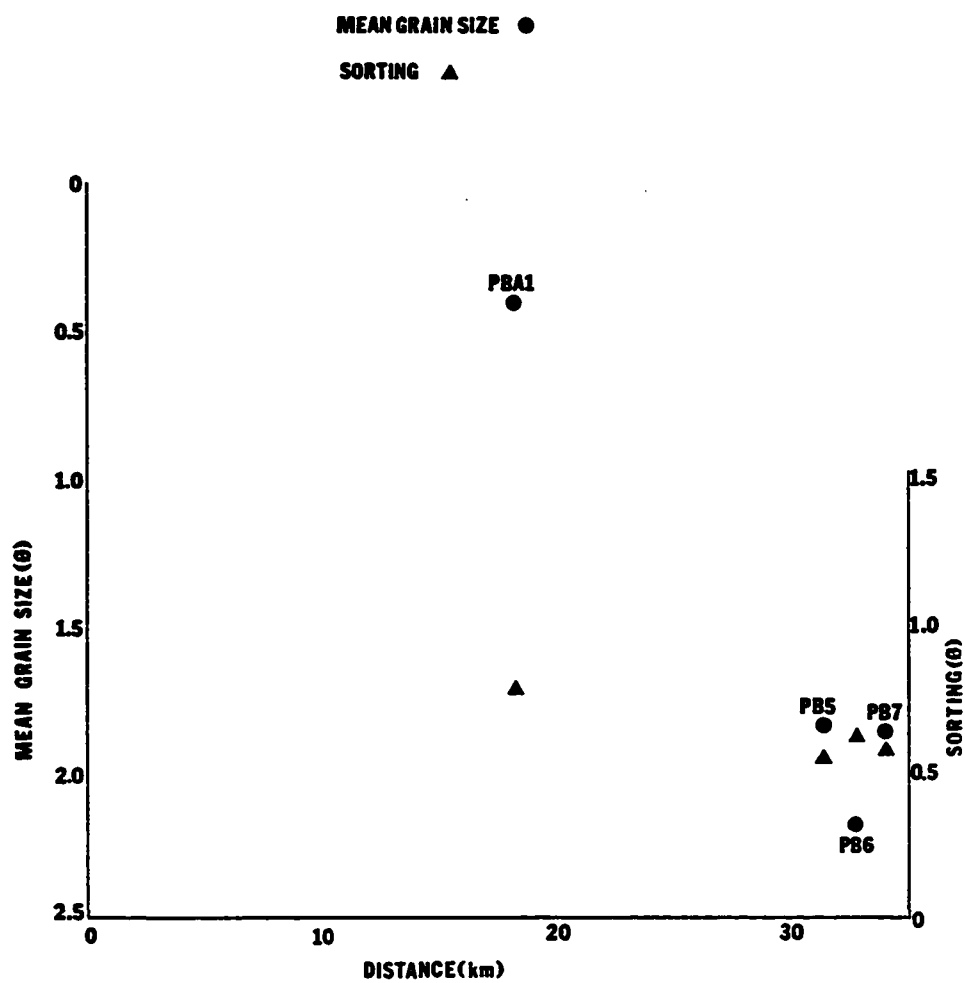


Figure 39. Plot of textural variations for point bar trench samples from Aurora to the mouth of the Rio Magui.

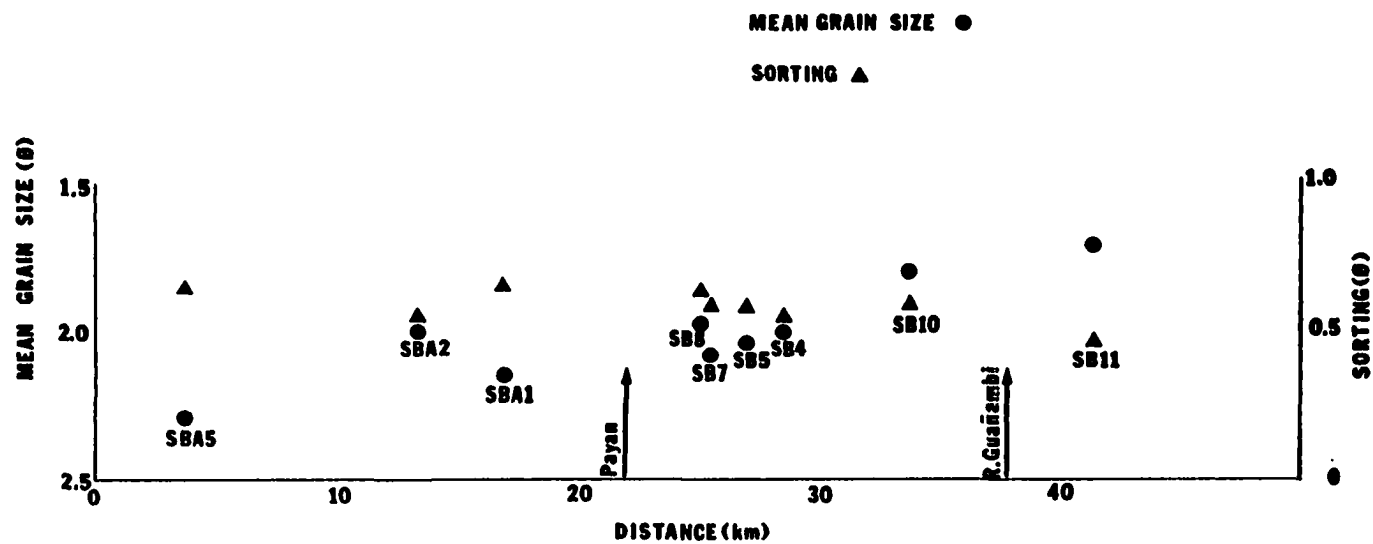


Figure 40. Plot of textural variations for trench samples of side bars from Aurora to the mouth of the Rio Magui.

with the work of Inman (1949) and later, Folk and Ward (1957). Other attempts to delineate sorting characteristics of sands in hopes of determining depositional environments using statistical and graphical methods were developed by Passega (1957) and later by Friedman (1961) among others.

It is generally accepted among geologists that mean grain size decreases and sorting increases with downstream transport (e.g., Middleton, 1976). Leopold et. al., (1964) discussed these trends and noted that localized fluctuations along the length of a stream may cause minor variations in the overall downstream decrease of grain size. For instance, along the Rio Magui erosion of terraces may add "new" material into the river sediment load directly or through the influx of smaller tributaries such as mine creeks into the main trunk.

Unfortunately, these types of extrinsic variables appear to have little influence upon the Rio Magui samples. The abundance of mine creek tributaries rapidly diminishes downstream of Payan, yet the textural trends continue. This further clouds an explanation for the strange but unique mean grain size and sorting trends which exist for channel bar samples of the Rio Magui.

CHAPTER VII

DEPOSITION OF ORGANIC MATTER

The purpose of this section is to document and interpret the variety of organic material and the spatial distribution of organic deposits along the Rio Magui. The size, orientation, location and abundance of organic debris provide the basis for determining the depositional processes for organic materials.

A. Methodology

A representative sampling of the three types of channel bars (mid, point and side) along a 40 km portion of the river from Aurora to the mouth of the Rio Magui provided compositional and size characteristics of major leaf mat accumulations and large wood debris. Orientations of wood debris was also noted with respect to current channel position.

B. Results

1. Description of Organic Debris and Deposits

Two major types of organic matter are transported and occasionally deposited along tropical streams such as the Rio Magui: 1) leaf mats and 2) wood debris. Leaf mats of varying sizes are relatively common along certain channel bars of the Rio Magui. The composition of these leaf mats is predominantly leaves of a wide variety of sizes and shapes which are blown into the river, although they also contain a lesser amount of small wood debris intermixed with the leaves.

Wood debris is also present in varying sizes and shapes. For this study "small" wood debris will include material up to 30 cm in length; any wood debris larger than 30 cm will arbitrarily be referred to as "large". Small wood debris is typically composed of twigs and branches approximately 2 cm in diameter and 15 cm long, but may contain somewhat larger or smaller material. Reeds and bamboo stems of similar size characteristics are also relatively common. Larger wood debris, logs, tree trunks, and in certain instances entire trees, are also abundant. The largest transported trunk observed was 21 meters long and 1 meter in diameter.

2. Size Characteristics of Organic Matter

Leaf mats can be large, extensive deposits or small and discontinuous, depending upon their location. Leaf mats are relatively rare on most mid-channel bars where they may exist as thin, discontinuous lenses or laminations, perhaps 2-3 cm thick and up to 20 cm long (Figure 41). On the few large mid-channel bars, mats can be interbedded with extensive sand accumulations towards the downstream end; small, low relief mid-channel bars do not exhibit leaf mat accumulations. Wood debris along both vegetated and unvegetated mid-channel bars is sparse and generally restricted to the downstream portions of the bar. One exception is a large vegetated bar (MCB6) which has both large and small debris present only at the upstream end. The relative frequency of occurrence for both leaf mats and wood debris generally increases with downstream distance.

Point bars and side bars contain organic deposits similar in composition and distribution. Leaf mat accumulations on point and side bars are very sizable, sometimes getting as large as 2.5 meters

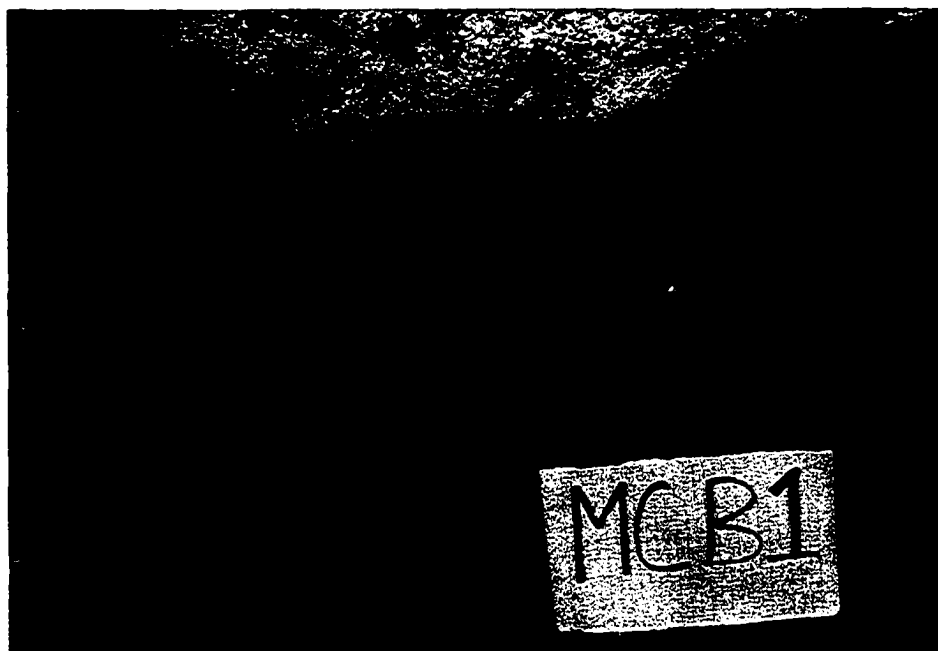


Figure 41. Photograph of thin leaf mat lamination typical of large mid-channel bars along the study area. Photograph is taken in a trench on Mid-channel bar 1.

thick and 20 meters long (Figure 42). Typically, these leaf mats form on the mid-to-downstream portions of the point and side bars. As with leaf mats, wood debris is very abundant on point and side bars and exist in both large and small sizes. Small wood debris 2-15 cm long is quite common (Figure 43); large debris, up to 21 meters in length, is somewhat less abundant but exists nevertheless, particularly on side bars (Figure 44). In virtually all instances, some leaf mats accumulated downstream of large wood debris. As on mid-channel bars, the relative frequency of organic matter generally increases with downstream distance.

3. Imbrication of Wood Debris

A cursory examination of orientations of modern organic matter in the field suggests that present-day wood debris is deposited in two basic orientations-either parallel to the direction of flow or at right angles to it. Many workers (Wasmund, 1926; Quenstedt, 1927; Schindewolf, 1928; Trusheim, 1931, and Seilacher, 1959) who have studied imbricated organic deposits have concentrated on organic remains of invertebrate organisms and other forms of aquatic life. Little information exists in the literature concerning orientations of wood debris along modern rivers. Along the Rio Magui small wood debris from approximately 7-20 cm in length is usually transported and deposited parallel to stream flow. Material smaller than this exhibits no apparent depositional orientation (Figure 43). Extremely large wood debris (10 meters or greater in length) also displays a depositional orientation parallel to the direction of flow. Large wood masses up to 10 meters in length, however, are inconsistent in their depositional orientations (Figure 45).

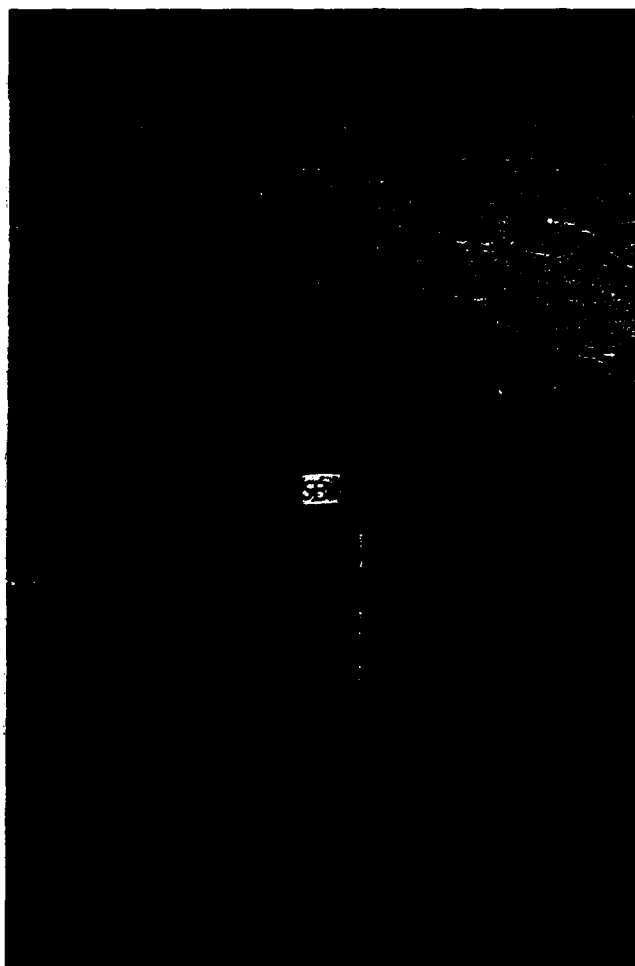


Figure 42. Photograph of large leaf mat accumulations typical of point and side bars of the Rio Magui. Rippled sands on top of the bar bury the leaf mat which extends back into the bar an unknown distance. The lower white segment of the scale is 20 cm in length.



Figure 43. Photograph of small wood debris typical of point and side bars along the Rio Magui. Direction of flow is from the left background to the right foreground. Note the orientation of the larger material parallel to the present flow direction. Smaller wood material displays no apparent orientation.



Figure 44. Photograph of large wood debris 21 meters long, as seen on Side bar 11, parallel to the direction of flow.

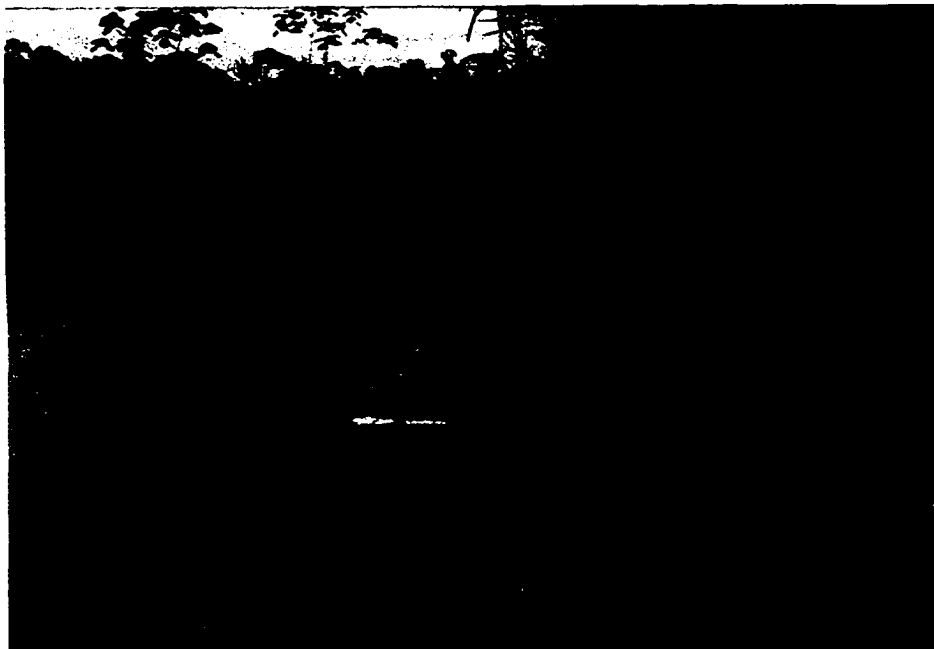


Figure 45. Photograph of large wood debris approximately 1.5 meters long (exposed) along the present river channel. This log is oriented perpendicular to the direction of flow.

C. Discussion

The primary thrust of earlier studies regarding organic debris and deposits in fluvial channels centers around the role of debris in streams of the Pacific Coast and Cascade Range of western North America (Froehlich, 1971; Lammell, 1972). Swanson et. al., (1976) discussed the history and physical effects of large organic deposits in streams of the western United States. In these areas, extremely large wood debris in small channels can dominate the flow patterns and locations of bedforms (Keller and Tally, 1979; Prestegard, (1984).

Numerous natural processes are responsible for the transfer of large organic debris into low gradient meandering channels, bank failure and blowdown being the two most prevalent mechanisms (Swanston and Swanson, 1976). Along the Rio Magui, the primary mechanisms of debris transfer into the river are 1) aeolian transport of leaves; 2) the floating, or "floodwash", of wood debris lying on the levee tops and floodplain which is transferred into the river at near-overbank flow conditions (Figure 46); and 3) bank failure due to undercutting of tree-lined channel margins (Figure 47).

While few authors have discussed the role of terrestrial organic debris transferred to and transported in stream channels, fewer still have attempted to discuss depositional processes of organic matter. Along the Rio Magui, the large size and similar characteristics and positions of leaf mats on both point and side bars imply that the processes of organic deposition active on these two bar types are the same. In contrast, the processes along mid-channel bars produce leaf mat laminations that are small, discontinuous and sporadic in extent.

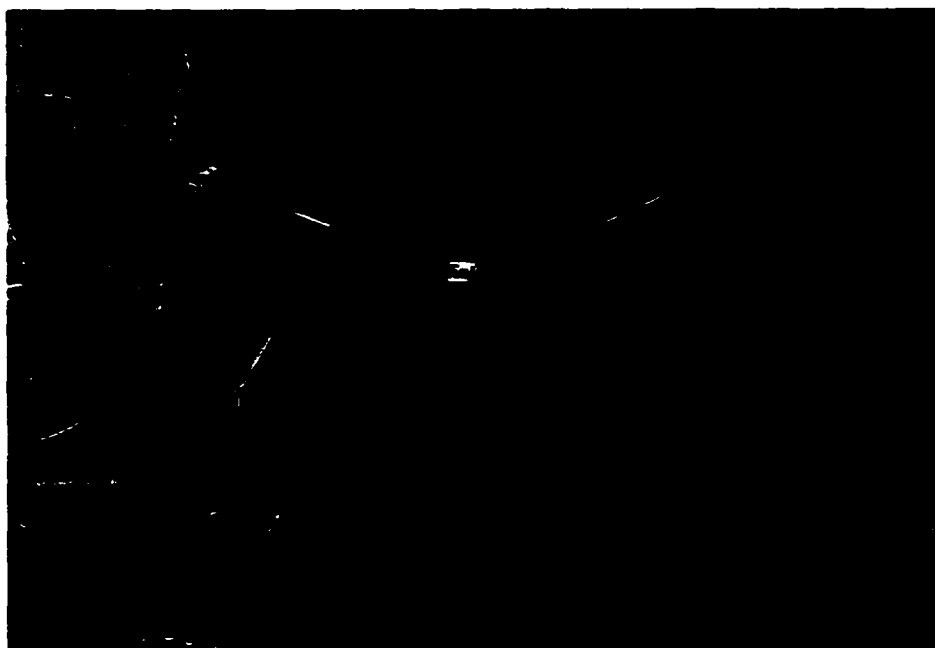


Figure 46. Photograph of small wood debris on levees of the Rio Magui. As floodwater rises, debris is carried down the river. Frequent cultivation of the floodplains by the villagers in this area account for much debris.



Figure 47. Photograph of bank collapse due to undercutting by flood waters.

Clearly, two distinct sets of processes co-exist along the Rio Magui and are responsible for the deposition of leaf mats and organic debris.

In order to understand why leaf mats are abundantly present on point and side bars but rarely expressed on mid-channel bars, we must examine the type of hydrodynamic processes and flow patterns which transport organic matter. The style and pattern of organic deposits on mid-channel bars is greatly controlled by the relief and vegetative cover of the bar. During periods of near bank-full to over-bank conditions, all point, side and mid-channel bars along the study area are completely submerged; some vegetation on four of the more stabilized mid-channel bars is emergent, however, during these flow conditions. As water flows over small mid-channel bars, the primary flow pattern is generally parallel to the flow in the channel. Additional secondary patterns of water movement such as eddies or helical flows are believed to exist over the surface of submerged channel bars (Allen, 1968). Because of the small size and low topographic relief of smaller mid-channel bars, few eddies or secondary flow patterns exist which might accumulate leaf mats. Most organic materials simply float over the bar and continue downstream. Greater topographic relief characteristics of all point and side bars and large mid-channel bars induces eddies and other secondary flow cells downstream of surface obstructions (Figure 48) which can lead to the formation of leaf mats on the downstream end of the bars. Stabilized vegetation upon large mid-channel bars which are emergent during periods of near bank-full flow can entangle large wood debris and aggrade a small "debris jam" (e. g., Swanson *et. al.*, 1976). During

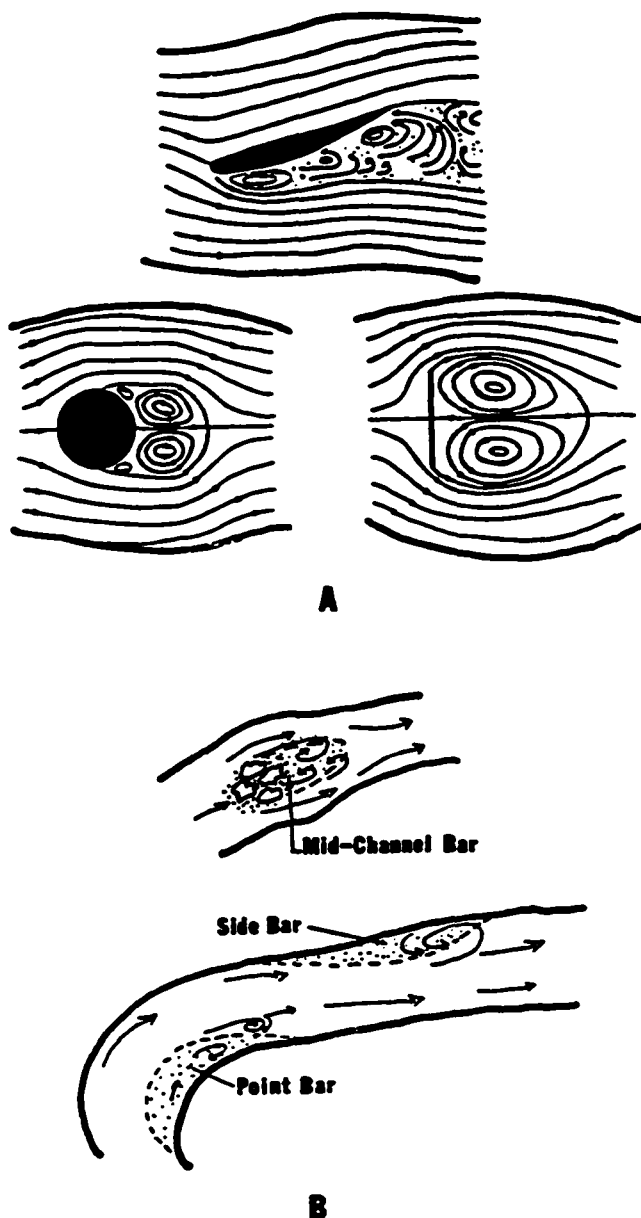


Figure 48. Sketch depicting examples of patterns of flow around obstacles and features of different shapes (modified after Allen, 1968). B. Observed locations of eddies on point, side and large mid-channel bars which collect leaf mats.

waning flow, wood debris of all sizes may become stranded upon bar surfaces.

Along point and side bars on the Rio Magui, three secondary flow mechanisms act as depositing agents for leaf mats: 1) eddies, or water currents with a circular motion formed at a point at which a current passes over an obstruction (Gary et. al., 1972), 2) vertical, unobstructed helical flows (Figure 49) resulting from stream hydraulics around meander bends (Allen, 1968) and 3) horizontal helical flow patterns which move water on the channel bottom towards the point bar as well as downstream (Dietrich and Smith, 1983). Collinson and Thompson (1982) following the work of Allen (1968), described how eddies and helical flows form on point bars and other irregularities along a channel margin in a flume stream channel. Along the Rio Magui, topographic relief on point bars leads to the formation of very turbulent eddies on the downstream end of the bars; more placid but prominent eddies form over side bars due to the position of the thalweg on the opposite bank. Some floating leaves are trapped in these eddies, and are deposited during waning flows. Not all of the leaf debris, however, remains on the surface; many leaves become easily "water-logged" and float below the surface. Horizontal helical flow patterns transport clumps of leaves across the bed of the channel towards the point bars and side bars. Some become entrapped in the eddies described earlier.

Eddies form on the downstream portion of most large mid-channel bars along the Rio Magui due to pronounced topographic and vegetative relief. Leaves transported on the rivers surface near these eddies are trapped and subsequently deposited during waning river flows.

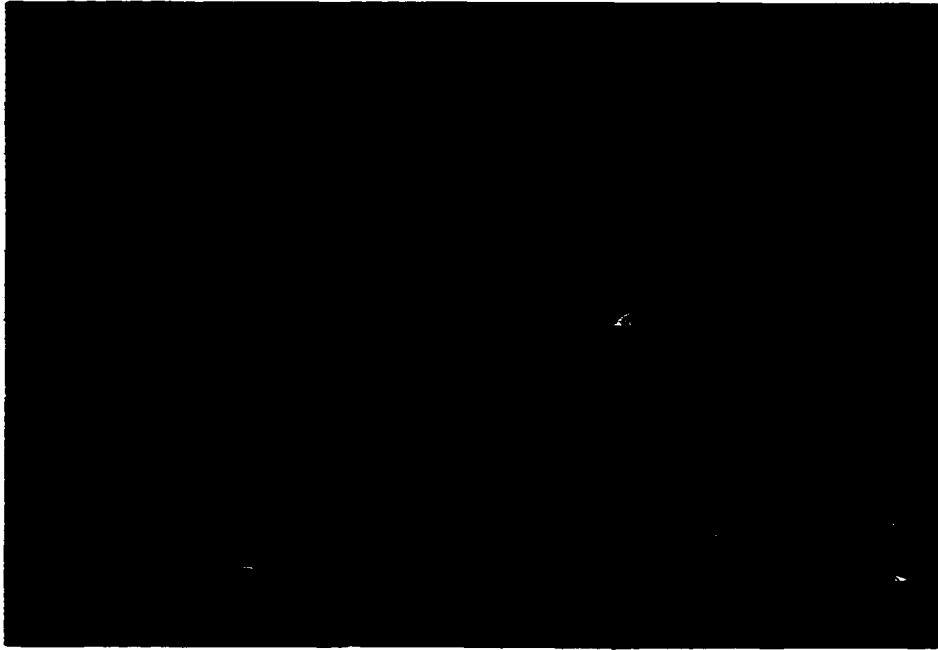


Figure 49. Photograph of helical flows or "boils" on the surface of the Rio Magui at high flow conditions. These helical cells are common to meander bends during all flow conditions, but more abundantly present at high flows.

Unlike conditions around point and side bars, helical flow around mid-channel bars transport submerged sediments away from the bars during large floods (Richards, 1982) thereby contributing little organic debris to any leaf mats forming there.

Large woody debris is input into the Rio Magui by similar means as rivers in other climates (e.g., bank collapse, blowdown) but unlike other rivers, debris is not permitted to collect or clog the channel; local villagers constantly traveling the river in dug-out canoes clear the fallen debris as soon as possible. Large mid-channel bars can collect woody debris on their vegetated, well-established portions. One bar located near the river mouth contained a small log jam on its upstream end (MCB6).

Some mention of the preservation potential of organic matter along the Rio Magui is also needed at this time. Leaf mats because of their nature, are highly susceptible to rapid decomposition and dispersal thus resulting in burial and preservation on an infrequent basis. Woody debris, however, is more "durable" and can be deposited, buried and ultimately preserved more readily as is seen in many of the older terraces of the Payan area.

CHAPTER VIII

LEVEE ENVIRONMENTS

The low broad levees along the Rio Magui typically rise 40 cm above the floodplain. Their sediments comprise the uppermost constituent of bank exposures on concave erosional banks. Levee sediments taken between the village of Payan and the mouth of the Rio Magui vary in their compositions, textures and sedimentary structures. In the following section we will examine lateral variations present in levee samples taken from bank exposures. These data reflect the depositional processes active at high-flow conditions in a tropical stream.

A. Methodology

Approximately 10 levee samples were collected at 1 km intervals between Payan and the mouth of the Rio Guañambi (Figure 50). An additional 15 samples were collected at 1/2 km intervals downstream of this junction to the mouth of the Rio Magui. The levee samples were initially weighed and wet-sieved through a 4.0 ϕ screen. After drying, the mud fraction (>4.0 ϕ) was weighed to give ratios of mud/sand for each sample. The sand fraction of each sample was sieved at half-phi intervals with the Ro-Tap following Folk (1974); weight percentages were input into a computer size analysis program developed by Darby and Wobus (1976) in order to determine mean grain size and sorting.

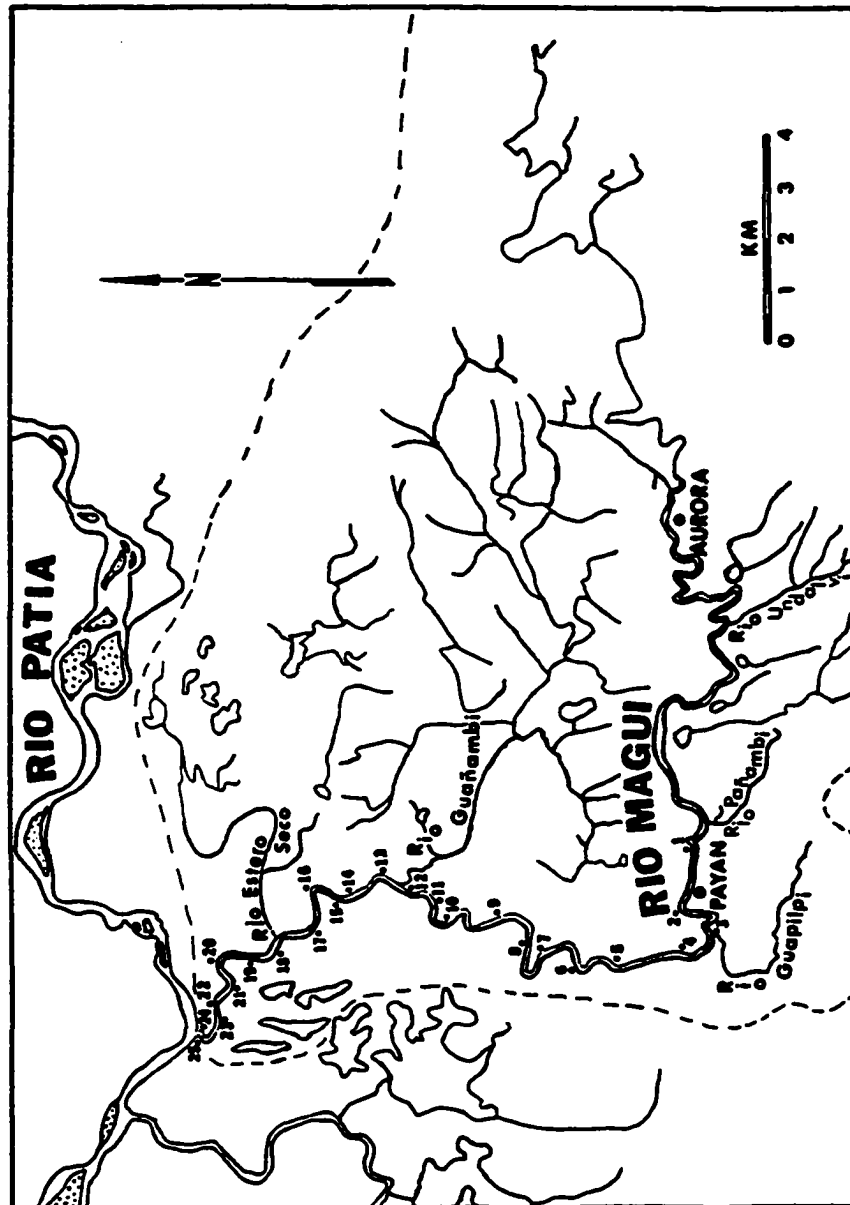


Figure 50. Location map of levee samples and major tributaries in the study area.

B. Results

1. Lateral variations in grain size parameters

a). Changes in Sand/Mud Ratio

Most of the 25 levee samples analyzed in this section are composed primarily of fine and very fine sand with minor mud (Figure 51). An irregular trend of increased mud with downstream distance is apparent from Figure 51. The mean sand size increases with increasing sand/mud ratio values (Figure 52). Levee samples with the highest proportion of mud contain the finest sands; coarser sands typically are present in samples with little mud. Thus, the amount of mud deposited on the levees is directly proportional to the grain size of the sand fraction. This linear relationship suggests that the processes of mud deposition and sand deposition are closely intertwined during levee formation and can not be easily distinguished.

b). Changes in Mean Grain Size

The plot of mean grain size versus river distance (Figure 53) initially appears as a scatter diagram with no apparent trends. Analysis of the morphology at each sample site greatly clarifies this diagram, however. Each site can be categorized as to the possible hydraulic and sedimentologic conditions at overbank flow (Table 2). Understandably, but unwittingly, all samples but one were taken from eroded banks on the outside of meanders or along straight reaches. Therefore little of the variation in Figure 53 is due to differences in the overbank hydraulics between sites. However, levee samples deposited immediately downstream of tributary mouths or coarse terrace banks eroded at high flow seem strikingly different than those

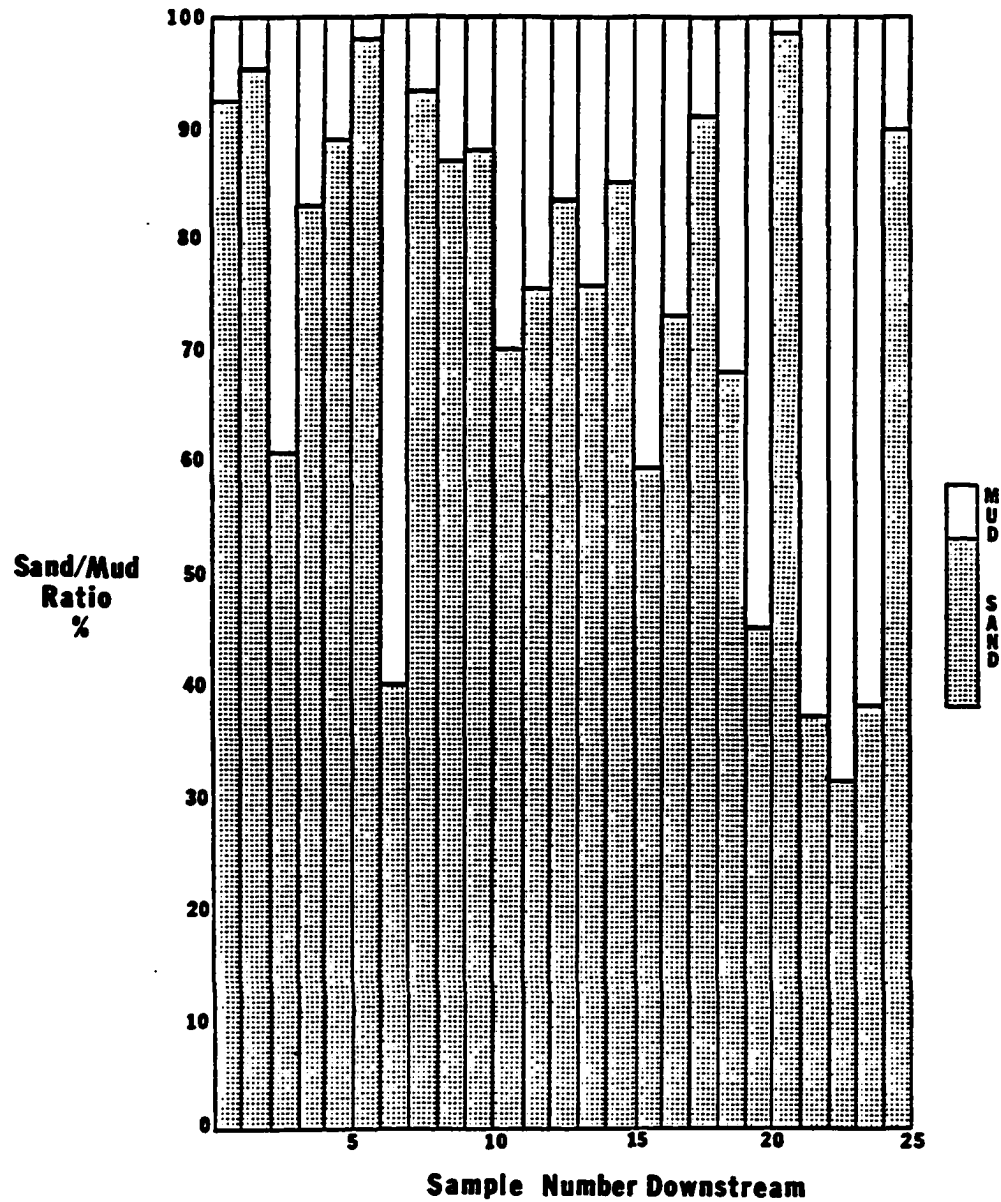


Figure 51. Plot of the percentage of sand/mud for each of the 25 levee samples.

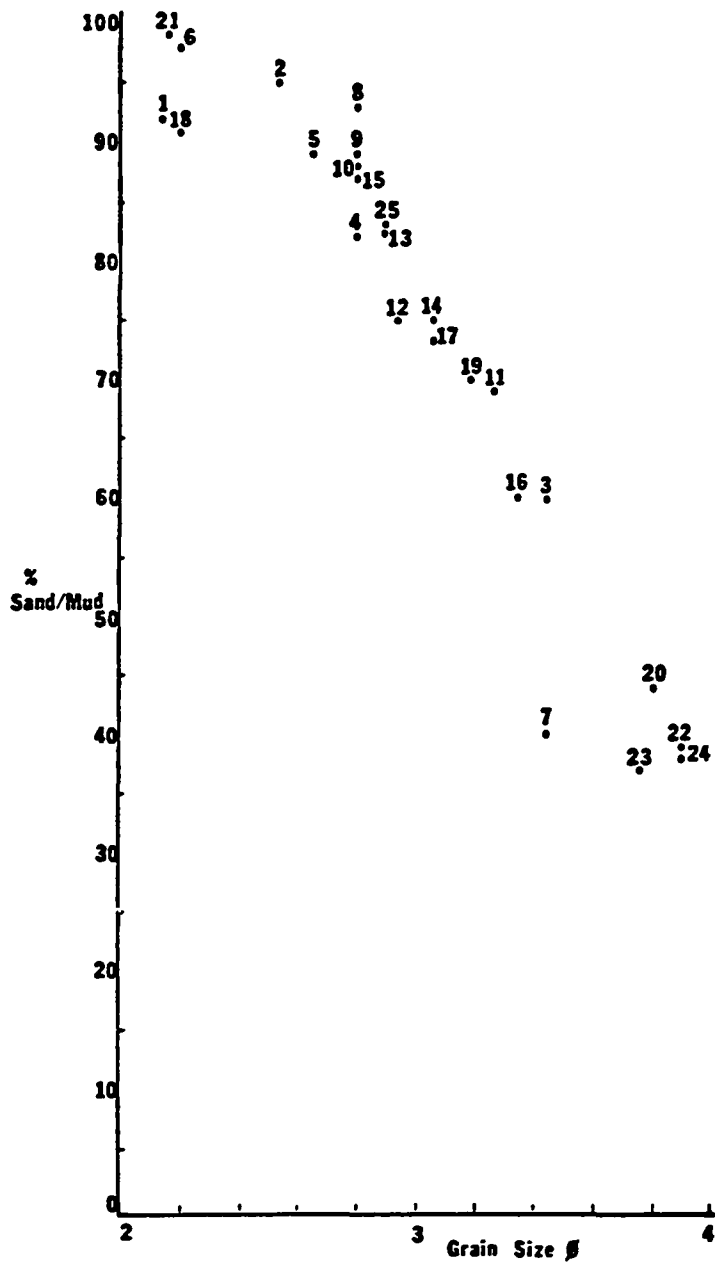


Figure 52. Plot of the percentage of sand/mud versus mean grain size (ϕ) for each of the 25 levee samples.

Table 2. Location of levee samples with respect to geomorphic features.

	Hydraulic Position			Other geomorphic Features	
	Straight Reach	Inside of Meander	Outside of Meander	Tributary mouth less than 50m upstream	High terrace bank less than 50m upstream
BS 1	x				x
BS 2			x		x
BS 3	x			x	
BS 4	x				
BS 5	x				
BS 6			x		x
BS 7			x		
BS 8	x				
BS 9	x				
BS10	x				
BS11			x	x	
BS12	x				
BS13	x				
BS14	x				
BS15			x		
BS16			x		
BS17			x		
BS18	x			x	
BS19	x				
BS20			x		
BS21			x		x
BS22			x		
BS23	x				
BS24			x		
BS25		x			

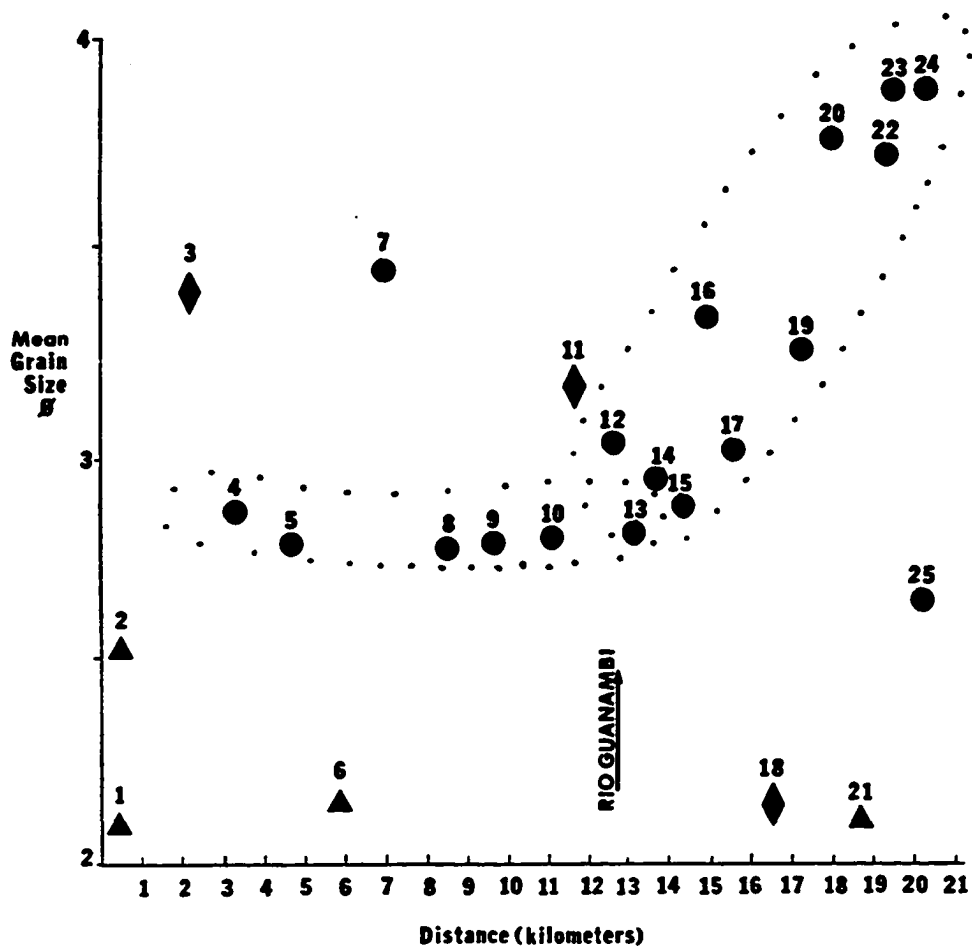


Figure 53. Plot of mean grain size (ϕ) versus downstream distance (km) from Payan for each of the levee samples. Samples taken within 50 meters downstream of a tributary mouth, \blacklozenge ; within 50 meters downstream of a high terrace bank, \blacktriangle ; unaffected by external influences, \bullet .

from sites without "external" influences. If tributary-or terrace-influenced (?) samples are disregarded, the mean grain size of levee sands along the Rio Magui exhibits two general trends. From Payan downstream to the junction of the Rio Guañambi, a relatively uniform mean particle size exists in the levee sands (samples 4, 5, 8, 9 and 10; Figure 53). A pronounced decrease in mean grain size with increased transport distance occurs from the Magui-Guañambi junction downstream to the mouth of the Rio Magui (samples 12-17, 19-20, 22-24) as shown on Figure 53.

The change of trends in the grain size data at the mouth of the Rio Guañambi coincides with a decrease of stream gradient. The longitudinal stream profile, based upon levee top elevation data on the bathymetric maps described in the channel morphology section, displays noticeable changes in gradient at four sites: 1) the junction of the Rio Guapilpi, 2) the junction of Piccinini Creek, 3) the junction of the Rio Guañambi, and 4) the junction of the Rio Estero Seco. In general the segments of the longitudinal profile (Figure 54) between these four points exhibit a generalized downstream decrease in stream gradient. The most significant and extensive decline in gradient occurs at the mouth of the Rio Guañambi. The low gradients maintained from this locality to the mouth of the Rio Magui may be responsible for the fining of levee samples downstream from the Rio Guañambi. The stream segment between the junction of the Rio Guapilpi and the mouth of Piccinini Creek also displays a low gradient (0.0003) compatible with those present along the lowest reaches of the Rio Magui (0.0004). Too few levee samples were taken along this reach, however, to reveal any change in grain size.

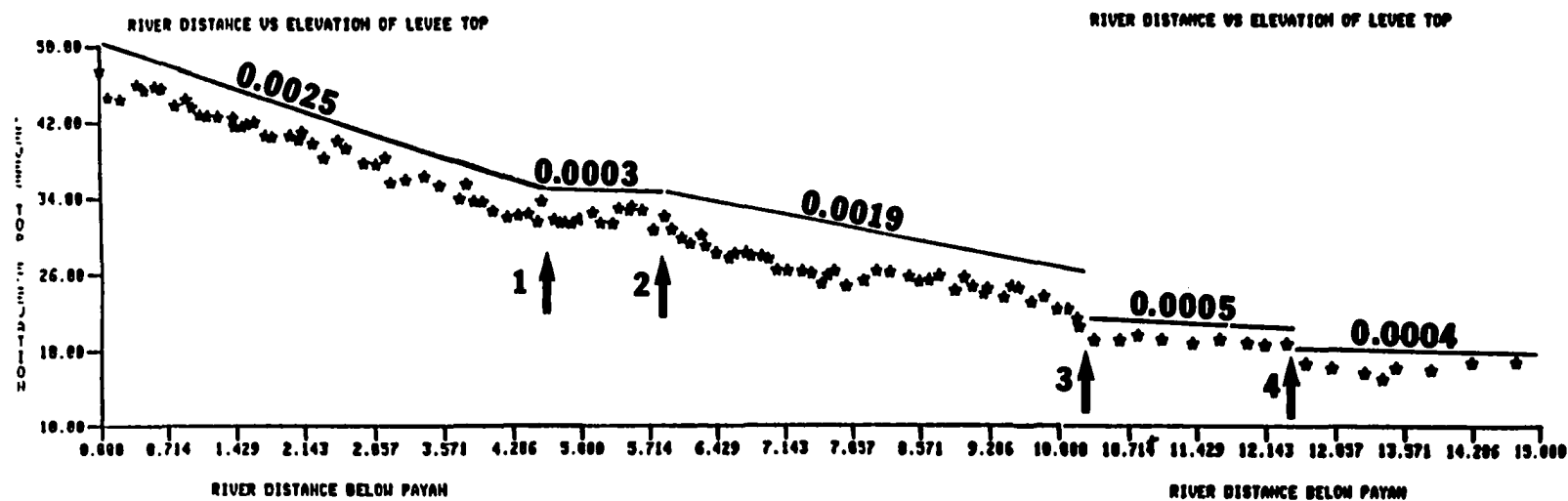


Figure 54. Longitudinal profile for the Rio Magui from Payan to the mouth of the Rio Magui. Average gradients for certain reaches are listed. Numbers indicate functions of major tributaries: 1 = Rio Guapilpi; 2 = Piccinini Creek; 3 = Rio Guañambi; 4 = Rio Estero Seco.

Each anomolous sample which falls outside of the two gradient-related trends in Figure 54 can be explained by a possible change in sediment source or depositional environment. Tributaries joining the Rio Magui at flood stage appear to add significant amounts of either very fine or very coarse-grained material to the channel levees. Two samples (nos. 3 and 11) were collected near the mouths of small creeks shown on Plate 4. One sample (no. 18) collected along the levee down and across the river from the mouth of the Rio Estero Seco is coarser than neighboring samples. No samples collected farther than 50 meters downstream from a tributary mouth have unusually coarse or fine sands. Materials present in high terrace banks contain cobble-to-boulder gravel with a medium-to-coarse-grained sand matrix (Figure 55). All four sites within 50 meters downstream of such terraces undercut by the Rio Magui at flood flows contain unusually coarse sands.

Another possible cause of mean grain size "anomalies" among the levee sands can be attributed to sediments transported in backwater flow from the Rio Patia at high flow conditions into the mouth of the Rio Magui. A cursory petrographic examination of Rio Magui levee sands indicates that only sample 25 at the mouth of the Rio Magui is significantly different than the remaining 24 samples analyzed for this study. Samples 1 through 24 contain primarily quartz with lesser amounts of volcanic fragments and accessory minerals. While many quartz grains are rounded, some display pronounced angularity. The volcanic fragments are generally sub-angular to angular in most instances. Sample 25 contains a greater abundance of amphibole minerals and volcanic fragments while

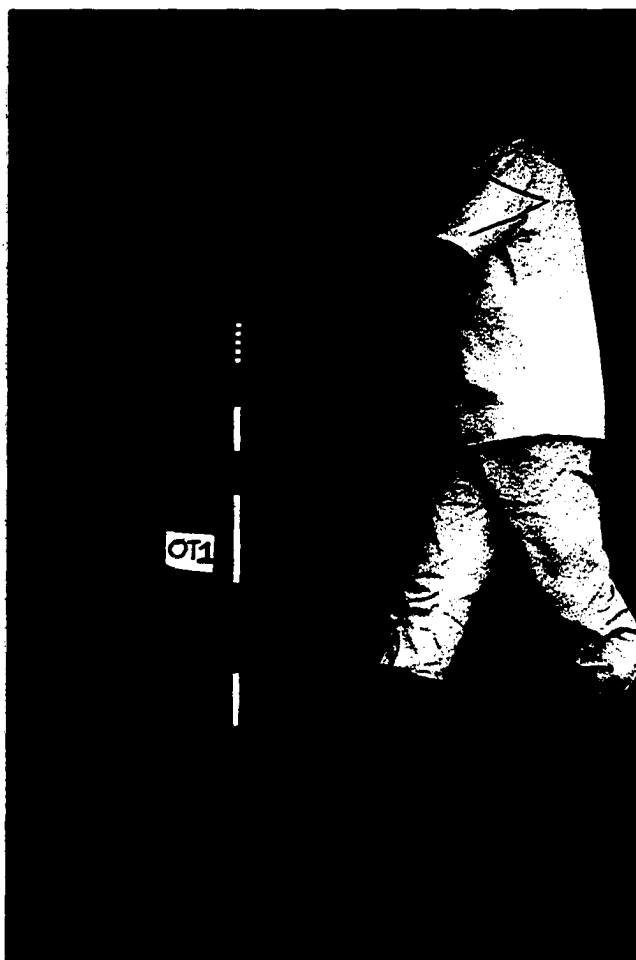


Figure 55. Photograph of typical composition of older terraces which deflect the course of the Rio Magui. Maximum cobble size is 32 cm, average is 7 cm. The white segments of the scale are 20 cm in length.

generally displaying a relatively high degree of rounding and sphericity, particularly of quartz grains. The unusually coarse sands in sample 25 are therefore attributed to an influx of sediment from the Rio Patia.

The final anomaly (sample 7), is significantly finer-grained than neighboring samples. The location of this sample coincides with a chute cut-off which is active at high flow conditions. As the river height increases during a rising flood-stage, water is diverted through a breach in the levee at this location and flows in a shallow channel across the neck of the meander before the rest of that meander's levees are flooded. Hence the bank sample collected at this point of diversion probably reflects sand deposited at different flood conditions than the other levee material analyzed.

c). Changes in Sorting

Sorting in the sands of levee samples along the study area exhibits two overlapping but distinct trends: 1) levee sands collected from Payan downstream to the mouth of the Rio Guañambi display relatively uniform sorting values, while 2) sands collected downstream from the mouth of the Rio Guañambi display pronounced decreasing values of sorting (Figure 56). The exceptions from these two trends are most of the samples related to eroding terraces and river junctions discussed earlier.

C. Discussion

Several of the parameters examined for this study are well documented by other workers in different climatic regimes. Most studies of variables pertaining to stream gradients have concentrated upon regional variations in slope rather than upon localized vari-

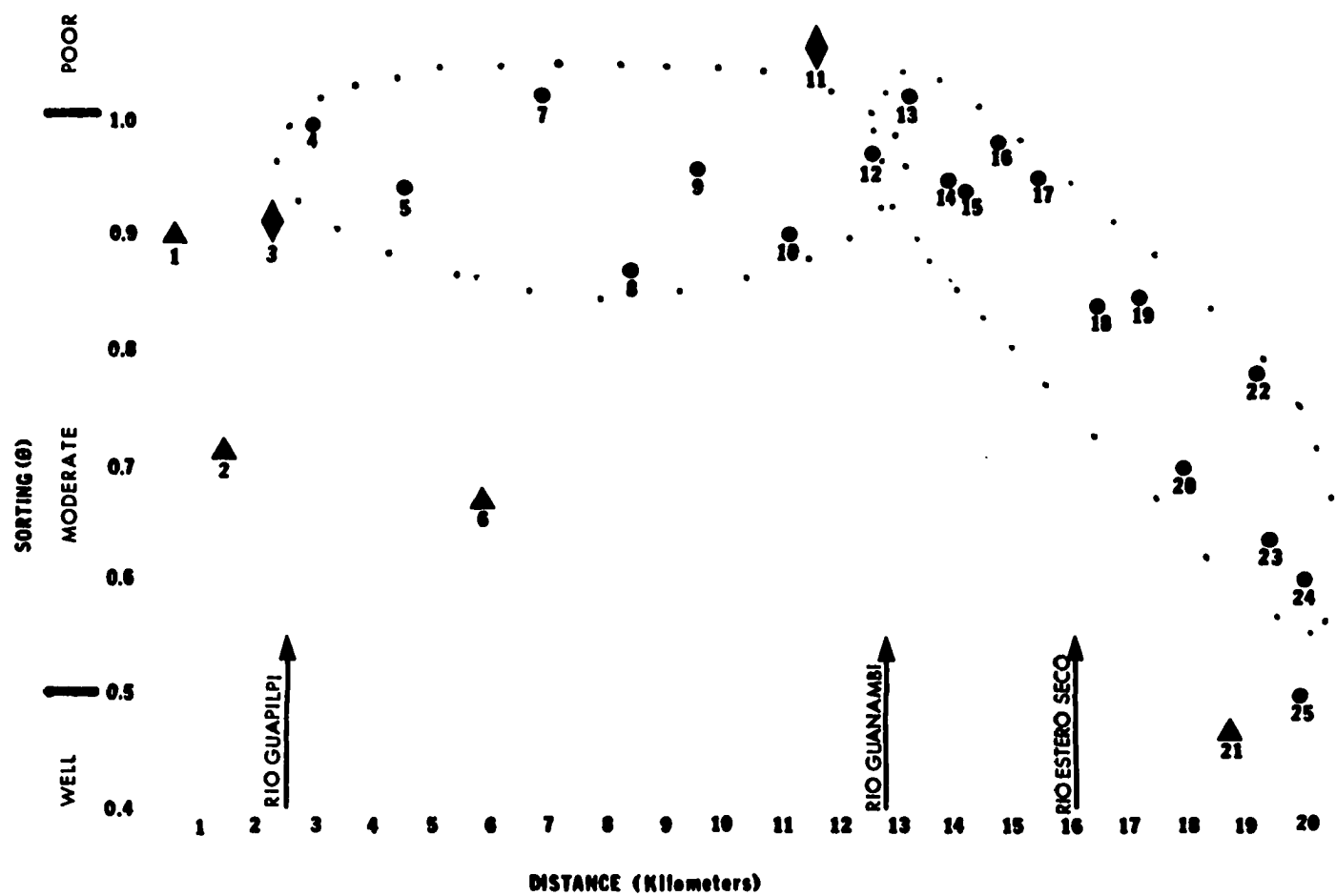


Figure 56. Plot of sorting versus downstream distance from Payan. Samples influenced (?) by terrace erosion less than 50 meters upstream: ▲ ; samples taken less than 50 meters downstream of tributary mouths: ◆ ; unaffected by external influences, ● .

ations (Prestegaard, 1983). It is generally accepted among geologists that river gradient tends to decrease with downstream distance (Leopold et. al., 1964; Schumm, 1977; Richards, 1982) in "normal" circumstances. Many early studies focused upon determining the cause for the "typical" concave character of longitudinal profiles. Sternberg (1875) concluded that decreasing downstream gradients are caused by a gradual diminishing of particle size for bed-load material in a downstream direction; Gilbert (1914) explained decreased gradients towards the lower reaches of a river primarily as a result of increased river discharges downstream. Not all streams exhibit a simple gently sloping, concave shape; several types of localized and regional variables along a river may exist and can influence stream gradients (Hack, 1957). Mackin (1948) discussed how the influx of tributaries into the main stream trunk will lower the stream gradient below the junction. Mackin also found that addition of sediments into the main trunk by tributaries, talus slides or terrace erosion will affect the hydraulic efficiency of the channel and concomitantly the entire stream gradient. On the other hand, Davies et. al., (1978) who discussed channel gradients for two rivers draining active volcanic regions in southern Guatamala, concluded that a hydrologic change in the stream (decreasing flood-water competence) was caused by decreasing slope. A major downstream decrease in grain size and sorting resulted. Several hydrologic variables within the river channel (e.g., roughness elements and resistance coefficients) are the most important influences on water-surface slope for five streams of the western United States (Prestegaard, 1982).

Morisawa (1962) discussed how any single path from the headwaters to a river mouth will display an irregular sequence of "line segments" with separate slope values, together which comprise a longitudinal stream profile. These line segments represent variability caused from tributary influx that increases trunk discharge.

On a broad scale, the Rio Magui decreases its gradient with downstream distance. Closer examination reveals, however, that the river slope is made of a series of straight line segments, each controlled by the water volume, sediment volume and sediment caliper being transported. Because the major break in stream gradient (Figure 54) coincides with the break in mean grain size and sorting data along the Rio Magui, two different depositional processes are believed to exist for the upper reach from Payan to the mouth of the Rio Guañambi, and the lower reach from this point downstream to the mouth of the Rio Magui. It is generally accepted that depositional processes (and the ensuing deposited material) will adapt to a change in channel slope. Therefore, the underlying question remains; "why does a major break in slope exist at the junction of the Rio Guañambi?". Three interrelated processes affect stream gradients along the Rio Magui: 1) The Rio Guañambi drains a relatively large basin (Figure 50), and its input into the Rio Magui adds a considerably greater amount of water into the main trunk. This influx could tend to decrease the channel slope. Thus, coarser material would cease to be transferred as it was upstream. 2) The stream load of the Rio Magui may be altered due to an influx of finer-grained material from the relatively low-relief Rio Guañambi basin. If so, a higher percentage of finer-grained material would be present, and the stream

would no longer be required to move as much bed-load material.

3) Localized uplift along the Rio Patia as it crosses a large anticline 15 km downstream of the Rio Magui results in a slight aggradation of the Rio Patia at the mouth of the Rio Magui. Many flooded tributary valleys seen along the Rio Patia and Rio Magui on both aerial photographs and radar imagery are formed by levees which can not be removed by the small discharge of the tributary networks (Whittecar et. al., 1984). Because of the relatively high discharge of the Rio Magui this aggradation would not dam the stream but would tend to flatten the gradient of the Rio Magui.

Between the junction of the Rio Gualpilpi and the junction of Piccinini Creek, the Rio Magui undergoes a significant decrease in slope to a gradient flatter than segments near the mouth of the river. The hypothesis that this flattening is caused by an increase in lateral stream processes is supported by the absence of channel bars as well as presence of several unusually sinuous and historically active meanders along this segment. Several explanations for the drop in gradient are possible: 1) Regional uplift, 2) Localized faulting, 3) Resistant sediments or bedrock in the channel and 4) Sediment input from the Rio Guapilpi.

Regional uplift is possible in this area considering the close proximity of the study area to the tectonically active Andes Mountains (Ramirez, 1975), but uplift usually influences a larger, more extensive area than the 700-meter segment of the river in question. Faulting may be responsible for the anomalous gradient in the stream being discussed. Numerous fracture traces crisscross the area (see Figure 12; also Barringer, in preparation). A major E-W lineament crosses

the Rio Magui at the downstream end of the flattened portion of the stream profile. If this lineament is a fault, recent uplift of the downstream side of the fault may have flattened the river gradient. However, the valley-bottom slope through this area does not change substantially. No single known factor adequately explains the flatter river slope and increased sinuosity between the Rio Guapilpi and Piccinini Creek; several causes may contribute to the apparent variations. Further investigation is needed to resolve this problem. The case for unusually resistant bedrock or sediment cut by the channel downstream of the relatively flat stretch is also not supportable by field data. No bedrock or any unusual accumulations of coarse gravel or obdurate oxbow-clay fillings were seen along this or any part of the Rio Magui. Although the Rio Guañambi provided a good explanation for a large change in gradient on the Rio Magui, the Rio Guapilpi can not. Its drainage area is small and geologically similar to the Rio Magui's to generate the volumes of water or fine-grained sediment needed to alter the Rio Magui's gradient so radically. Furthermore the effects of any such tributary input should probably influence downstream gradients farther downstream than is seen in this case. On the other hand, it is possible that large quantities of fine grained tailings from centuries of mining were carried by the Rio Guapilpi to the Rio Magui.

In order to determine whether sands which comprise modern levees along the Rio Magui were deposited by traction or suspension, shear and settling velocities were calculated. The following equation developed by Shields (1936) was used to determine shear velocities of

the Rio Magui at bank-full flow.

$$\text{Shear velocity} = U^* = \frac{U}{5.75 \log \frac{z}{k}}$$

The components for this equation are defined as follows:

U = The average velocity of the deepest part of the channel at bank-full flow.

z = The height of velocity measurement above the bed.

k = The bed roughness or ripple height (in this case 0.5 meters represents the maximum height of a sand wave; smaller values for "k" would decrease the resultant shear velocity).

At Payan the Rio Magui has the following values for the above mentioned components:

U = 180 centimeters per second

z = 120 centimeters

k = 50 centimeters

Thus the shear velocity for the Rio Magui at bank-full stage is:

$$U^* = \frac{180 \text{ cm/sec}}{2.18} = 82.3 \text{ cm/sec.}$$

Using an average water temperature for the Rio Magui of 20°C and the coarsest size (0.5 mm) in the levee deposits, the resulting settling velocity for this levee sand during flood conditions is approximately 7.5 cm/sec (Rouse, 1937 in Blatt et. al., 1980). Because the shear velocity is significantly greater than the settling velocity and the conditions for fully developed suspension is $W(\text{settling velocity}) \leq 0.8 U^*$ (Shields, 1936), it is apparent that levee sands along the Rio Magui were deposited from suspension.

In conclusion, two sets of depositional processes on levees exist along the river from Payan to the mouth of the Rio Magui. Those

processes active from Payan to the mouth of the Rio Guañambi deposit moderately sorted fine sand onto the levees at high flow conditions. The processes active from the junction of the Rio Guañambi downstream to the mouth of the Rio Magui are greatly influenced by an influx of finer-grained material which causes the stream gradient to adjust accordingly, and by regional uplift near the mouth of the Rio Patia which causes hydraulic ponding of Rio Patia flood waters into the main trunk of the Rio Magui.

CHAPTER IX

BACKSWAMP ENVIRONMENTS

Five sites in backswamp environments were selected along the Rio Magui for detailed analyses (Figure 57). For this study, a backswamp is defined as the low area adjacent to the river channel levees which is covered by water as the Rio Magui exceeds bank-full flow conditions. Backswamps along the Rio Magui are relatively flat with minor ridges and swales which generally trend parallel to the present river.

A. Methodology

1. Plane Table and Alidade

The sequence of minor ridges and swales characteristic of Rio Magui backswamps were mapped at each of the five sites with plane table and alidade. The purpose for these surveys was to pinpoint the exact lateral location and elevation of these topographic features and to designate localities for subsurface (auger) analysis.

2. Augering

A hand auger with 3 meters of extension pipe was used to analyze sediment samples at depth from each of the localities described earlier. Mean grain size, sorting composition and color characteristics were identified in the field for samples at each auger site.

Several unexpected problems inhibited the overall backswamp

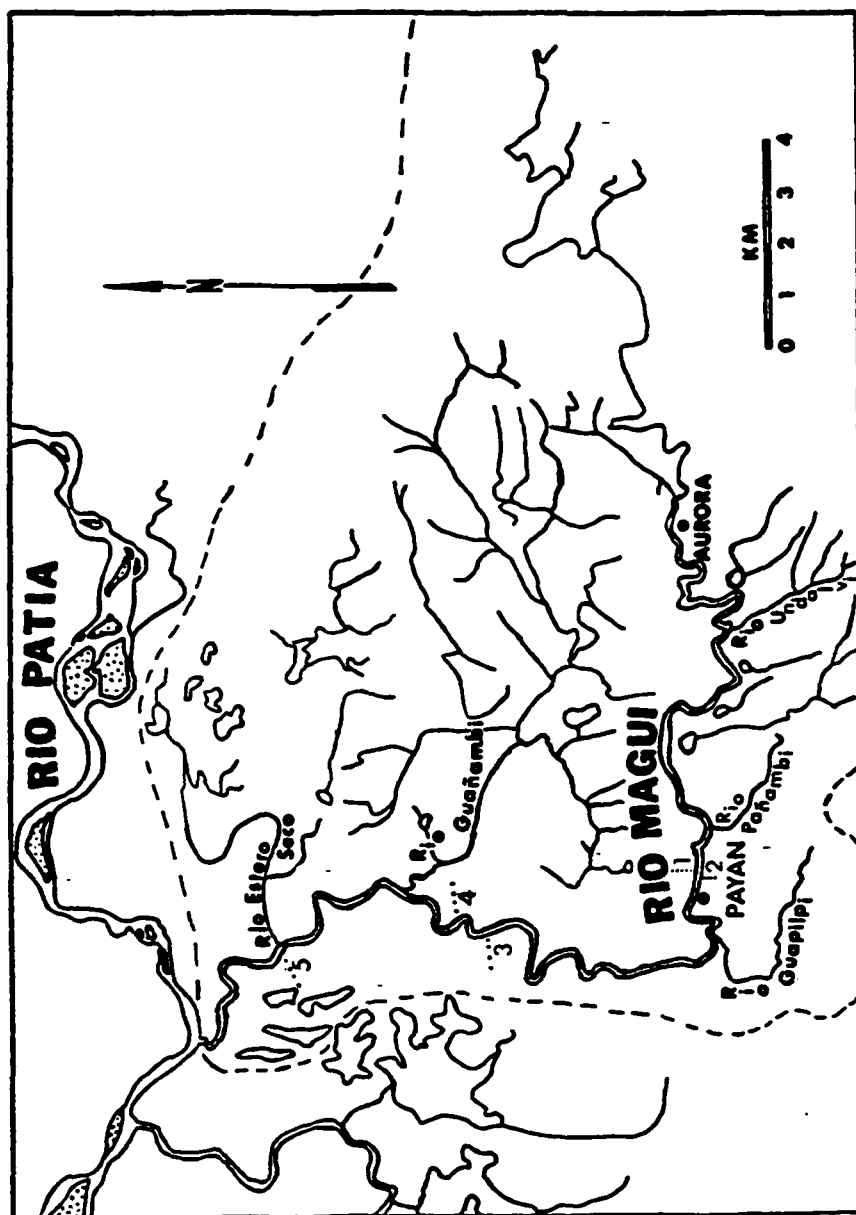


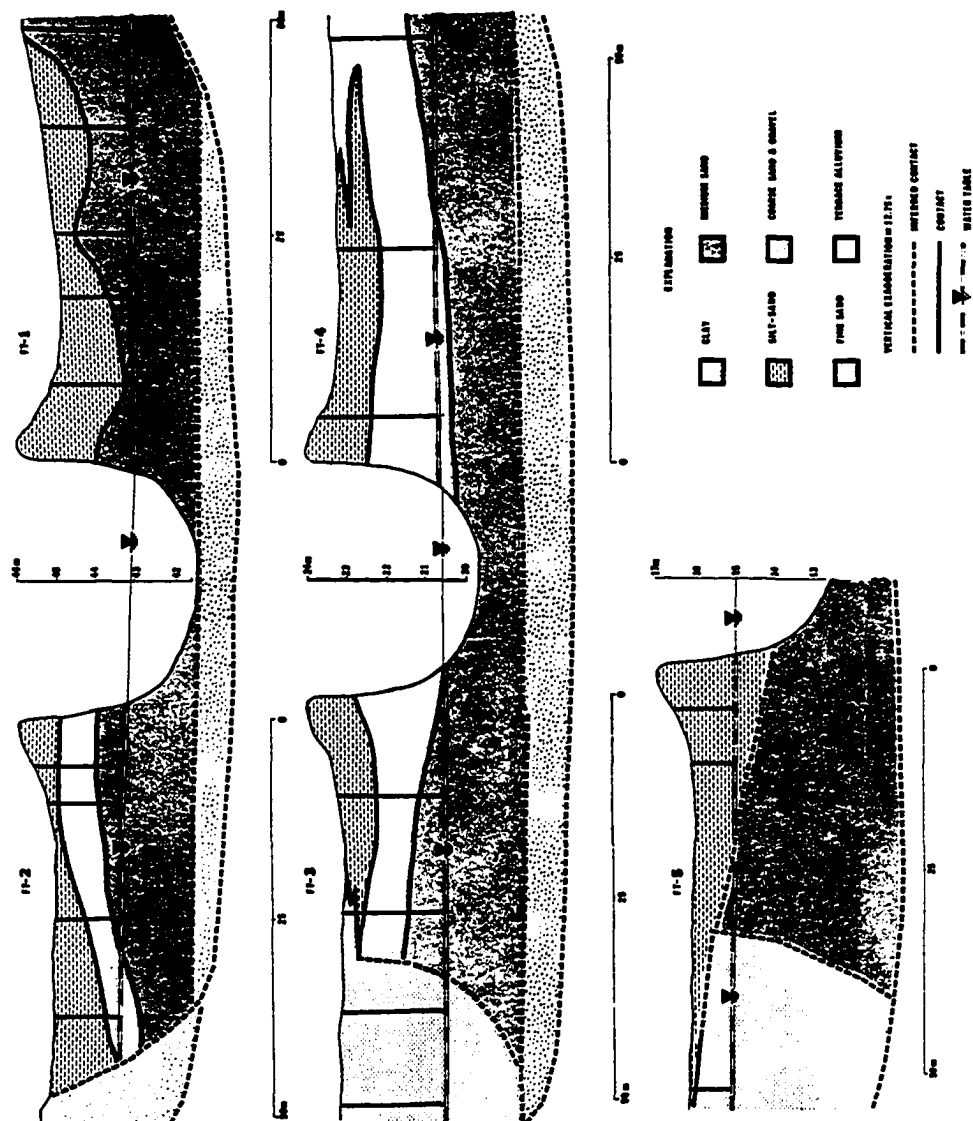
Figure 57. Location map of the five floodplain traverses along the Rio Magui.

analysis. Firstly, the selection of traverse sites was modified to avoid areas of active farming by local villagers. The majority of the inhabitants living along the Rio Magui depend on the produce which they cultivate on the river's floodplain and on whatever is available to eat from the surrounding rain forest. In order to avoid straining diplomatic relations with the villagers, only uncultivated segments of the floodplain were used. Also, of the remaining backswamp areas suitable for analyses, many were at (or near) the water table which inhibited augering. Areas near the channel margins were usually not saturated; sandy sediments located at depth at sites approximately 15 meters or more from the channel margins, however, were saturated and had virtually no cohesion. In addition, in order to prepare a working surface several villagers equipped with machetes were required to cut a path through the dense vegetation.

B. Results

Surficial floodplain deposits along the Rio Magui are generally composed of a silty, fine-grained sand. Additionally, several zones of clay exist along two of the floodplain traverses (FT-3 and FT-5). This surface layer overlies a bed of fine- or medium-grained sand up to 3 meters thick. Beneath the sand layers, a coarse-grained sand and gravel zone exists. This gravel comprises the bed of the Rio Magui from near the headwaters downstream to the junction of the Rio Estero Seco, where at this point, the channel bed is composed predominantly of sand due to the lower bed-flow velocities. As indicated on the cross-sections (Figure 58) the basal extent of the gravel is unknown.

Figure 58. Cross-section of the five floodplain
traverses along the Rio Magui.



While some areas of the Rio Magui's floodplain are suitable for field analysis, the majority are inaccessible backswamps or lakes (Figure 59) which generally exhibit two basic shapes. Large dendritic lakes (Figure 60) are especially prevalent in the backswamps from the mouth of the Rio Guañambi downstream to the mouth of the Rio Magui (Plates 4-6). Floodplains from Payan to the mouth of the Rio Guañambi (Plates 1-3) contain lakes which are generally smaller and irregular in shape (Figure 61).

C. Discussion

Although many floodplain deposits located in other regions display grain size characteristics similar to those observed along the Rio Magui, floodplain deposits exposed along the Rio Magui did not often show sedimentary structures (e.g., convolute bedding; climbing ripples; horizontal laminations) commonly seen elsewhere (McKee et. al., 1967). The reason for the absence of these sedimentary structures is generally unknown but may be due in part to periodic cultivation of the floodplain by the villagers.

Textural variations noted by workers in other regions were seen in Rio Magui bank exposures but not in augered holes. The depth of each auger hole was limited to the 3 meters of auger pipe available for this study which clearly was insufficient to fully penetrate the modern alluvial sequence (Figure 58). Additionally, the presence of the water table tended to cave-in the holes and further inhibited augering. If these two obstacles could have been overcome, coarse-grained sands and gravels would have been observed and the variations in grain size would be more apparent. Fortunately, bank-cuts exposed



Figure 59. Photograph of a wide backswamp along the Rio Magui at bank-full flow. Note the levee top marked by vegetation in the foreground.

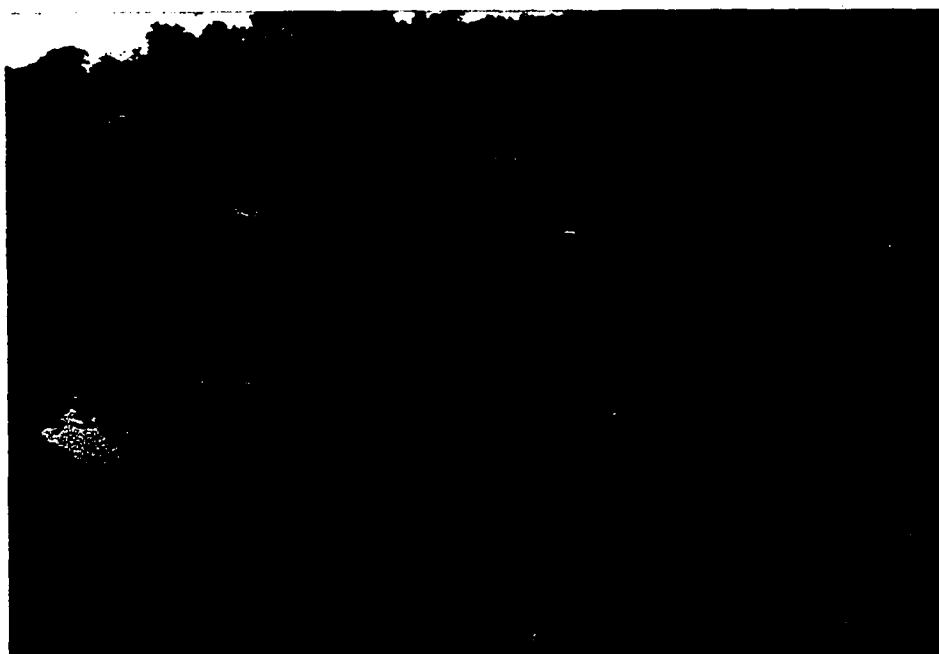


Figure 60. Photograph of dendritic lakes common to the Rio Magui floodplain from the junction of the Rio Guañambi downstream to the mouth of the Rio Magui. Note the dammed levee in the upper right corner.



Figure 61. Photograph of an irregular lake (center) representative of the segment of the Rio Magui located around the town of Payan.

during low-water flow (1/4-bank-full or less) exposed coarser material deposited in the channel bed along the majority of the Rio Magui (Figure 62), thus aiding in stratigraphic correlations beneath the surface of the floodplain beyond the extent of the boreholes.

In the first scientific analysis of the Rio Magui area (Isenor, 1941), several boreholes were drilled to depths up to 16.8 meters across the Rio Magui near Payan. They showed that floodplain muds overlie up to 15 meters of sand and gravel; approximately 1 to 2 meters beneath the Rio Magui floodplain. The present river has cut a channel less than 15 meters in depth into indurated sand (Darby, 1983). The majority of the material in this buried channel which is the modern channel in most instances, is comprised of fluvial gravels.

Many similarities exist between the floodplain transects located near Payan and the ones located downstream near the junction of the Rios Guañambi and Estero Seco. For instance, all transects show a general sequence of sandy silt or silty sand overlying either fine-grained or medium-grained sands which generally have the same overall thickness regardless of location downstream. Several differences do exist, however, which are worth mentioning at this time. Firstly, the transects downstream of Payan suggest that ox-bow cut-offs may exist based upon aerial photographs of the region and upon evidence of abrupt facies changes at depth, namely, the introduction of cohesive clay zones found at two traverse sites. Another difference between the transects near Payan and the others located further downstream is the absence of gravel along the channel bed. Apparently, flow velocities downstream of Payan beyond the junction of the Rio



Figure 62. Photograph of bank exposure near Payan at less than 1/4-bank-full stage delineating much of the modern alluvial sequence typical of the Rio Magui floodplains. Note the cross-bedded gravels underlying the cohesive silty sands in the stream bank.

Guañambi are insufficient to fully transport cobbles and other coarse-grained material (as discussed in Chapter VI). Contacts for the gravel near Payan are therefore based upon known bank exposures at low-water stage, while all other gravel contacts located along transects downstream of Payan are inferred due to lack of visual confirmation.

Three mechanisms are suggested for the formation of lakes on the floodplains of the Rio Magui. The first, and perhaps the most dominant, is the aggrading of drowned river channels. Recent slope adjustments of the Rios Patia and Magui and their adjoining tributaries due to localized uplift near the southwestern coast of Colombia have induced aggradation of levees upstream of the uplift and subsequent damming and flooding of large tributary valleys (Whittecarr *et. al.*, 1984). This regional uplift is believed to have influenced the Rio Magui from the junction of the Rio Guañambi downstream to the mouth of the Rio Magui and beyond. Many drowned river channels exist along this reach and subsequently form the large finger-like lakes which are common to this area. The second method for lake formation includes the surge of water over the levee tops during times of over-bank flooding. The daily torrents of rainfall characteristic of tropical climates and the relatively high water table also aid in keeping these low-lying areas submerged. Therefore, inundated portions of the floodplain rarely dry out and subsequently exist as pools of standing water. These pools or shallow lakes are generally small, appear irregular in plan view, and generally lie between minor topographic ridges which are believed to represent

remnants of older levee tops. Ox-bow lakes (half-moon shaped) formed by periodic shifting of the river channel, are infrequently represented on the Rio Magui's floodplains and seem to be more prevalent near the town of Payan.

CHAPTER X

SUMMARY AND CONCLUSIONS

The preceding chapters focus upon characteristics and processes of the Rio Magui. The depositional process model for the Rio Magui which follows is a summary of data described in earlier sections. This model is organized to explain which specific processes, features and characteristics form during the various stages of a flood. The following summary is based upon my observations and ideas as well as upon concepts of other workers developed elsewhere as described throughout the preceding nine chapters of this manuscript.

A typical flood along the Rio Magui can be sub-divided into four stages: 1) baseflow, 2) rising limb, 3) flood peak, and 4) falling limb. Near Payan, baseflow conditions (less than 1/4-bank-full flow) usually develop within approximately 15 hours after cessation of major rain storms (13 cm/day); discharge measurements and suspended sediment concentrations are at a minimum, usually less than $25\text{m}^3/\text{sec}$ and 18 mg/l, respectively. Such low-flow conditions occurred during 25% of the period studied and exposed all channel bars and many riffles along the Rio Magui. Because only fine-grained sand and some suspended sediments are transported during these flow conditions, almost no sedimentary structures form during this stage. Helical flows and eddies are smaller and less vigorous than during greater flows.

The rising limb stage is characterized by increasing river heights that begin to rise within one hour of a significant rain. Depending upon the intensity and duration of the precipitation, discharge varies between 25 and $325\text{m}^3/\text{sec}$. Suspended sediment concentrations often increase rapidly to as much as 260 mg/l. As the river rises, relatively small channel bars devoid of vegetation and topographic relief are submerged leaving only the larger, vegetated islands partially emergent. It is very possible that during rising limb flow conditions, sedimentary structures are formed. Unfortunately, few of these structures are preserved due to scour by greater flows during the floods peak. As velocities continue to increase, medium- and coarse-grained sand and some pebbles are probably transported with the river flow. Deepening pools and increasing channel widths create additional, more vigorous eddies and helical flows than previously existed during baseflow conditions.

The flood peak represents the interval with greatest transportational and erosional capacity. During this period, river stage height is at or greater than 3/4-bank-full flow conditions. The majority of the floods along the Rio Magui do not breach the top of the levees. Larger floods that flow overbank are the ones which form the levees. Generally, river discharges may become greater than $325\text{ m}^3/\text{sec}$ while suspended sediment concentrations can exceed 260 mg/l. High discharges such as these primarily scour and transport coarse-grained sediments including cobbles and boulders along the channel bar. The surfaces of all river channel bars during the flood peak are typically submerged. Furthermore, the main flow around a meander bend may be diverted through a chute or neck cut-off as described earlier. During

the flood peak for large floods that flow over the levee tops, flow travels across the floodplain and may deposit fine-grained sands carried in suspension as far as 45 meters away from the channel. Numerous helical flows and eddies are visible on the surface of the river, especially over submerged river channel bars. These eddies and helical flows represent the highest velocities for flows characteristic of this interval.

The final stage of a typical Rio Magui flood, the falling limb, is further divided into three unique flow regimes which have successively diminishing discharges. Immediately after the flood peak, relatively low-intensity upper flow regime conditions prevail. During this period river discharges and suspended sediment concentrations drop to as low as $140 \text{ m}^3/\text{sec}$ and 120 mg/l , respectively. If the flood went overbank, when river heights drop to below bank-full conditions, the flow of water over the floodplain ceases although fine-grained deposition on the floodplain continues.

During this part of the falling limb, all but a select few of the larger channel bars along the Rio Magui remain submerged. The formation of large-scale cross-bedding by the migration of sand-waves and lunate megaripples probably occurs during this interval followed by the formation of lunate and lingoid ripples as velocities continue to drop. Larger material such as boulders, cobbles, and pebbles that could be transported as bed-load only during the flood peak are deposited along what will become visible as the channel bar margins during low flows. Eddies and helical flows continue to transport and erode sediment along the channel. This

initial division of the falling limb is expressed by the sedimentary structures found along the channel bars as previously mentioned. On bars where large-scale cross-bedding or other varieties of large-scale sedimentary structures are not represented, it is possible that velocities dropped very rapidly following the flood peak, that the flood in question did not generate velocities (depths) sufficient to produce large structures, or that slower flows reworked the sand waves and megaripples into smaller bedforms.

Following this initial division of the falling limb is a relatively high-intensity low-flow regime interval. River height continues to diminish to approximately 3/4-bank-full flow while discharge and suspended sediment concentrations decrease as well ($75 \text{ m}^3/\text{sec}$ and 65 mg/l , respectively). Smaller channel bars still remain submerged, but larger bars begin to emerge. The sedimentary structures which form during these flow conditions include primarily undulatory ripples composed of coarse- and medium-grained sand. All of the previous flood stages maintain organic matter in suspension. During this interval, however, leaves moving at depth and at the water's surface by helical flows collect in eddies on the lee sides of point and side bars. Standing water on the backswamps continues to recede and may form irregular-shaped lakes in the low-lying portions of the floodplain; suspended sediments will continue to settle out from these waters.

The final episode of a receding flood along the Rio Magui is a relatively low-intensity low flow regime. River discharge is at a minimum (approximately $25 \text{ m}^3/\text{sec}$) as it was during the baseflow

stage, but the suspended sediment concentrations can be comparatively higher than immediately before the flood (40 mg/l). The stage height is approximately 1/2-bank-full flow, and most of the channel bars along the river are partially exposed. The initial sedimentary structures which form during this interval are straight-crested ripples which produce small ripple cross-beds. As river flow drops further, heavy mineral laminations are winnowed out along the channel margins and channel bar edges. The dominant type of sediment transported during this period is probably fine-grained sand. Helical flows and eddies continue to transport and deposit organic debris as described earlier. On top of the backswamps, partial drying of some of the irregular lakes may occur, but the frequent recurrence of subsequent flooding and almost daily rainfall generally inhibit floodplain desiccation.

The preceding summary describes major depositional processes active within the Rio Magui from the headwaters to the river mouth. It is appropriate to point out, however, that lateral differences in timing and intensity of processes do exist. Most of these variations appear to be due to the increase of discharge downstream and to external factors that influence stream behavior such as the possible hydraulic ponding that may occur along the lower third of the Rio Magui.

"Does this suite of processes described for the Rio Magui adequately represent a typical model for rivers located in the humid tropics?" Although many authors discuss several specific processes active along rivers throughout the humid tropics, no one to date has

proposed a complete depositional model for rivers in tropical climates that might serve as a basis for comparison. Therefore, in order to answer the proposed question, the major depositional processes of the Rio Magui will be compared to fluvial processes documented elsewhere by other workers in similar tropical regimes.

For the most part, the Rio Magui model contains processes and characteristics similar to those found within other tropical streams. For instance, Pain (1969, in Douglas, 1977) documented rates of precipitation for high-intensity, high magnitude tropical rainstorms of the Orere catchment of north-east New Zealand which closely parallel precipitation rates in the Payan region. Douglas (1977) discussed how moments of highest discharge are associated with highest concentrations of suspended sediments for a large flood along the Barron River in the humid tropics of north Queensland, Australia. As mentioned earlier in Chapter II, a similar situation exists for floods along the Rio Magui.

Budel (1977) explains that most lakes found in the humid tropics generally have an outlet leading to a tributary. As explained earlier in Chapter IX, this is generally not the case for lakes on Rio Magui backswamps, particularly along the lower third of the Rio Magui near the Rio Patia. A few of the floodplain lakes near Payan, however, do have outlets that lead to a tributary channel. A rare documentation of several lakes along the Pahang River in west Malaysia (Douglas, 1977) shows that lakes form when levees block the outlets of tributary channels due to great quantities of sediment deposition onto the levee tops during floods. Unfortunately, Douglas does not

offer an explanation for the cause of the excess deposition. This occurrence of blocked outlets closely parallels the formation of lakes within the backswamps of the Rio Magui from the junction of the Rio Guañambi downstream to the mouth of the Rio Magui.

While many processes and characteristics along the Rio Magui are similar to those active in other tropical streams, several distinct differences exist. For instance, Douglas (1977) noted that most meandering streams located in tropical rain forests display relatively high sinuositities such as the Horrigan Creek in north Queensland, Australia. Recent work by Baker (1978) also supports this idea. As previously discussed in Chapter III, the Rio Magui has a relatively low sinuosity (1.3); its channel morphology is greatly dependent upon the location of large terraces which restrict many segments of the present river. Another interesting difference between the Rio Magui and other tropical streams is the abundance of gravels as bed-load within the channel. Kajetenowicz (1958, in Douglas, 1977) and Baker (1978) note the general absence of bed-load in meandering tropical streams. Regional tectonism towards the Pacific coast may induce low stream gradients along the Rio Magui that inhibit necessary stream velocities required to transport coarse-grained sediments.

Perhaps the most unusual difference between Rio Magui processes and processes found along other tropical streams, is the textural trends unique to Rio Magui levee samples. As described previously in Chapter VIII, abrupt changes in stream gradient near the junction of the Rio Guañambi due to tectonic uplift along the Rio Patia

and adjoining areas may alter the mean grain size and sorting trends in levee samples on the Rio Magui. Clearly these trends differ with other textural trends common to many rivers located elsewhere which generally exhibit decreasing grain size and improving sorting trends with downstream transport. Once again, active tectonism common to southwest Colombia is believed to account for the unusual textural trends of the Rio Magui levee sands.

In conclusion, the Rio Magui is a meandering tropical stream which originates in the coastal lowlands of southwest Colombia and continually reworks older sediments deposited by the ancestral Rio Patia, a large high-gradient river originating in the Cordillera Occidental to the east. Generally the depositional model proposed for the Rio Magui adequately agrees with processes active along other tropical and temperate zone streams located elsewhere. Recent slope adjustments of the Rio Magui caused by tectonic uplift towards the Pacific Coast have induced significant differences in deposits and landforms which are unique to the Rio Magui. Because of these characteristics, it appears that no single model can fully explain or define a complete and standardized set of depositional processes and features for a "typical" tropical stream.

REFERENCES CITED

- Allen, J. R. L., 1963. Asymmetrical ripple marks and the origin of water-laid cosets of cross-strata. *Liverpool Manchester Geological Journal*, vol. 3, no. 2, 187 p.
- _____, 1965. A review of the origin and characteristics of recent Alluvial Sediments. *Sedimentology*, vol. 5, p. 89-191.
- _____, 1968. Current ripples: Their relations to patterns of water and sediment motion. *Amsterdam, Holland*, 433 p.
- Arango, J. L. and Ponce, M., 1982. Mapa Geologico Generalizado del Departamento de Nariño. Inst. Nat. de Invest. Geológico-Mineras, Bogota.
- Baker, V. R., and Penteado-Orellana, Margarida Maria, 1978. Fluvial sedimentation conditioned by Quaternary climatic change in Central Texas. *Journal of Sedimentary Petrology*, vol. 48, no. 2, p. 433-451.
- Barringer, R. A. (in preparation). The sedimentologic character, depositional history, and stratigraphic correlation of auriferous alluvial terraces near Payan, Southwestern Colombia.
- Blatt, H., Middleton, G. and Murray, R., 1980. Origin of Sedimentary Rocks. Prentice-Hall, Inc., Englewood Cliffs, New Jersey, 781 p.
- Bogen, J., 1980. The hysteresis effect of sediment transport systems. *Norsk Geografisk Tidsskrift*, vol. 34, p. 45-54.
- Büdel, Julius, 1977. *Klima Geomorphologic*. Borntraeger, 1 Berlin-7 Stuttgart, 443 p.
- Carson, M. A., Taylor, C. H. and Grey, B. J., 1973. Sediment production in a small Appalachian watershed during spring run-off: The Eaton Basin, 1970-1972. *Canadian Journal of Earth Sciences*, vol. 10, p. 1707-1734.
- Clifton, H. Edward, 1969. Beach Lamination: Nature and Origin. *Marine Geology*, vol. 7, p. 553-559.
- Collinson, J. D., 1970. Bedforms of the Tana River, Norway. *Geogs. Annals.*, vol. 52-A, p. 31-56.
- Collinson, J. D. and Thompson, D. B., 1982. Sedimentary Structures, George Allen & Unwin, London, 194 p.

- Conybeare, C. E. B., and Crook, K. A. W., 1968. Manual of Sedimentary Structures, Commonwealth of Australia. Dept. of National Development, Bureau of Mineral Resources, Geology and Geophysics. Bull. No. 102, 75 p.
- Darby, D. A., 1982. Bathymetric map of the Rio Magui at Payan, Colombia, South America. Old Dominion University Research Foundation Technical Report.
- _____, 1983a. Hydrologic assessment of the planned hydraulic mining along the Rio Magui, S. W. Colombia, S. A. Old Dominion University Research Foundation Technical Report GSTR-83-1, 11 p.
- _____, 1983b. Geology and sedimentology of the Rio Magui terraces near Payan, Colombia, South America. Old Dominion University Research Foundation Technical Report GSTR-83-3, 24 p.
- Darby, D. A. and Whittecar, G. R., 1984a. Envir impact of the proposed mining at Payan, Nariño, Colombia. Old Dominion University Research Foundation Technical Report GSTR-84-1, 47 p.
- Darby, D. A. and Whittecar, G. R., 1984b. Geology and Gold Evaluation of the Payan Mining District, Nariño, Colombia. Old Dominion University Research Foundation Technical Report GSTR-84-11, 98 p.
- Darby, D. A., and Wobus, H. B., 1976. A versatile computer program for sediment size analysis. Old Dominion University Research Foundation Technical Report No. PGS-TR-GE-76-25, 44 p.
- Davies, David K., Vessel, Richard K., Miles, Robert C., Foley, Michael G., and Bonis, Samuel B., 1978. Fluvial transport and downstream sediment modifications in an active volcanic region. C. S. P. G. Memoir No. 5, p. 61-84.
- Davies, T. R. H., and Tinker, C. C., 1984. Fundamental characteristics of stream meanders. Geol. Soc. Amer. Bull. vol. 95, No. 5, p. 505-512.
- Dietrich, W. E., and Smith, J. D., 1983. Influence of the Point Bar on flow through curved channels: Water Resources Research, v. 19, p. 1173-1192.
- Doeglas, D. J., 1962. The structure of sedimentary deposits of braided rivers. Sedimentology, vol. 1, p. 167-190.
- Douglas, Ian, 1977. Humid Landforms. The MIT Press, Cambridge, Massachusetts, 288 p.
- Dunne, T. and Dietrich, W., 1982. Sediment sources in tropical drainage basins. American Society of Agronomists Special Publication No. 43, p. 41-55.

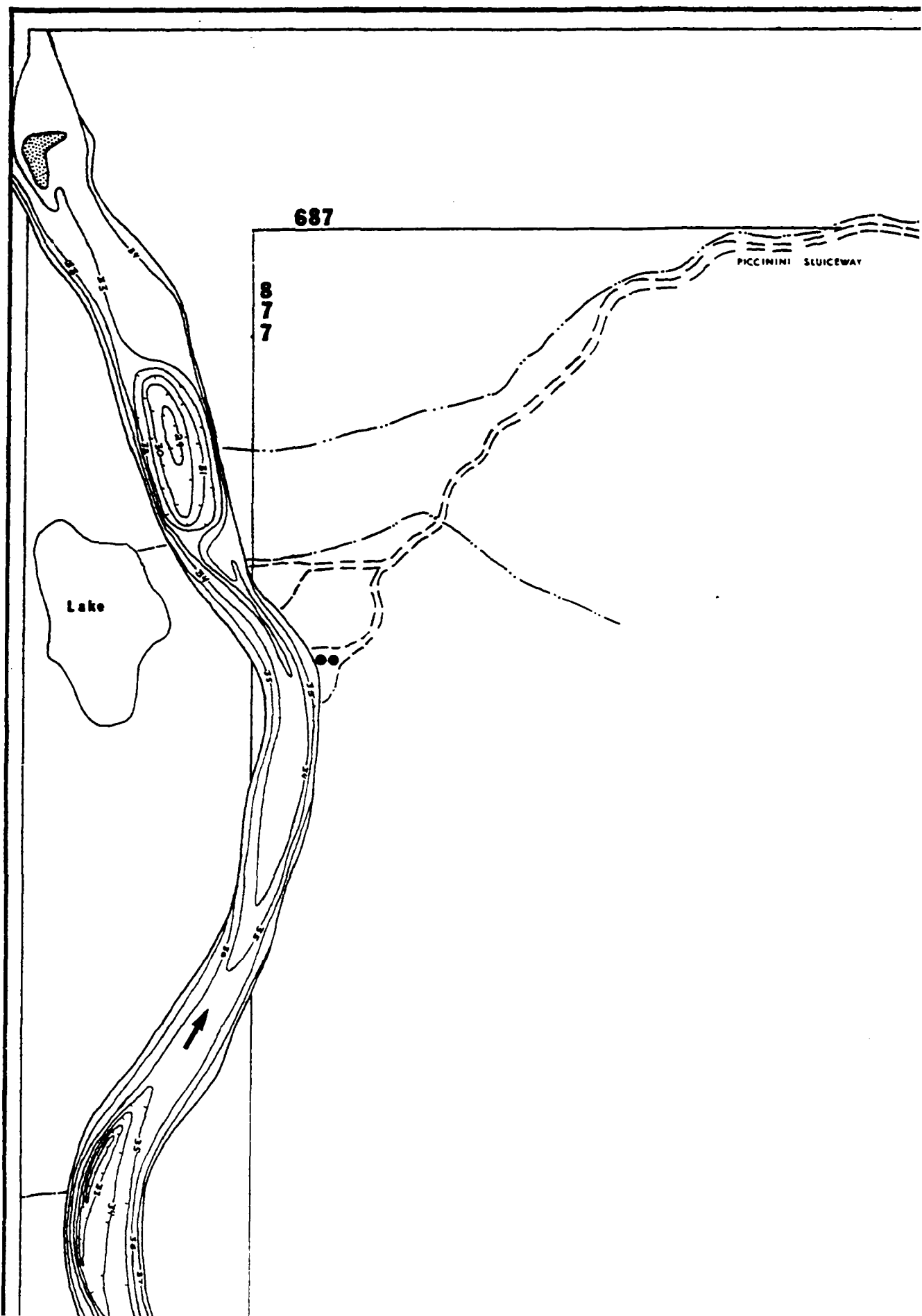
- Ferguson, R. I., 1976. Disturbed periodic model for river meanders: *Earth Surface Processes*, vol. 1, p. 337-347.
- Fisk, H. N., 1947. Fine grained alluvial deposits and their effects on Mississippi River activity. Mississippi River Commission, Vicksburg, Mississippi, 82 p.
- Folk, R. L., and Ward, W. C., 1957. Brazos River Bar: A study in the significance of grain size parameters: *Jour. Sed. Pet.* vol. 27, p. 3-26.
- Folk, R. L., 1974. Petrology of Sedimentary Rocks. Hemphill Publishing Company, Austin, Texas, 182 p.
- Freidman, G. M., 1961. Distinction between dune, beach and river sands from their textural characteristics. *Jour. Sed. Pet.*, vol. 31, p. 514-529.
- Froehlich, H. A., 1971. Logging debris--managing a problem. In: *Forestry land uses and stream environments a symposium*. J. T. Krygier and J. D. Hall, (eds.), Oregon State University, Corvallis, Oregon, p. 112-117.
- Gary, Margaret, McAfee, Robert, Jr., and Wolf, C. L. (eds.), 1972. *Glossary of Geology*: American Geological Institute, 805 p.
- Ghosh, A. K. and Scheidegger, A. E., 1971. A study of natural wiggly lines in hydrology: *Jour. of Hydrol.*, vol. 13, p. 101-126.
- Gilbert, G. K., 1914. The transportation of debris by running water. U. S. G. S. Prof. Paper 86, 263 p.
- Gupta, A., 1975. Stream characteristics in Eastern Jamaica. An Environment of seasonal flow and large floods. *American Journal of Science*, vol. 275, p. 825-847.
- Hack, J. T., 1957. Studies of longitudinal stream profiles in Virginia and Maryland: U. S. Geol. Sur. Prof. Paper 294-B, 97 p.
- Häntzschel, W., 1938. Bau und Bildung Von Grob-Rippeln im Watten-Meer. *Senckenbergiana* 20, p. 1-42.
- Harms, J. C., 1969. Hydraulic significance of some sand ripples. *Geol. Soc. Am. Bull.*, vol. 80, p. 363-396.
- Harms, J. C. and Fahnestock, R. K., 1965. Stratification, bedforms, flow phenomena (with an example from the Rio Grande). *S. E. P. M. Spec. Pub.* 12, p. 84-115.

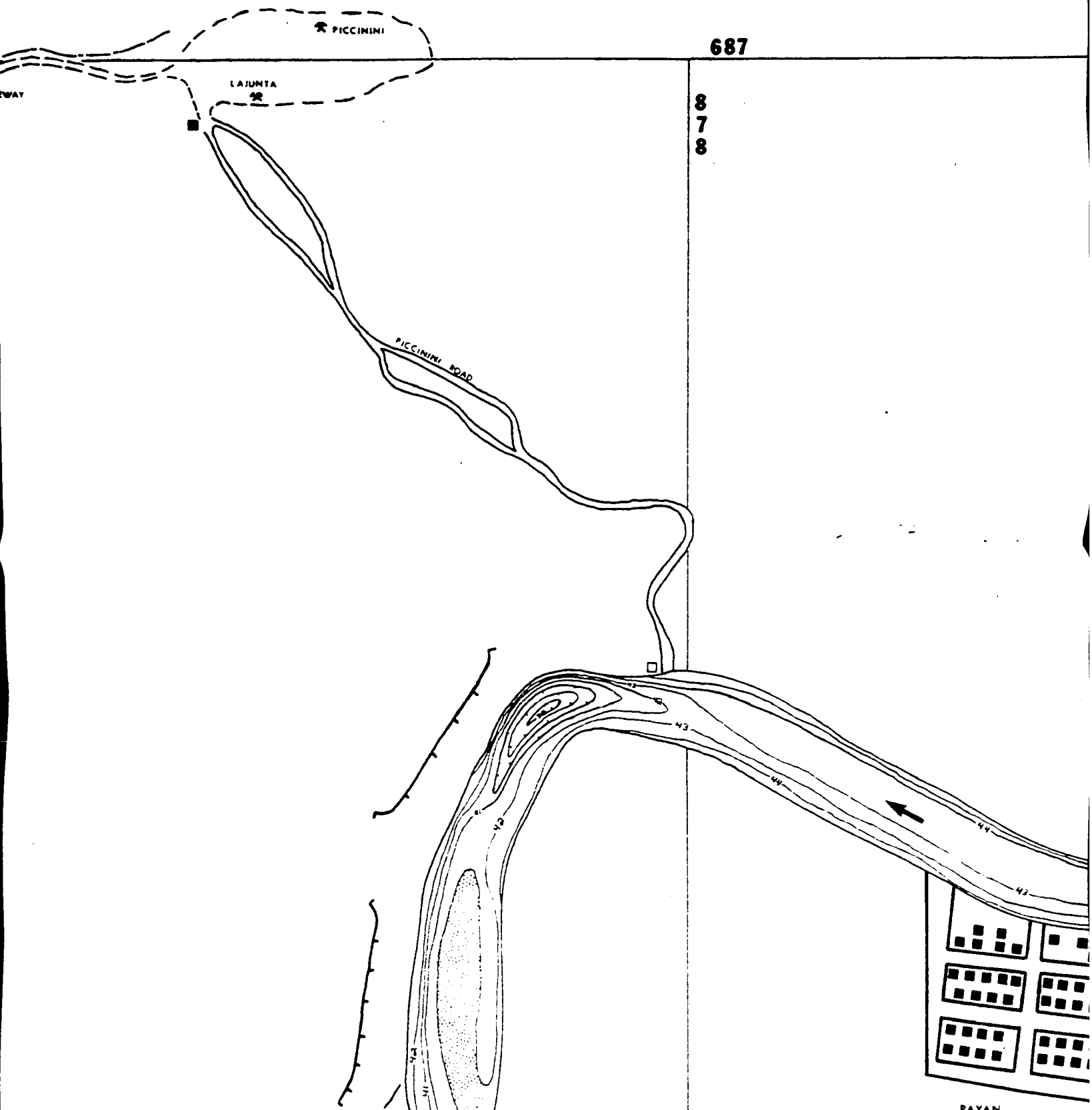
- Harms, J. C., Southard, J. B., Spearing, D. R. and Walker, R. G., 1975. Depositional environments as interpreted from primary sedimentary structures and stratification sequences. Soc. Econ. Paleon. Mineral Spec. Pub. No. 2, 226 p.
- Inman, D. L., 1949. Sorting of sediments in the light of fluid mechanics: Jour. Sed. Pet., vol. 19, p. 51-70.
- Isenor, A., 1941. Cross-sections through drill lines, Magui River, Unpubl. doc. Compañía Minera de Nariño.
- Kajetenowicz, A., 1958. La dependance de la grosseur de la granulation du materiel du lit dans les rivieres montagneuses de leurs qualites physiographiques Publs. Ass. Int. Hydrol. Scient., vol. 43, p. 323-326.
- Keller, E. A. and Tally, T., 1979. Effects of large organic material on channel form and fluvial processes in the coastal redwood environment, in: Rhodes, D. D., and Williams, G. P. (eds.), Adjustments of the Fluvial System: Kendall Hunt Company, Dubuque, Iowa, p. 169-197.
- Krumbein, W. C., 1934. Size frequency distribution of sediments: Jour. Sed. Pet., vol. 4, p. 65-77.
- Lammel, R. F., 1972. Natural debris and logging residue within the stream environment. M. S. thesis, Oregon State University, Corvallis. 49 p.
- Lane, E. W., 1957. A study of the shape of channels formed by natural streams flowing in erodable material. M.R.D. Sediment Series No. 9, U. S. Army Engineer Division, Missouri River, Corps Engineers, Omaha, Nebraska.
- Langbien, Walter B., and Leopold, Luna B., 1966. River meanders-theory of minimum variance, U. S. G. S. Prof. Paper 422-H.
- Leopold, Luna B., and Wolman, M. G., 1957. River channel patterns: braided, meandering, and straight. U. S. Geol. Surv. Prof. Paper, 282-B.
- Leopold, Luna B., Wolman, M., Gordon and Miller, John P., 1964. Fluvial Processes in Geomorphology, W. H. Freeman and Company, San Francisco, 517 p.
- Lisle, T., 1979. A sorting mechanism for a riffle pool sequence. Geol. Soc. Amer. Bull., vol. 90, p. 1142-1157.
- Ljunggren, P. and Sundborg, A., 1968. Some aspects on fluvial sediments and fluvial morphology. II A study of some heavy mineral deposits in the valley of the river Lule Alv: Geog. Annaler, vol. 50, p. 121-135.

- Mackin, J. H., 1948. The concept of the graded river: Geol. Soc. Amer. Bull., vol. 59, p. 463-512.
- McKee, E. D. and Weir, G. W., 1953. Terminology for stratification and cross-stratification in sedimentary rocks. Geol. Soc. Amer. Bull. 64, p. 381-390.
- McKee, E. D., Crosby, E. J., Berryhill, H. L., 1967. Flood Deposits, Bijou Creek, Colorado. Jour. Sed. Pet., vol. 37, p. 829-851.
- Middleton, G. V., 1976. Hydraulic interpretation of sand size distributions: Jour. Geol., vol. 84, p. 405-426.
- Morisawa, M., 1962. Quantitative geomorphology of some watersheds in the Appalachian Plateau. Geol. Soc. Amer. Bull., vol. 73, p. 1025-1046.
- Mueller, J. E., 1968. Introduction to hydraulic and topographic sinuosity indexes. Annals of the Association of American Geographers, vol. 58, p. 371-385.
- Ortiz, Hernan, 1982. Proyecto Payan, Reconocimiento geologico de depositos de placer: Progress Report No. 1, Compañia Minera de Colombia y Texas, S. A., Inc., 13 p.
- Pain, C. F., 1969. The effect of some environmental factors on rapid mass movement in the Hunua Ranges, New Zealand. Earth Sci., J., Vol. 3, p. 101-107.
- Passega, R., 1957. Texture as characteristics of clastic deposition. Am. Assoc. Petrol. Geol. Bull., v. 41, p. 1952-1984.
- Pettijohn, F. J., 1957. Sedimentary Rocks. Harper & Row, New York, 718 p.
- Potter, P. E., Pettijohn, E. F., 1963. Paleocurrents and basin analysis. Berlin-Gottingen-Heidelberg: Springer, 296 p.
- Prestegard, K. L., 1982. Variables influencing water surface slope in gravel and coarse sand streams (Ph.D. Thesis): Berkeley, California, University of California, 150 p.
- _____, 1983. Variables influencing water-surface slopes in gravel-bed streams at bankfull stage. G. S. A. Bull., vol. 94, no. 5, p. 673-678.
- _____, 1984. Progress in understanding fluvial processes. Jour. Geol. Educ., vol. 32, p. 254-260.

- Quenstedt, W., 1927. Beiträge zum Kapitel fossil And sediment vor und bei der Einbettung. Neues Jahrb. Mineral Etc., Beil., vol. 58B, p. 253-432.
- Ramirez, Emilio Jesus, 1975. Historia de los terremotos en Colombia. Instituto Geografico "Augustin Codazzi", 250 p.
- Raudkivi, A. J., 1963. Study of sediment ripple formation. Am. Soc. Civ. Engrs. Proc., Hyg. 89, p. 15-34.
- Reading, H. G., 1978. (Ed.) Sedimentary Environments and Facies. Elsevier North-Holland, Inc., New York, N. Y., 557 p.
- Reineck, H. E., 1963. Sedimentgefüge Im Bereich der südlichen Nordsee. ABH. Senckenbergische naturforsch. Ges. 505, 138 p.
- Reineck, H. E. and Singh, I. B., 1975. Depositional sedimentary environments. Springer-Verlag Berlin, Heidelberg, New York, 439 p.
- Richards, K. S., 1978. Simulation of flow geometry in a riffle-pool stream. Earth Surface Processes, vol. 3, p. 345-354.
- _____, 1982. Rivers: Form and process in alluvial channels. Methuen and Co., Ltd., London, 358 p.
- Rouse, Hunter, 1937. Nomogram for the settling velocities of spheres. Div. Geol. Geo. Exhibit D, Rept. Comm. Sedimentation (1936-1937) Natl. Res. Council, Washington, D. C., p. 57-64.
- Schindewolf, O. H., 1928. Über volborthella tenuis Schm. Palaeontol., Z., vol. 10, p. 1-68.
- Schumm, S. A., 1977. The Fluvial System. John Wiley & Sons, New York, N. Y., 337 p.
- Seilacher, D., 1959. Fossilien als Strömungsanzeiger. Aus Der Heimat, vol. 67, p. 171-177.
- Shields, A., 1936. 'Anwendung der Aehnlichkeitsmechanik und der turbulenzforschung auf die geschiebebewegung', Mittheilung der Preussischen versuchsanstalt fuer Wasserbau und Schiffbau, Heft 26, Berlin.
- Smith, David Ingle and Stoop, Peter, 1978. The River Basin: An introduction to the study of hydrology. Cambridge University Press., London, 120 p.
- Sternberg, H., 1875. Untersuchungen über Längen-und Querprofil Geschiebeführende Flüsse, in: Zeitschrift für Bauwesen, vol. 25, p. 483-506.

- Swanson, F. J., Lienkaemper, G. W. and Sedell, J. R., 1976. History, physical effects and management implications of large organic debris in western Oregon streams. U. S. D. A. For. Serv. Gen. Tech. Rep. PNW-56, 15 p.
- Swanston, D. N., and Swanson, F. J., 1976. Timber harvesting, mass erosion and steep-land forest geomorphology in the Pacific Northwest, In: Geomorphology and Engineering D. R. Coates, (ed.), Dowden, Hutchinson and Ross, Inc., Stroudsburg, PA. p. 199-221.
- Tanner, W. F., 1960. Shallow water ripple mark varieties. Jour. Sed. Pet., vol. 30, p. 481-485.
- Thakur, T. R., and Scheidegger, A. E., 1968. A test of the statistical theory of meander generation: Water Resources Research, v. 4, p. 317-329.
- _____, 1970. Chain model of river meanders: Jour. of Hydrol., vol. 12, p. 25-47.
- Trusheim, F., 1931. Versuche über transport und ablagerung von mollusken. In: Lüders, K., Truseim, F., (eds.), Beiträge zur Ablagerung Mariner mollusken in der flachsee. Senckenbergiana, vol. 13, p. 124-139.
- Udden, J. A., 1914. Mechanical composition of clastic sediments. Geol. Soc. Amer. Bull., v. 25, p. 655-744.
- Visher, G. S., 1956. Fluvial processes as interpreted from ancient and recent fluvial deposits. Soc. of Econ. Paleon. and Miner. Spec. Pub., No. 12, p. 116-132.
- Wallis, I. G., 1978. The random component in stream meandering: Water Resources Bulletin, v. 14, p. 576-586.
- Wasmund, E., 1926. Bioconose und Thantoconose. Arch. Hydrobiol., vol. 17, p. 1-116.
- West, Robert C., 1957. The Pacific Lowlands of Colombia. The Louisiana State University Press, Baton Rouge, Louisiana, 278 p.
- Wentworth, C. K., 1922. A scale of grade and class terms for clastic sediments. Jour. Geol., v. 30, p. 377-392.
- Whittecar, G. Richard, Darby, Dennis A., Barringer, Richard A., Garrett, Jim R., and Babuin, Michael L., 1984. (Abstract) Changes of quaternary fluvial systems in a high-relief humid tropical environment. Geol. Soc. Amer. Abstracts with Programs, v. 16, no. 6, p. 397.
- Wood, P. A., 1977. Suspended sediment in a tropical environment of seasonal flow and large floods: Hope River, Jamaica. Jour. of Trop. Geog., v. 45, p. 65-69.





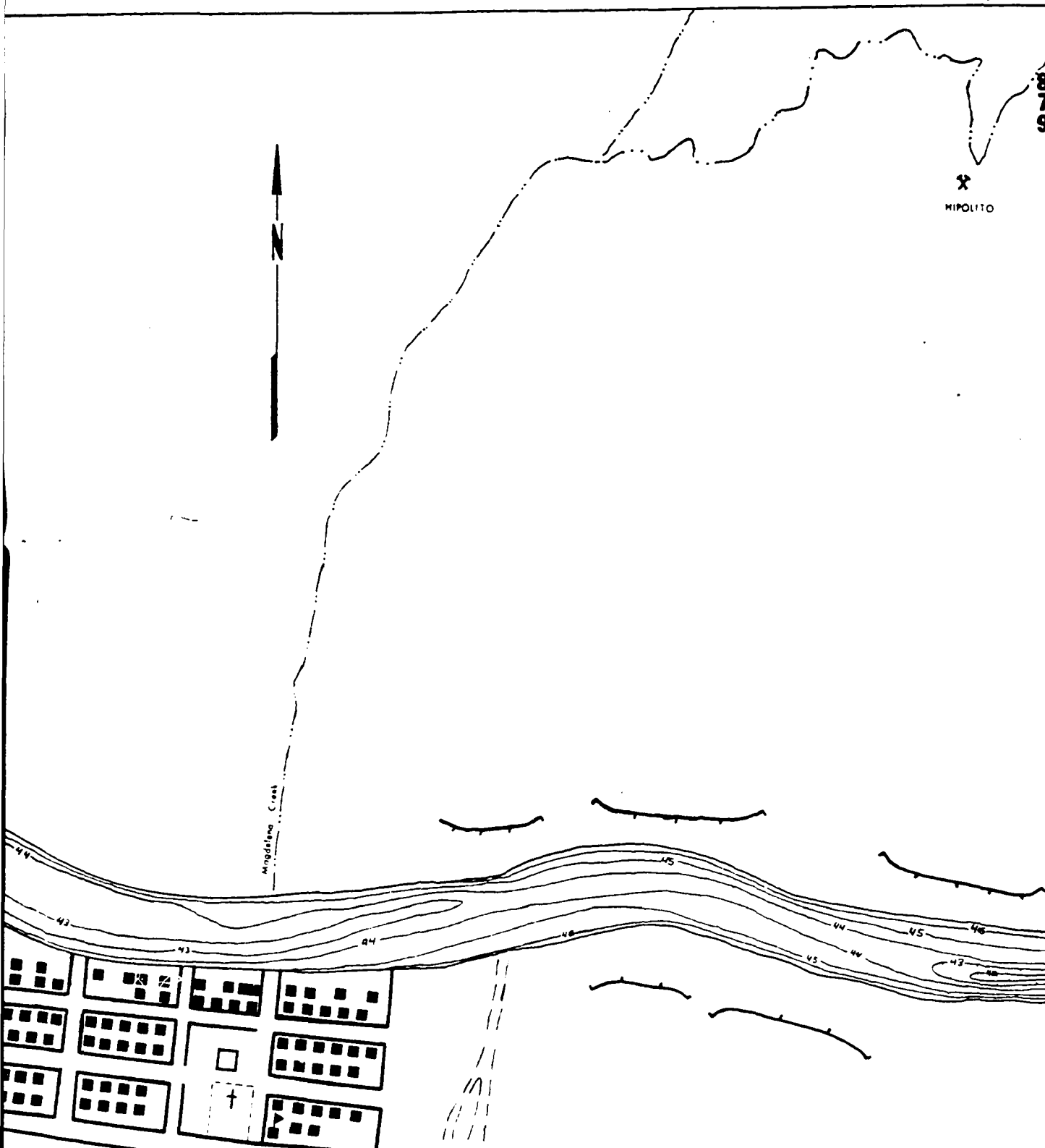
687

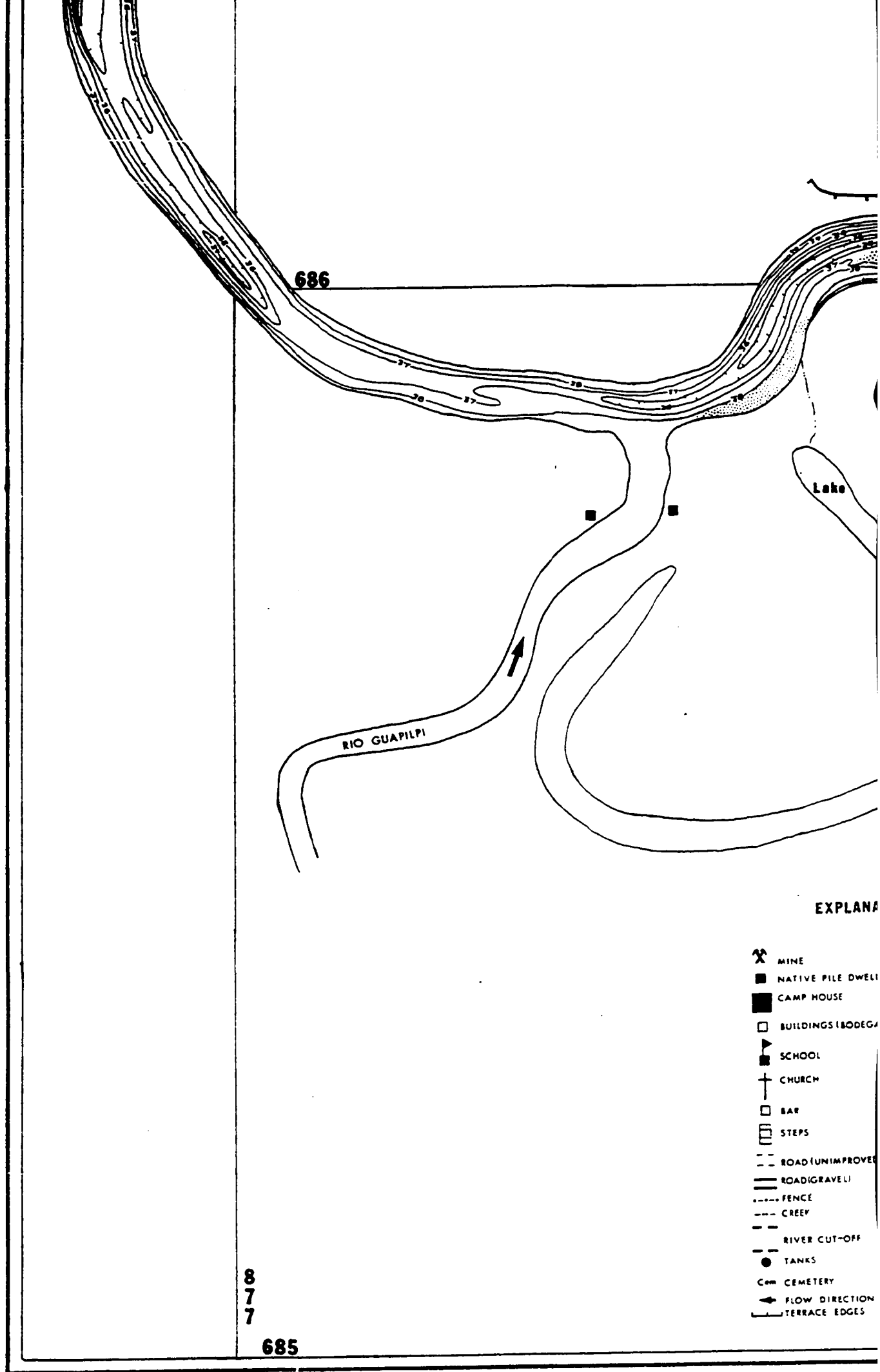
879

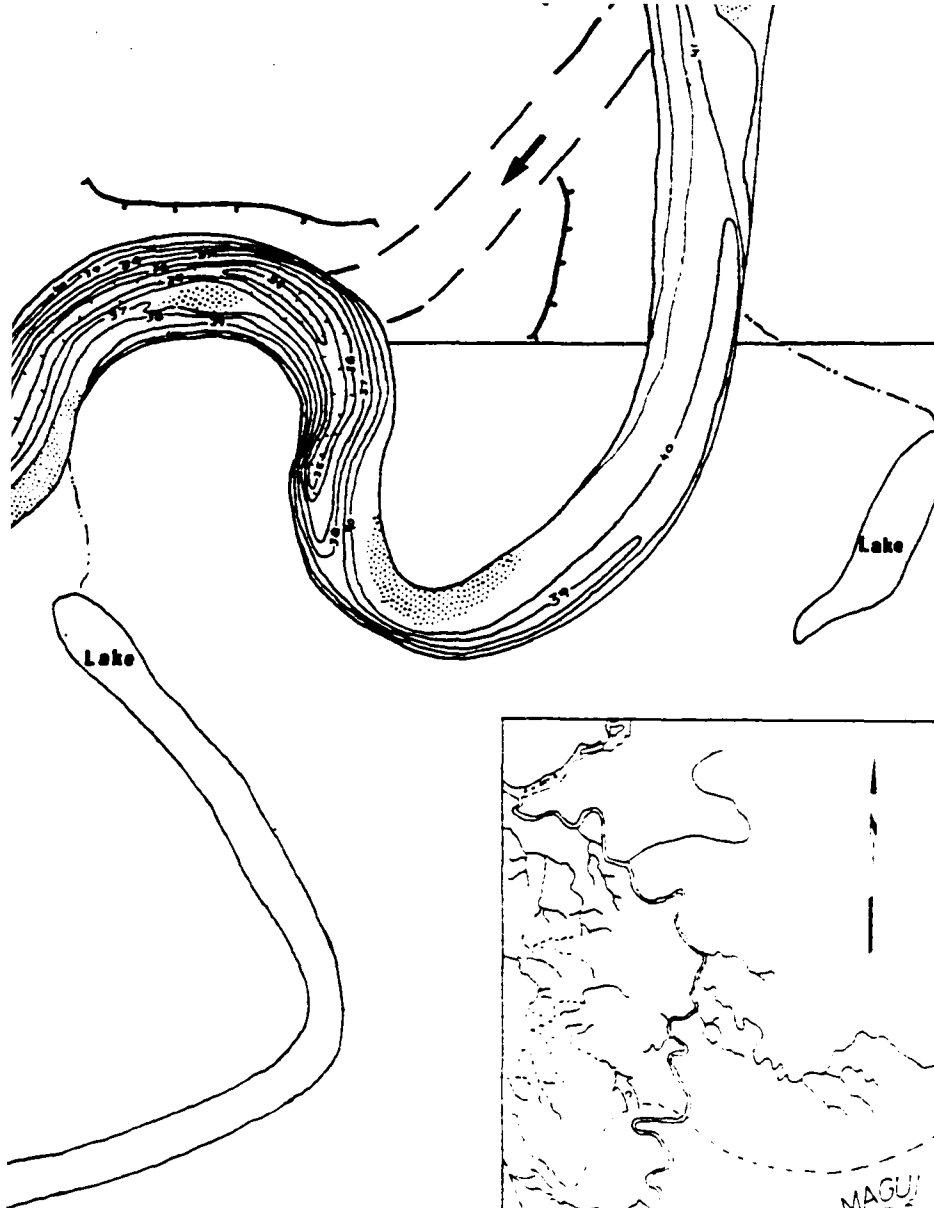
X
HIPOLITO



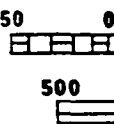
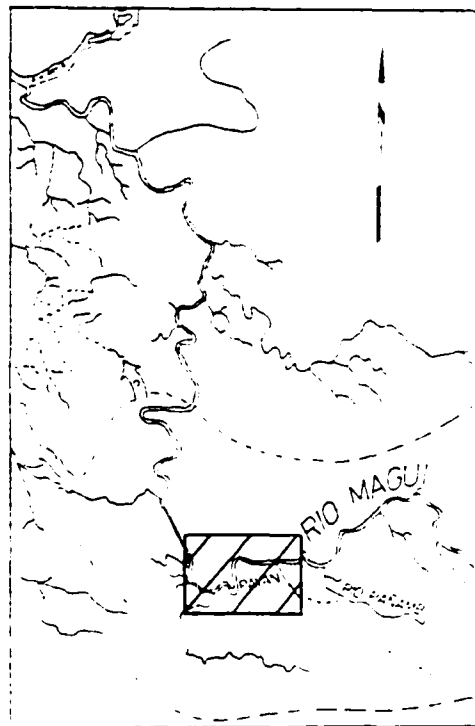
Mangrove Creek







686



EXPLANATION

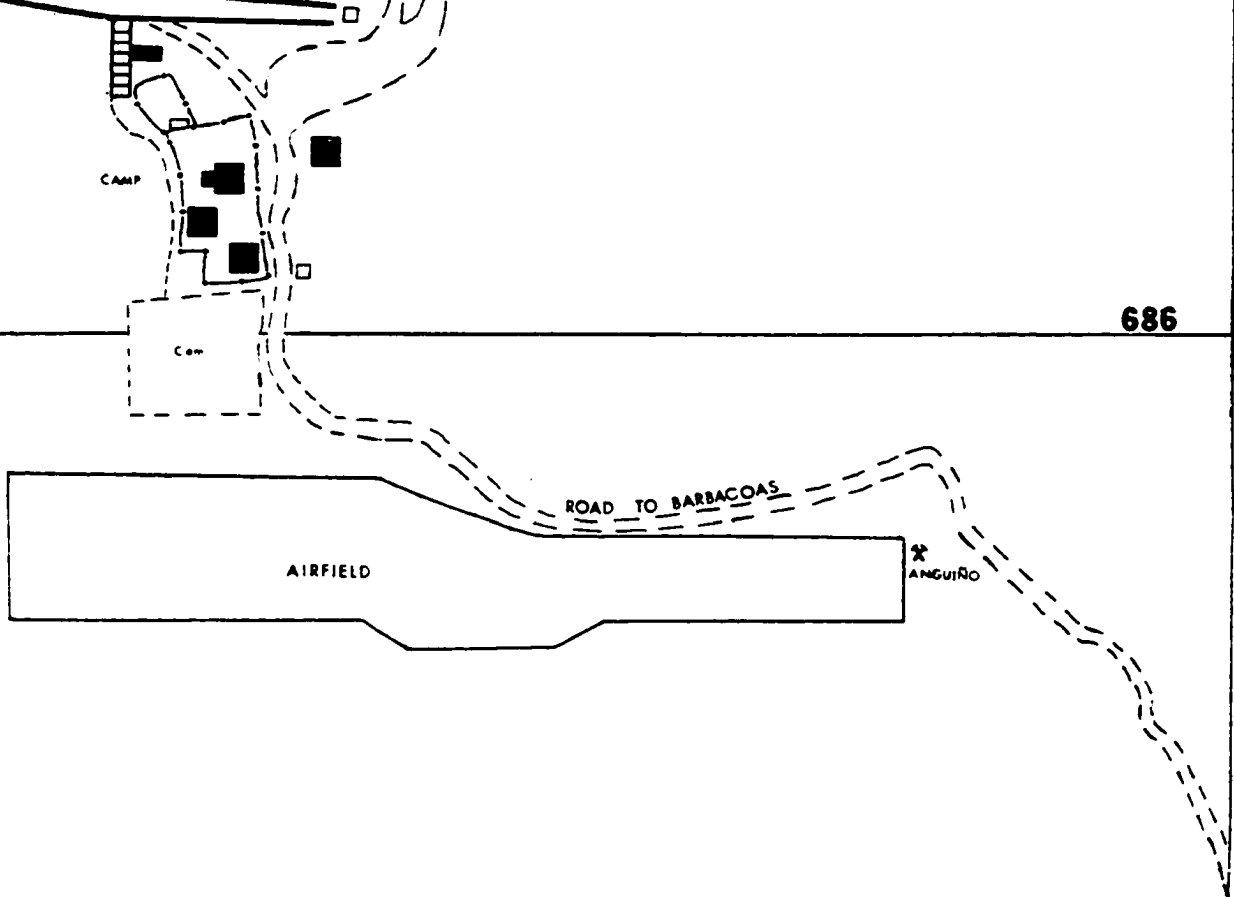
BATHY

M

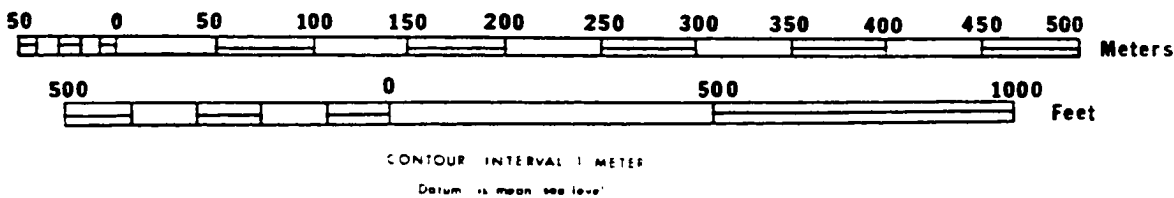
- MINE
- NATIVE PILE DWELLING
- CAMP HOUSE
- BUILDINGS (BODEGA)
- SCHOOL
- CHURCH
- BAR
- STEPS
- ROAD (UNIMPROVED)
- ROAD (GRAVEL)
- FENCE
- CREEK
- RIVER CUT-OFF
- TANKS
- CEMETERY
- FLOW DIRECTION
- TERRACE EDGES

8
7
8

685



686

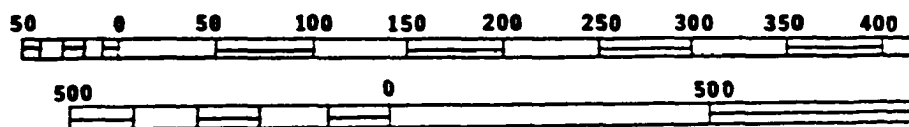


THYMETRIC MAP OF THE PAYAN QUADRANGLE

By
M.L. BABUIN, R.A. BARRINGER and J.R. GARRETT
1984

8
7
9

685



CONTOUR INTERVAL 1 METER

Datum is mean sea level

BATHYMETRIC MAP OF T AGUA DERECHO QUADRAI

By
M.L. BABUIN, R.A. BARRINGER and J.R. GARRETT
1984

8
7
6

689

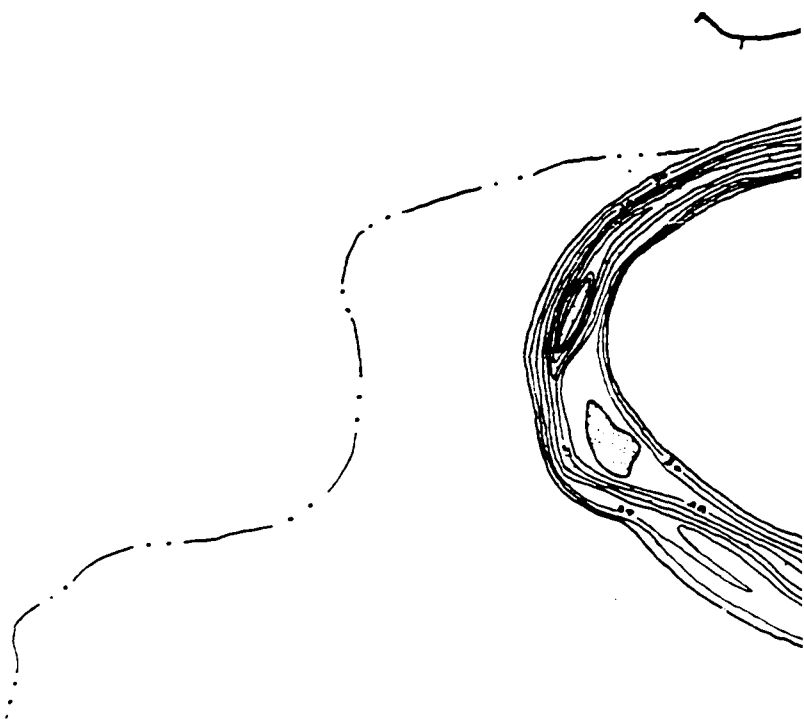


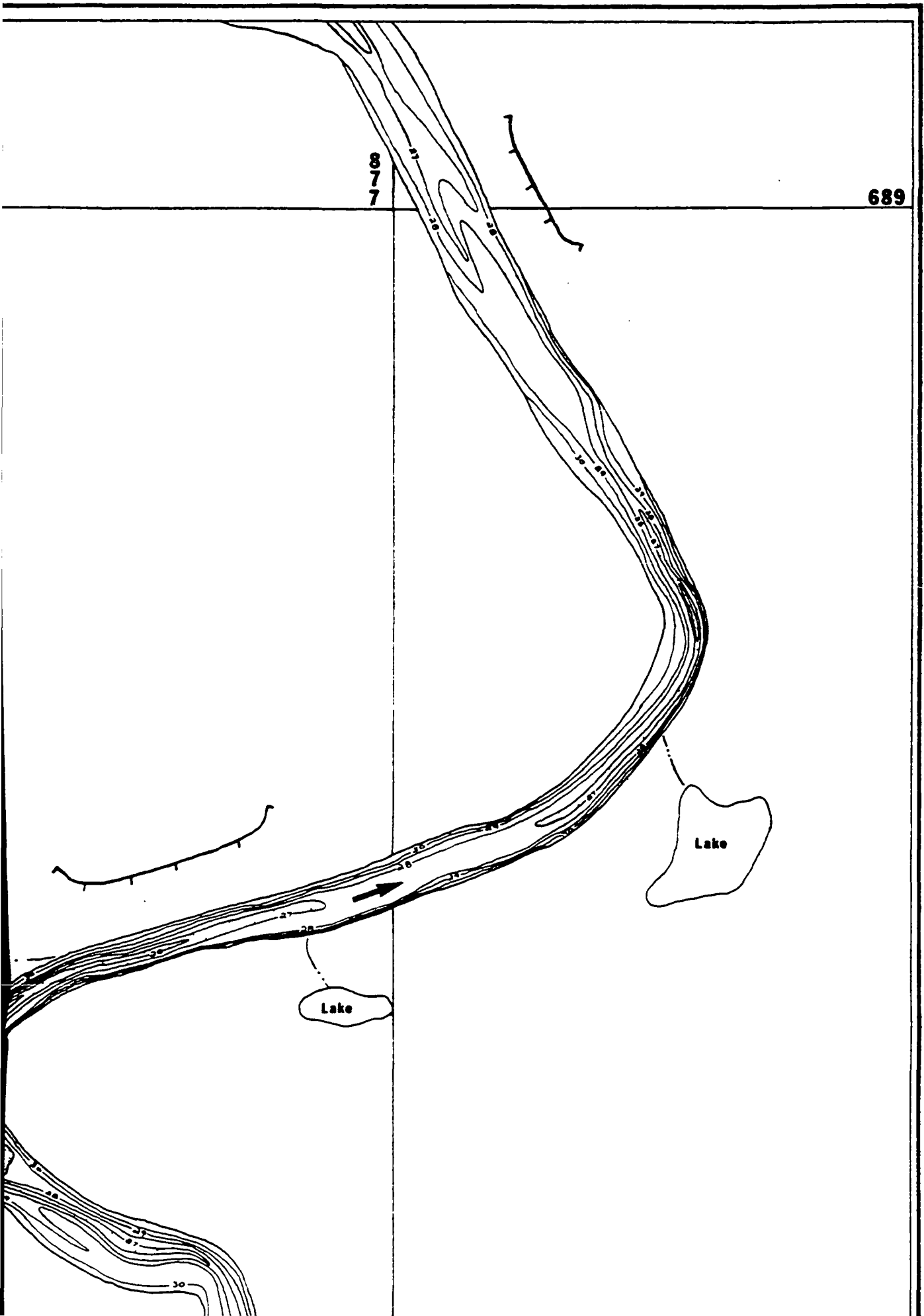
350 400 450 500 Meters

1000 Feet







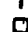



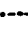
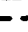





OF THE
ORANGLE

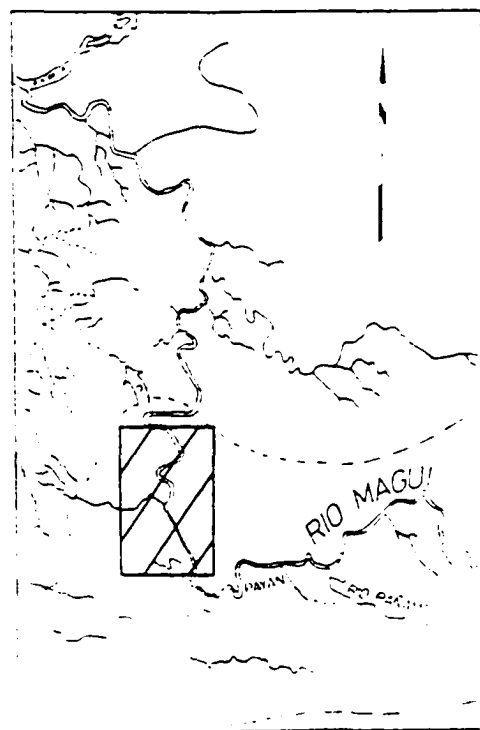
ARRETT





EXPLANATION

-  MINE
-  NATIVE PILE DWELLING
-  CAMP HOUSE
-  BUILDINGS (BODEGA)
-  SCHOOL
-  CHURCH
-  BAR
-  STEPS
-  ROAD (UNIMPROVED)
-  ROAD (GRAVEL)
-  FENCE
-  CREEK
-  RIVER CUT-OFF
-  TANKS
-  CEMETERY
-  FLOW DIRECTION
-  TERRACE EDGES





688

Lake

Lake

Lake

108








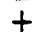

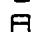



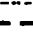
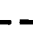


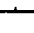

688

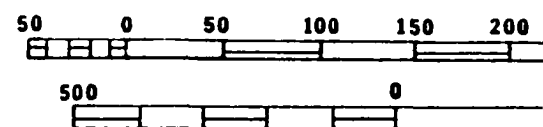
87

Lake

691

8
7
6

-  MII
-  NA
-  CA
-  BUI
-  SCI
-  CHI
-  BAI
-  STE
-  RO
-  ROA
-  PEN
-  CRE
-  RIV
-  TAI
-  Com CEI
-  FLC
-  TER




















CONTOUR
Datum

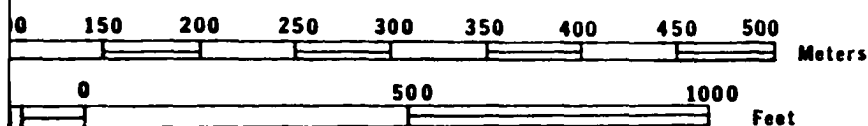
BATHYMETRIC M HORSESHOE MEAND

M.L. BABUIN, R.A. BARR

19

EXPLANATION

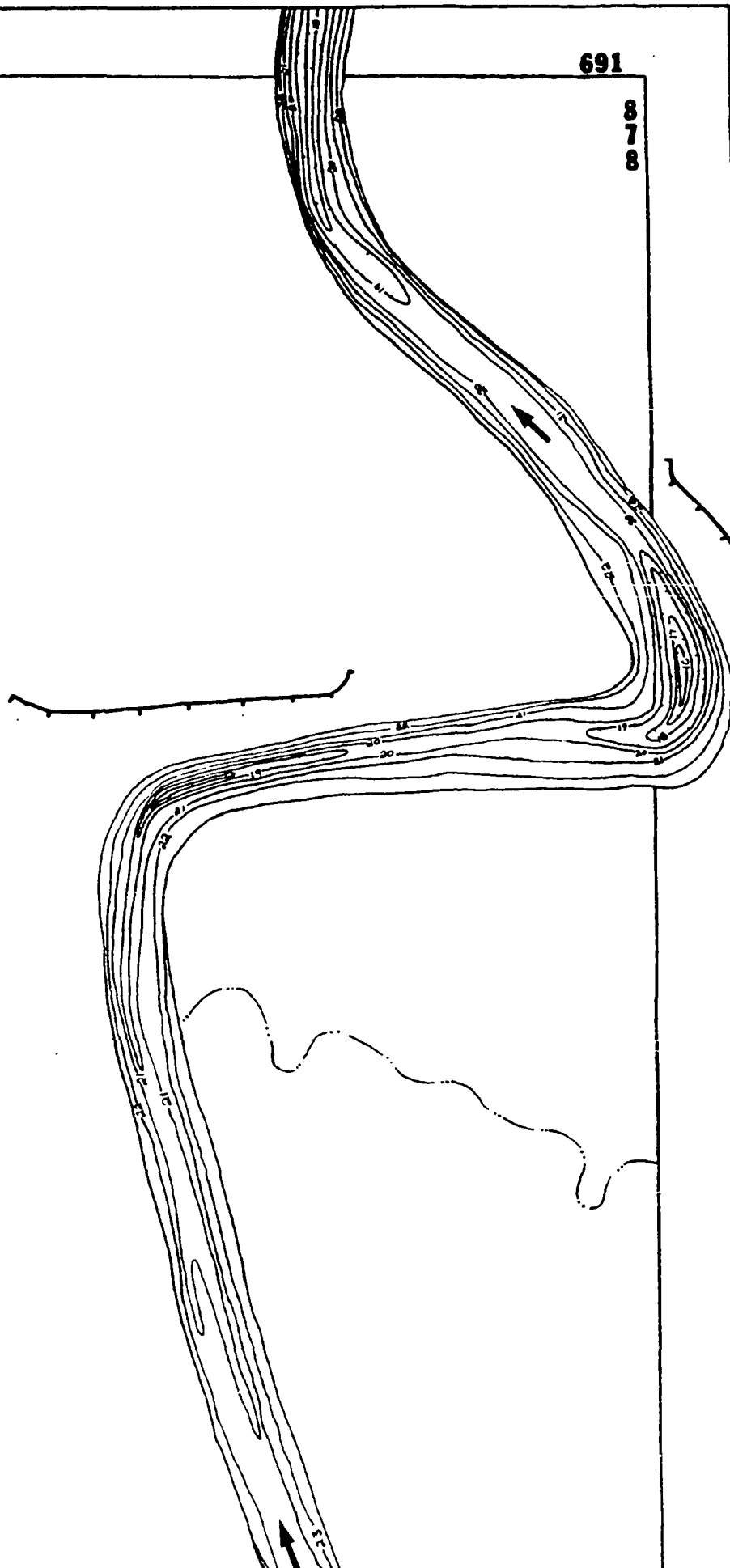
-  MINE
-  NATIVE PILE DWELLING
-  CAMP HOUSE
-  BUILDINGS (BODEGA)
-  SCHOOL
-  CHURCH
-  BAR
-  STEPS
-  ROAD (UNIMPROVED)
-  ROAD (GRAVEL)
-  FENCE
-  CREEK
-  RIVER CUT-OFF
-  TANKS
-  CEMETERY
-  FLOW DIRECTION
-  TERRACE EDGES

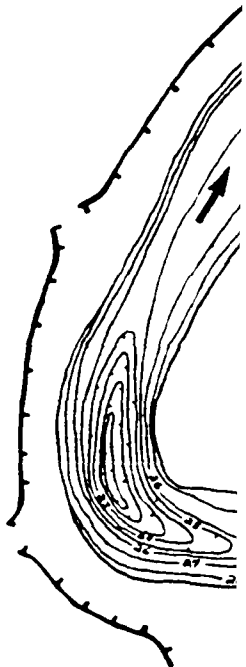
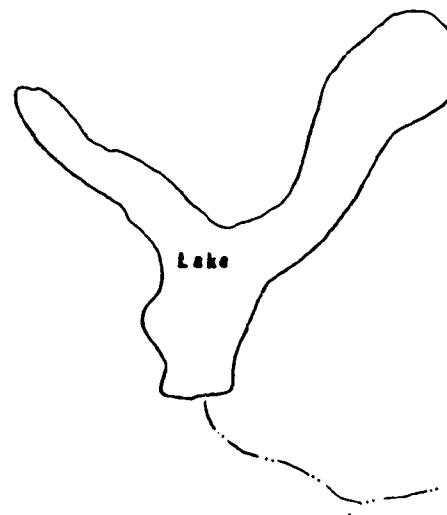
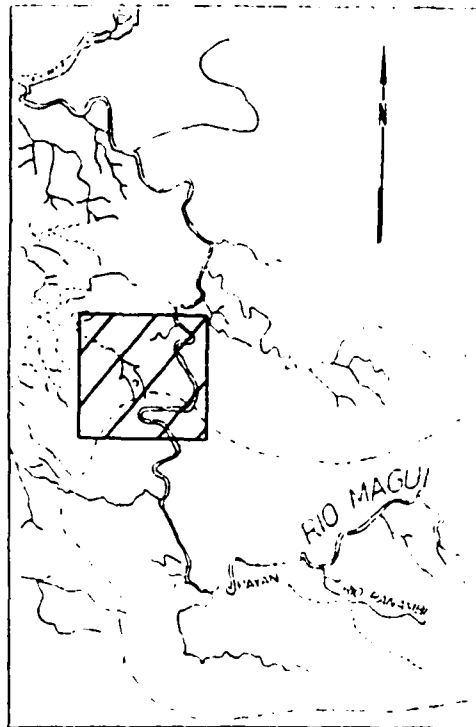


CONTOUR INTERVAL 1 METER
Datum is mean sea level

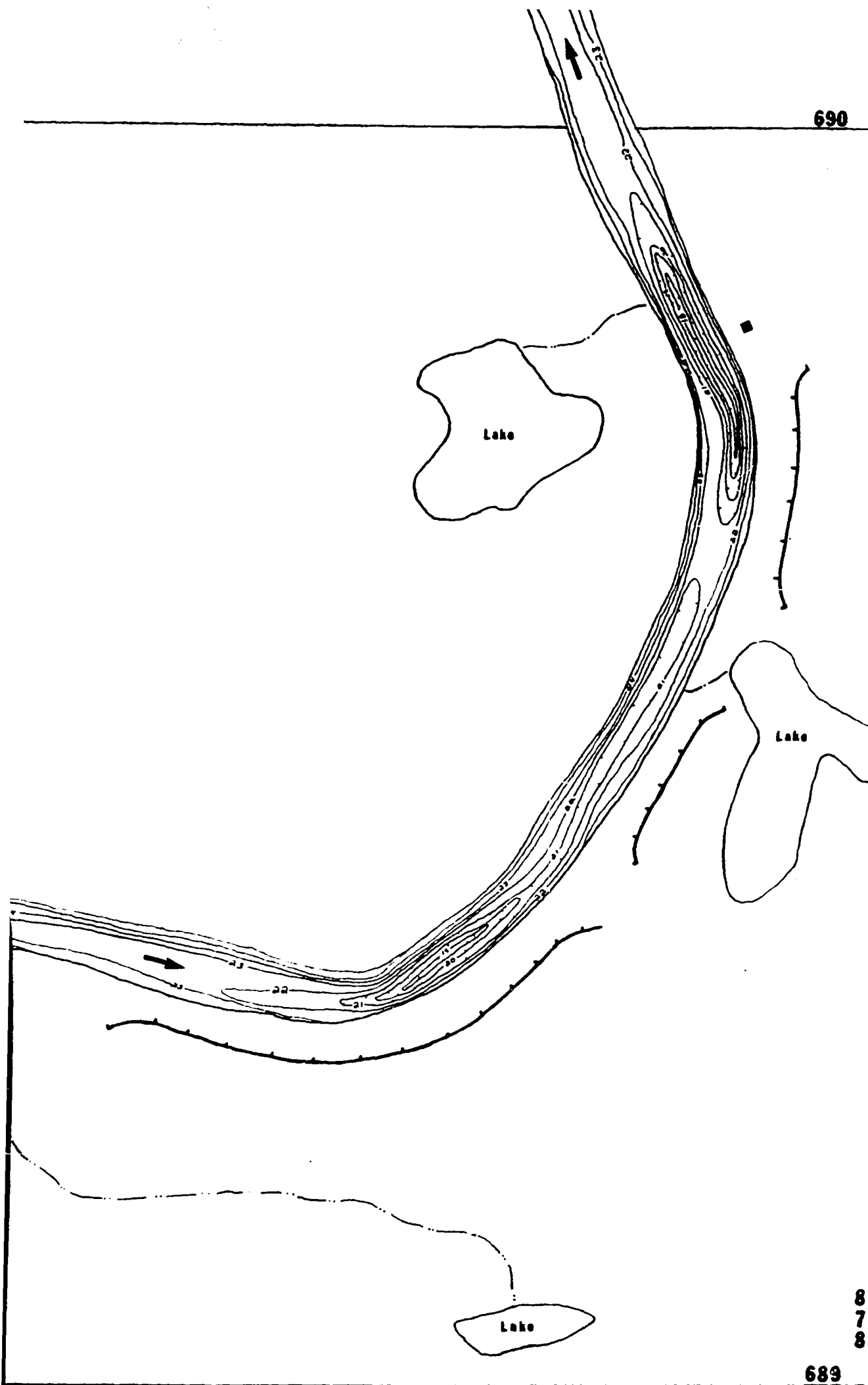
TRIC MAP OF THE EANDER QUADRANGLE

By
JIN, R.A. BARRINGER and J.R. GARRETT
1984



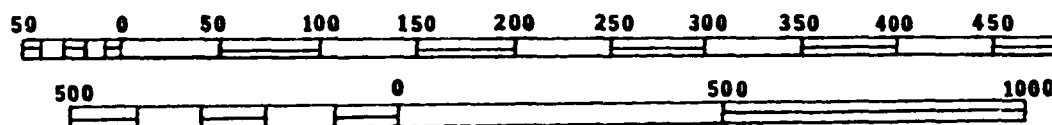






693

8
7
7

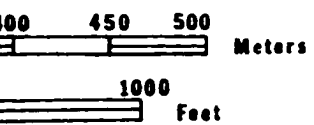


CONTOUR INTERVAL 1 METER

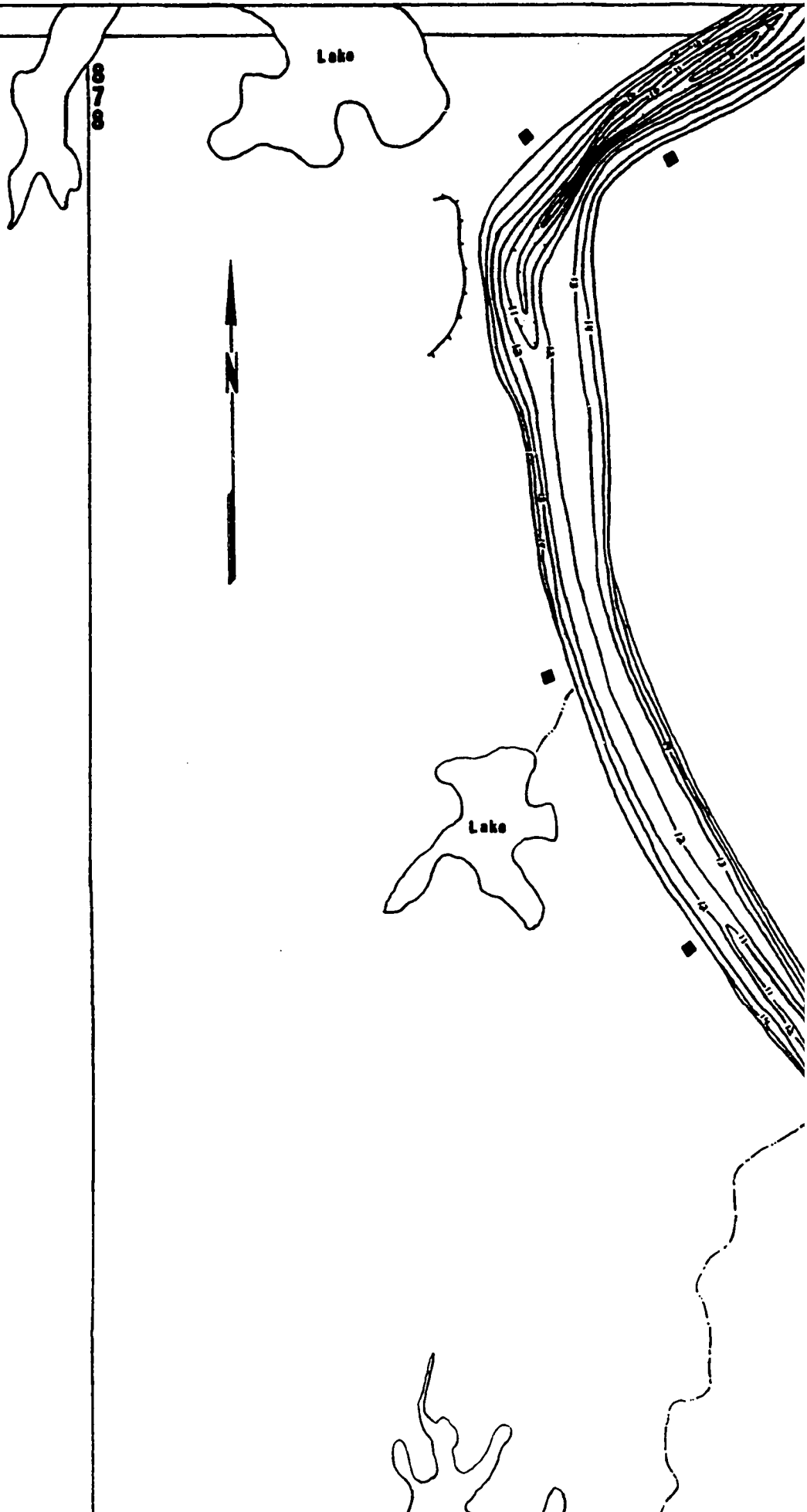
Datum is mean sea level

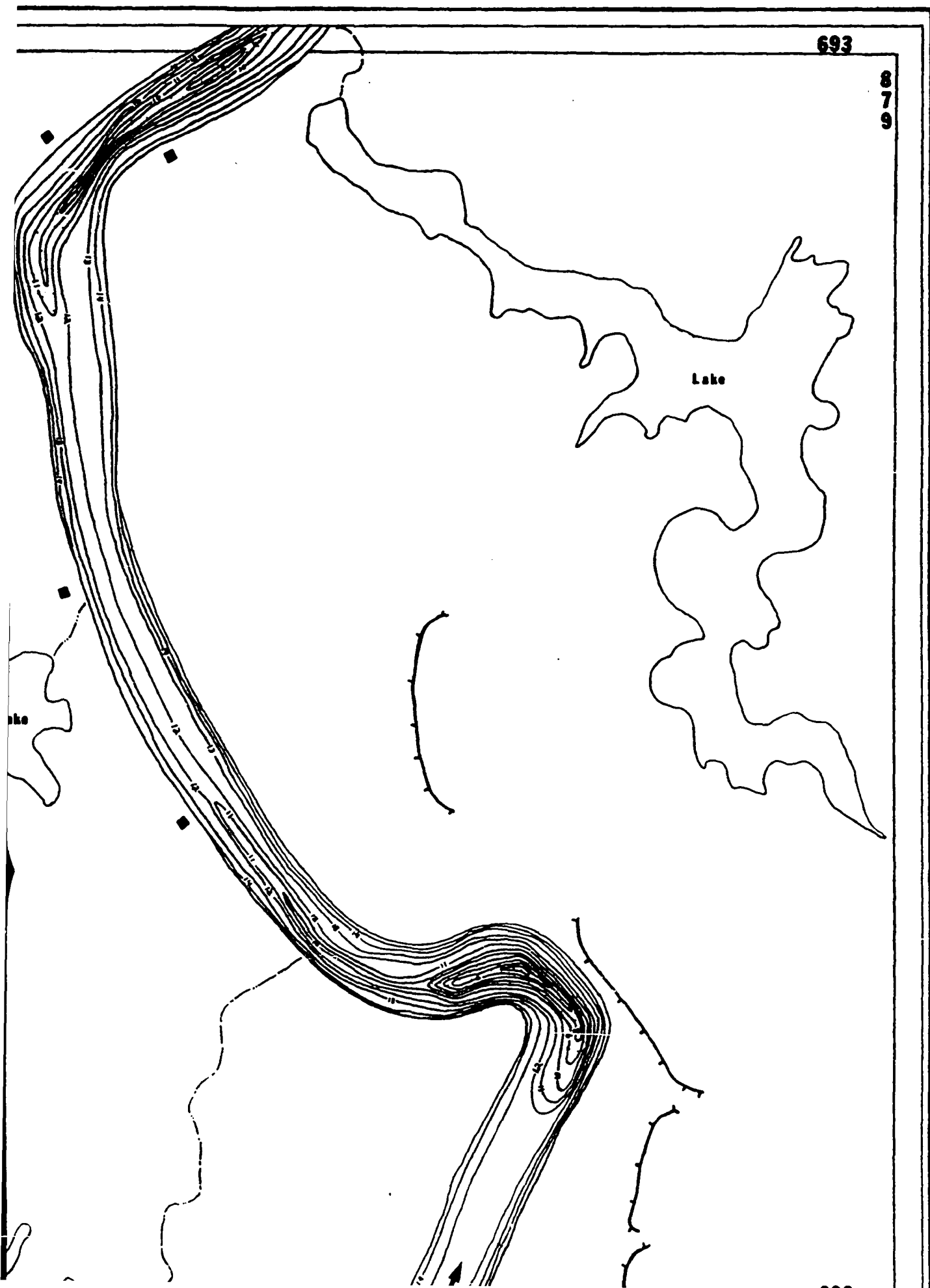
BATHYMETRIC MAP OF THE GUAÑAMBI QUADRANGLE

By
M.L. BABUIN, R.A. BARRINGER and J.R. GARRETT
1984









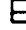
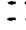

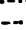







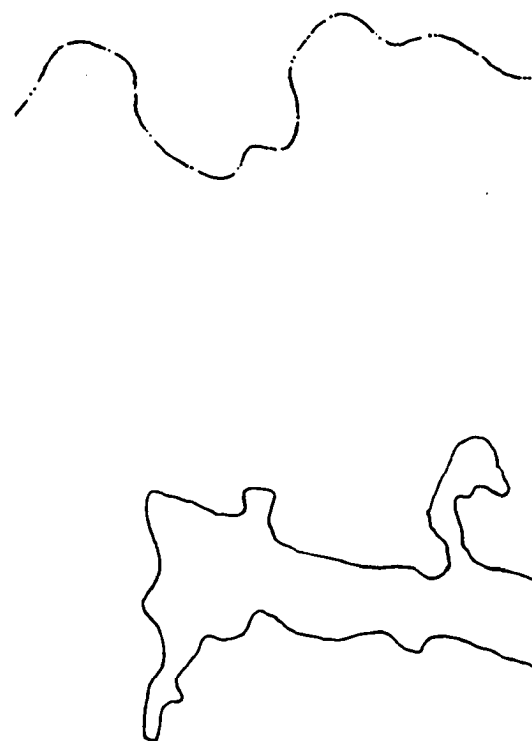
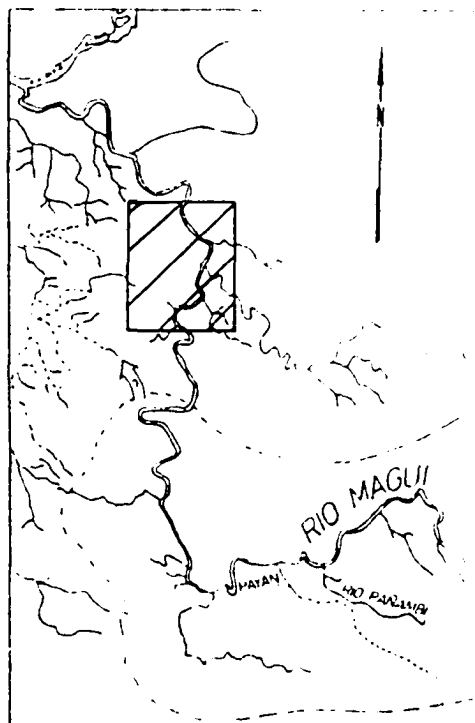
THE
GLE

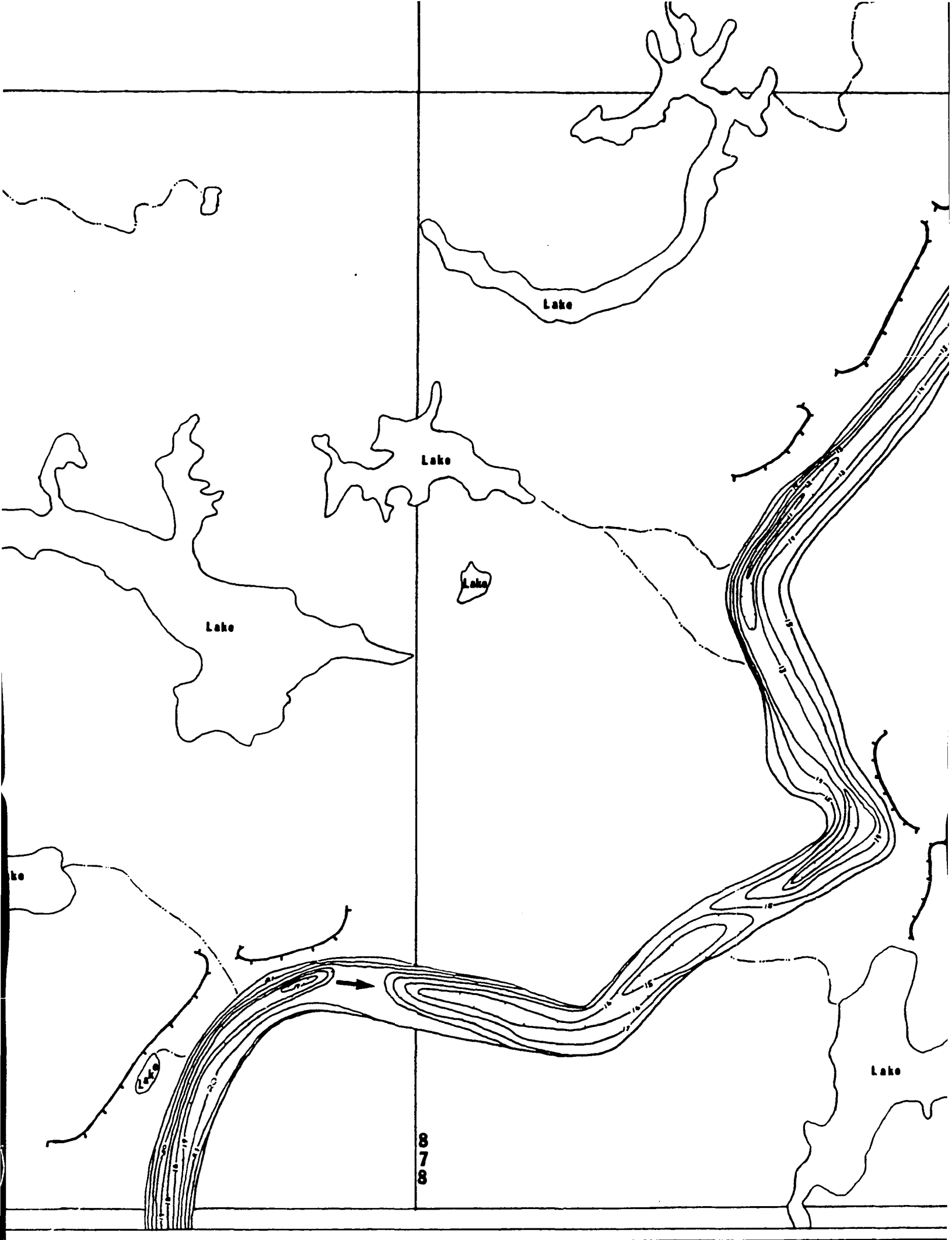




EXPLANATION

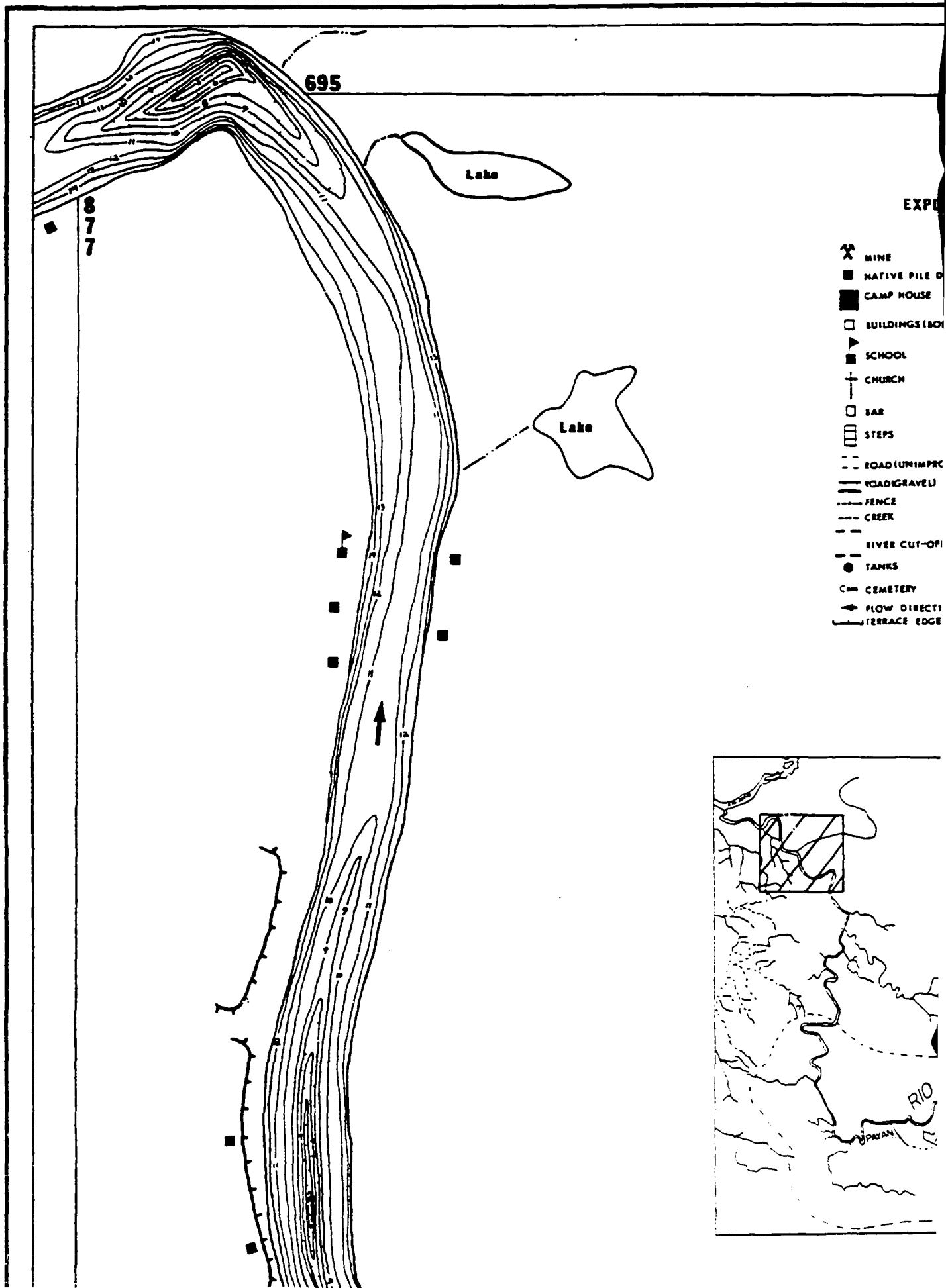
-  MINE
-  NATIVE PILE DWELLING
-  CAMP HOUSE
-  BUILDINGS (BODEGA)
-  SCHOOL
-  CHURCH
-  BAR
-  STEPS
-  ROAD (UNIMPROVED)
-  ROAD (GRAVEL)
-  FENCE
-  CREEK
-  RIVER CUT-OFF
-  TANKS
-  CEMETERY
-  FLOW DIRECTION
-  TERRACE EDGES






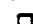















8
7
8

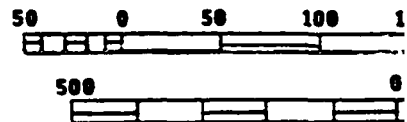




EXPLANATION

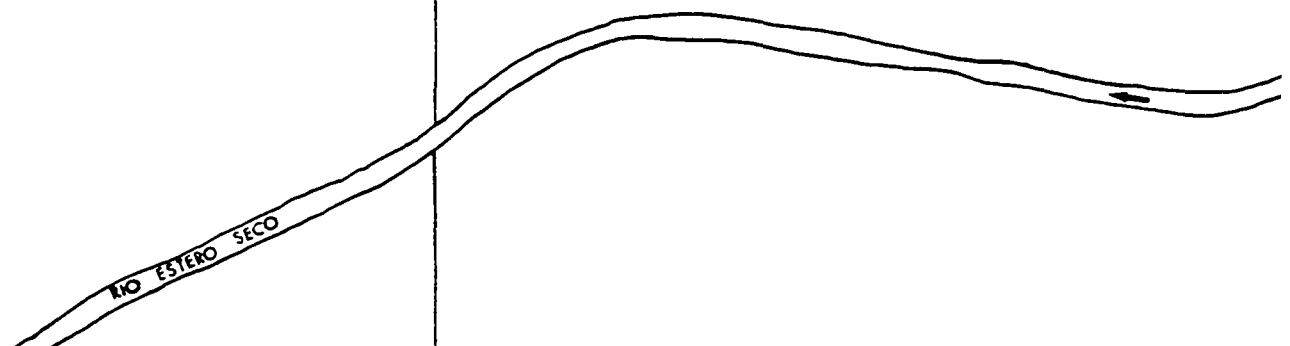
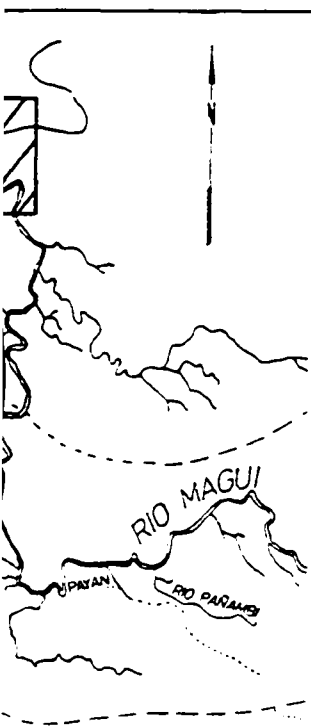
-  MINE
-  NATIVE PILE DWELLING
-  CAMP HOUSE
-  BUILDINGS (BODEGA)
-  SCHOOL
-  CHURCH
-  BAR
-  STEPS
-  ROAD (UNIMPROVED)
-  ROAD (GRAVEL)
-  FENCE
-  CREEK
-  RIVER CUT-OFF
-  TANKS
-  CEMETERY
-  FLOW DIRECTION
-  TERRACE EDGES

8
7
8



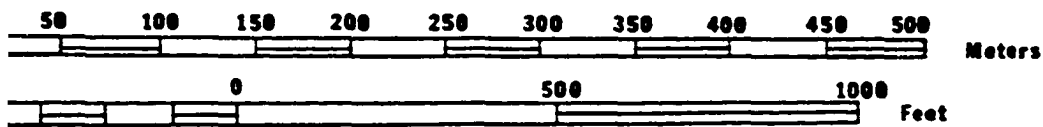
BATHYMETRIC ESTERO SECO

M.L. BABUIN, R.A.



695

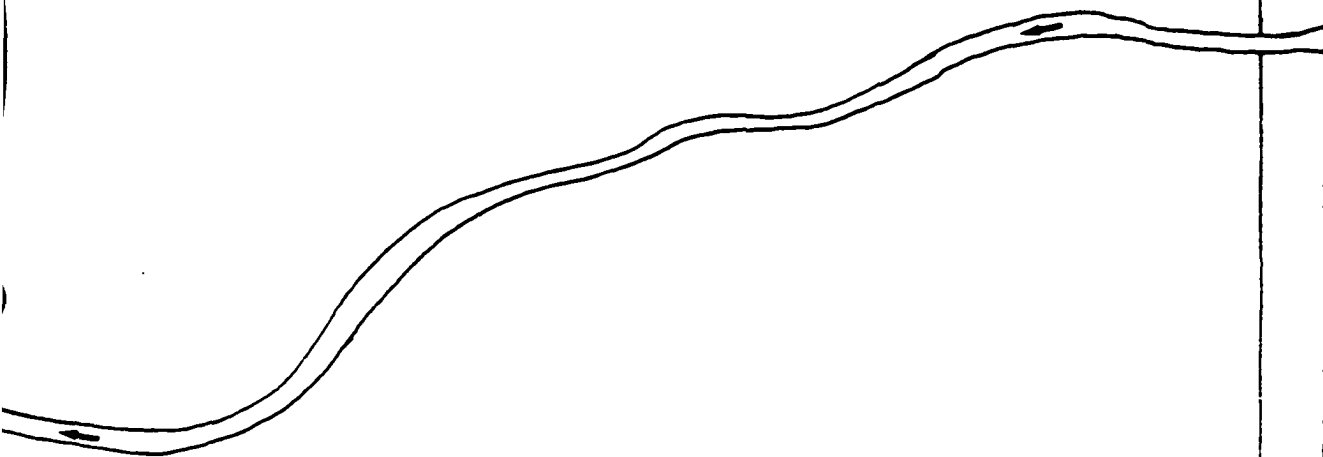
8
7
9



CONTOUR INTERVAL 1 METER
Datum = mean sea level

METRIC MAP OF THE SECO QUADRANGLE

By
M.L. BABUIN, R.A. BARRINGER and J.R. GARRETT
1984



694

8
7
7

693

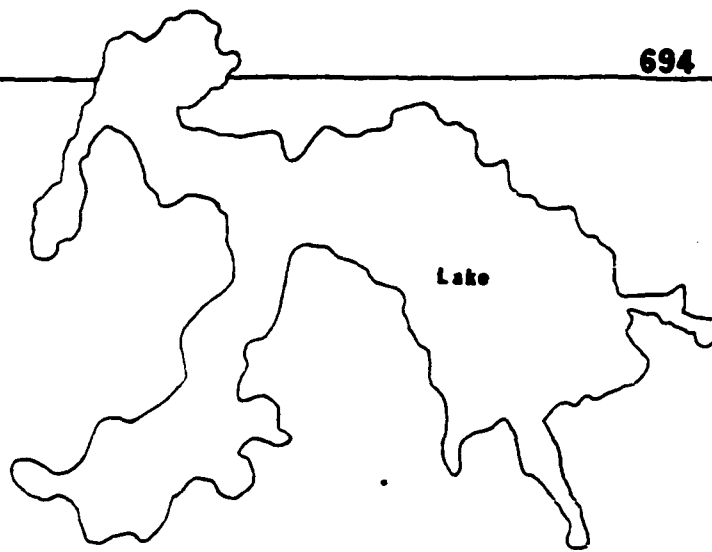
Lake

Lake



•

694



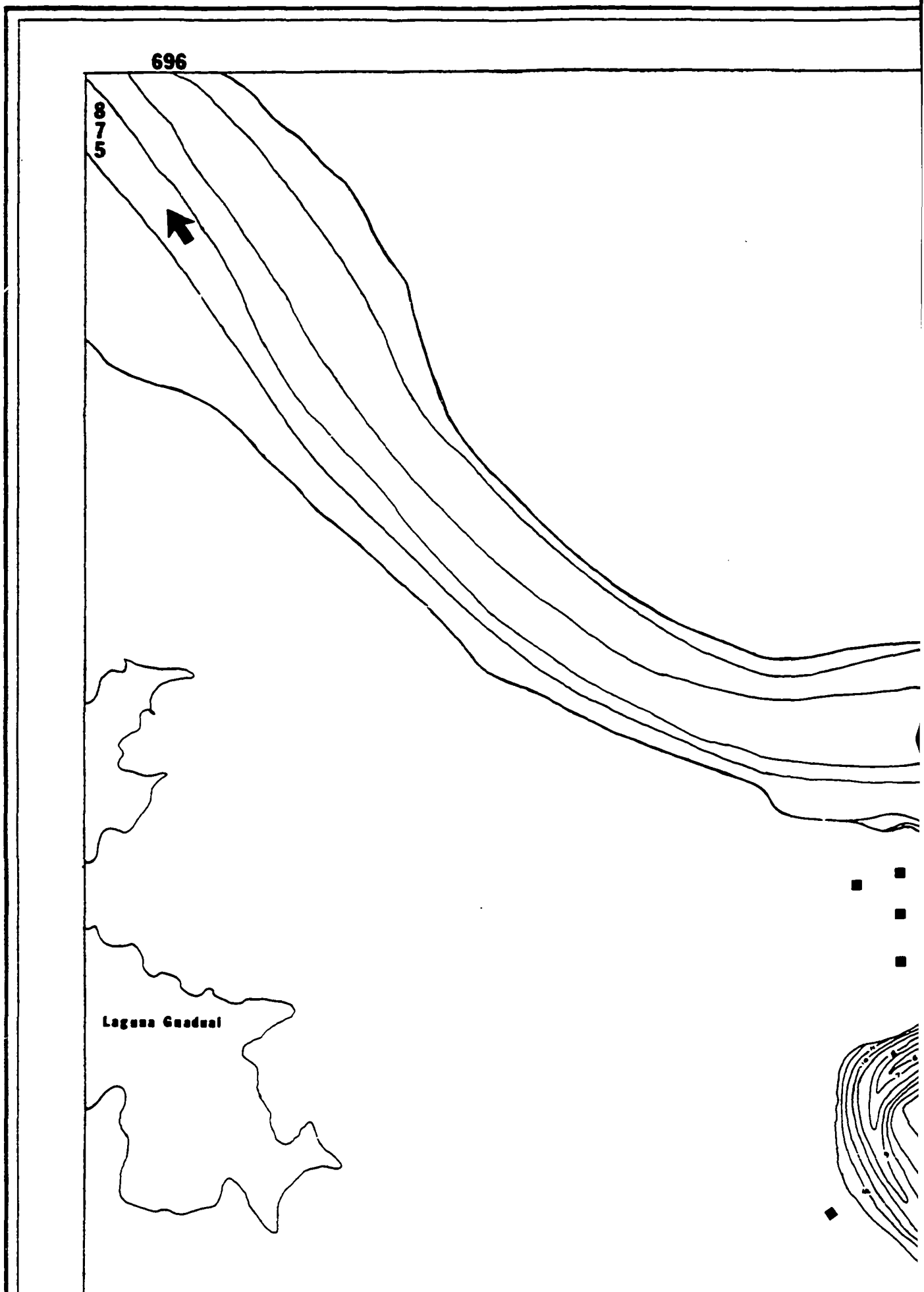
Bellavista



Lake

8
7
9

693













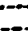
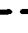





8
7
6

RIO PATIA



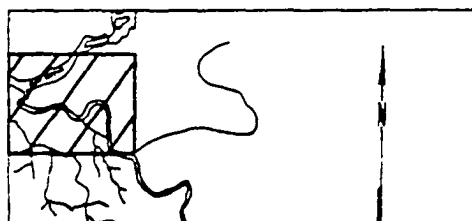


EXPLANATION

-  MINE
-  NATIVE PILE DWELLING
-  CAMP HOUSE
-  BUILDINGS (BODEGA)
-  SCHOOL
-  CHURCH
-  BAR
-  STEPS
-  ROAD (UNIMPROVED)
-  ROAD (GRAVEL)
-  FENCE
-  CREEK
-  RIVER CUT-OFF
-  TANKS
-  CEMETERY
-  FLOW DIRECTION
-  TERRACE EDGES



Lake

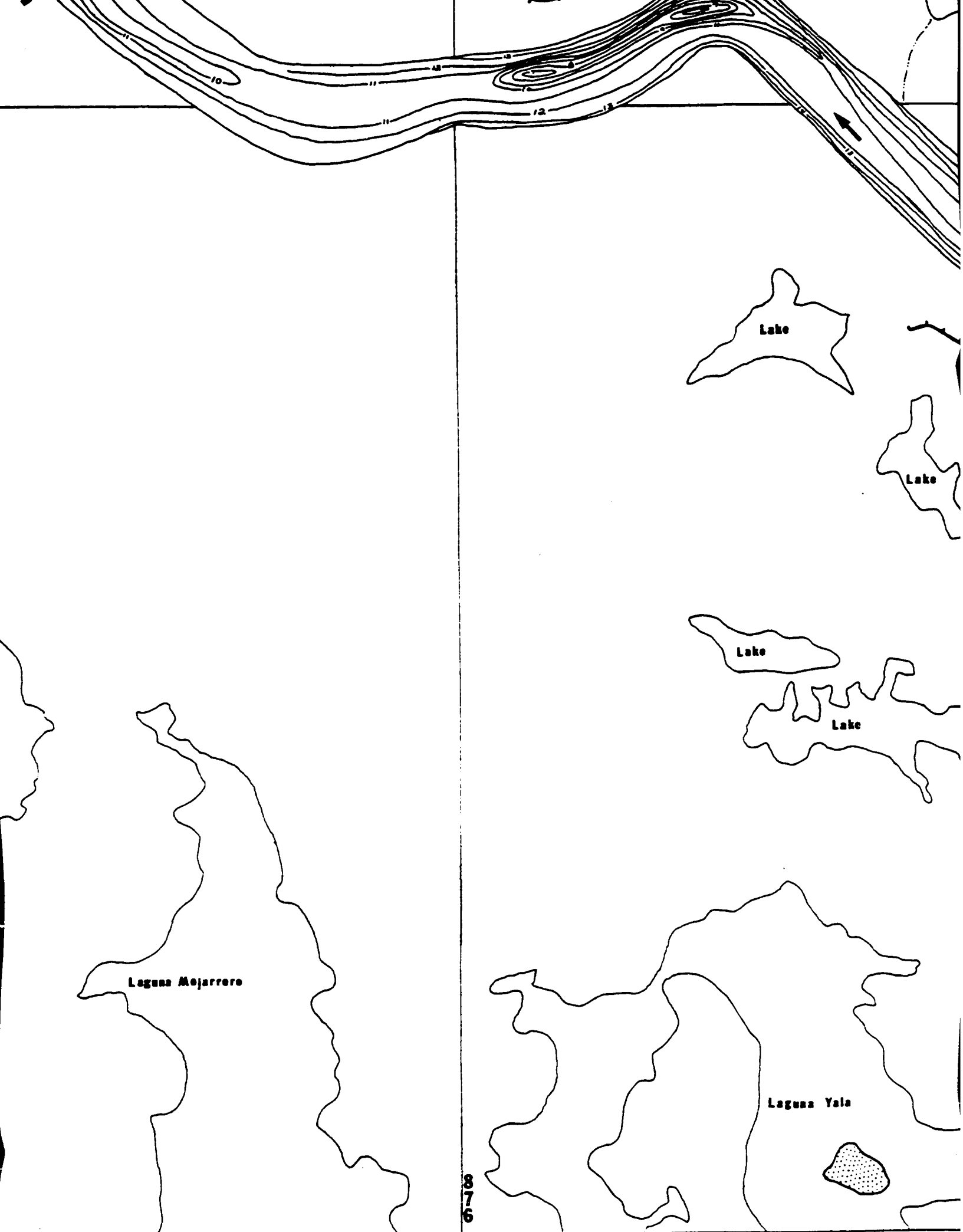


695

Laguna Carlo

8
7
5

694



876

Laguna Mojarrero

Lake

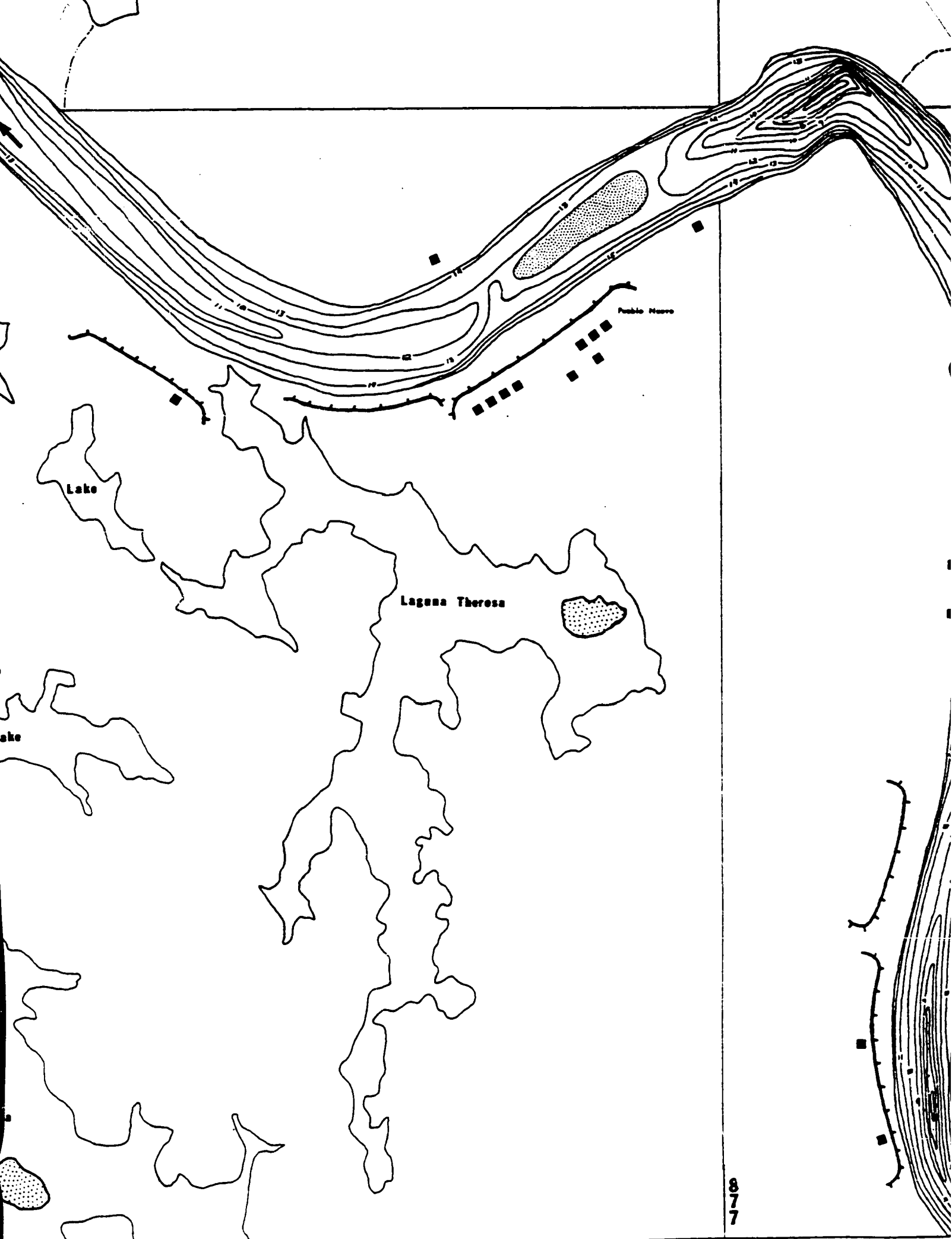
Lake

Lake

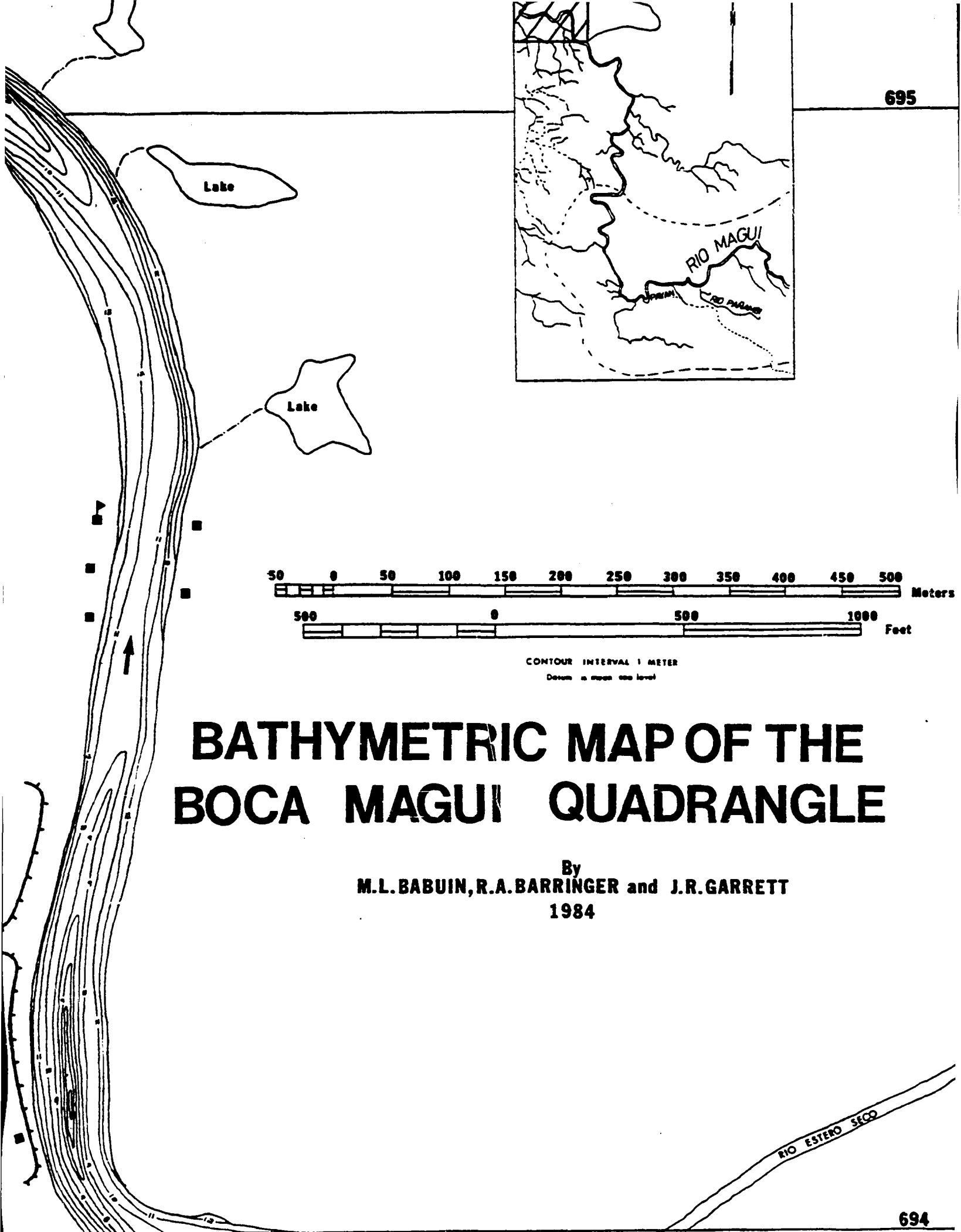
Lake

Laguna Yala





877



BATHYMETRIC MAP OF THE BOCA MAGUI QUADRANGLE

By
M.L. BABUIN, R.A. BARRINGER and J.R. GARRETT
1984

